Master's thesis

NTNU
Norwegian University of Science and Technology
Faculty of Engineering
Department of Civil and Environmental Engineering

Markus Nikolai Berner

Application of Data Mining Techniques to Soil Stabilization

Master's thesis in Civil and Environmental Engineering
Supervisor: Yutao Pan
Co-supervisor: Stefan Ritter and Sølve Hov
June 2023

NTNU
Norwegian University of
Science and Technology

Markus Nikolai Berner

Application of Data Mining Techniques to Soil Stabilization

Master's thesis in Civil and Environmental Engineering
Supervisor: Yutao Pan
Co-supervisor: Stefan Ritter and Sølve Hov
June 2023

Norwegian University of Science and Technology
Faculty of Engineering
Department of Civil and Environmental Engineering

NTNU
Norwegian University of
Science and Technology

Preface

This master's thesis represents the final part of my master degree in Geotechnical Engineering at the Norwegian University of Science and Technology (NTNU). It was conducted in the spring of 2023 for the Department of Civil and Environmental Engineering. The assignment was carried out in collaboration with Norwegian Geotechnical Institute (NGI).

This study aims to find correlations in soil stabilization databases using Data Mining.

The work done in this master's thesis is a further development of the work done in the initial project thesis carried out in the fall of 2022.

Trondheim, 12.06.2023

Markus Nikolai Berner

Acknowledgments

I would like to thank my main supervisor, Yutao Pan, for his excellent guidance through the entire process of my master's thesis. I have really appreciated our discussions and that you were always available when I needed help.

I would also like to thank Sølve Hov who provided all the data in this thesis and gave great help in establishing the databases. His expertise and support were crucial in enabling me to carry out the various analyses.

Furthermore, I would like to thank Stefan Ritter for providing this thesis. I have really appreciated his constructive feedback and meaningful discussions related to this work.

Lastly, I would like to thank Dominik Gächter and Nejla Helvacioglu from Keller for their involvement in the early stages of this master's thesis.

Abstract

Deep Dry mixing (DDM) is a soil stabilization method for clays and other weak soils. The method combines the dry binder with the soil, which increases its strength. This study aims to determine whether reliable correlations between in-situ soil parameters and stabilized soil strength can be detected. To establish the correlations, both linear and non-linear methods were used. The findings in this study are intended to provide a further understanding of what affects strength development in DDM soils, which are useful insights for future DDM projects.

The analyzed data came from three different sources. Two databases were already established ([1] and [2]), which consisted of laboratory-improved soils from Norway and Sweden. In addition, two new databases were created for this thesis: A CPTU database and a laboratory database. These consisted of data from 167 field strength measurements of stabilized soil, 33 CPTUs, and various laboratory tests from 14 different test series, all from the E6 Kvithammar-Åsen project. There were challenges related to large distances between the tests performed and a lack of laboratory data, which resulted in uncertainty in the analyses.

The linear correlation analysis of the CPTU database showed no observed correlation between the CPTU data and the column strength, as indicated by the highest obtained coefficient of determination (R^2) value of 0.05. However, weak correlations were discovered in the laboratory database from E6 Kvithammar-Åsen, where the plastic limit showed the highest correlation with an R^2 value of 0.32. Although assumptions were made to address the challenges of the distance between the various tests in addition to missing laboratory data, the correlations from the laboratory database were generally consistent with the Norwegian laboratory-improved database. However, varying correlations were seen in the corresponding Swedish database. The water binder ratio was the only variable with similar correlations in all laboratory databases.

Gradient Boosting and Random Forest models were created using the different databases, where 80% of the data were used to train the models, and the remaining 20% were used for evaluation. The models from the E6 Kvithammar-Åsen databases showed poor results, while the models based on laboratory data from Norway and Sweden managed to predict the stabilized strength of the soil with a best R^2 value of 0.82.

Sammendrag

Kalksementstabiliseringer er en grunnforbedringsteknikk for leire og andre svake jordtyper. Metoden blander den tørre bindemiddelet med grunnen, noe som øker styrken. Hensikten til studien er å finne ut om det kan påvises pålitelige sammenhenger mellom in-situ jordparametere og skjærstyrken til den stabiliserte grunnen. Det ble brukt både lineære og ikke-lineære metoder for å utforske og identifisere eventuelle korrelasjoner. Resultatene i denne studien har til hensikt å gi ytterligere forståelse av hva som påvirker styrkeutviklingen i kalksementpeler, noe som er nyttige innsikter for fremtidige kalksementprosjekter.

De analyserte dataene kom fra tre forskjellige kilder. To databaser var allerede etablert ([1] og [2]), som besto av laboratorieforbedrede jordprøver fra Norge og Sverige. I tillegg ble to nye databaser opprettet for denne avhandlingen: En CPTU-database og en laboratoriedatabase. Disse bestod av data fra 167 feltmålinger av skjærstyrken til kalksementpelene, 33 CPTU-målinger og ulike laboratorietester fra 14 ulike prøveserier, alt fra E6 Kvithammar-Åsen prosjektet. Det var utfordringer knyttet til store avstander mellom de utførte testene og mangel på laboratoriedata, noe som resulterte i usikkerhet i analysene.

Den lineære korrelasjonsanalysen av CPTU-databasen viste ingen observert sammenheng mellom CPTU-dataene og den stabiliserte styrken til kalksementpelene, som indikert av den høyeste oppnådde determinasjonskoeffisienten (R^2) på 0,05. Imidlertid ble det oppdaget svake korrelasjoner i laboratoriedatabasen fra E6 Kvithammar-Åsen, der plastisitetsgrensen viste den høyeste korrelasjonen med en R^2 verdi på 0,32. Selv om det ble gjort antakelser for å håndtere utfordringene med avstanden mellom de ulike testene i tillegg til manglende laboratoriedata, var korrelasjonene fra laboratoriedatabasen generelt konsistente med den norske laboratorie databasen. Imidlertid ble varierende korrelasjoner sett i den svenske laboratorie databasen. Vann bindemiddel tallet var den eneste variabelen med tilsvarende korrelasjoner i alle laboratoriedatabasene.

Gradient Boosting og Random Forest modeller ble laget ut ifra de ulike databasene, der 80% av dataene ble brukt til å trene modellene, og de gjenværende 20% ble brukt til evaluering. Modellene basert på E6 Kvithammar-Åsen-databasene viste dårlige resultater, mens modellene basert på laboratoriedata fra Norge og Sverige klarte å forutsi den stabiliserte jordens styrke med den beste R^2 verdien på 0,82.

Contents

List of figures

List of tables

Acronyms

DDM	Deep Dry Mixing
UCS	Unconfined Compressive Strength
BRN	Blade Rotation Number
DM	Data Mining
KDD	Knowledge Discovery in Databases
ANN	Artificial Neural Networks
DT	Decision Trees
RF	Random Forest
GB	Gradient Boosting
SVM	Support Vector Machines
MR	Multiple Regression
RMSE	Root Mean Square Error
MAE	Mean Absolute Error
R^2	Coefficient of Determination
R	Correlation Coefficient
KPS	Kalk Pelar Sondering
FOPS	Förinstallerad Omvänd Pelar Sondering
wbr	Water Binder Ratio
wbr_{corr}	Corrected Water Binder Ratio

1 Introduction

1.1 Background

Deep dry mixing is a standard method of soil stabilization in Scandinavia. The technique is called dry because the binder utilizes the existing water in the soil to start the hardening processes. The strength development in the DDM columns is affected by various mechanisms, each consisting of several influencing factors. Spatial variation provides further uncertainty related to the performance of the soil improvement. That is why strict requirements for quality control are required. This applies to the entire execution: Before, during, and after installing the DDM columns.

Large amounts of data from both unstabilized and stabilized soil were obtained from the E6 Kvithammar-Åsen project. The data included both CPTU and laboratory readings and the measured shear strength of the stabilized columns. Since the executive parameters from the installed columns were relatively similar, this provides a reasonable basis for investigating the relationship between in-situ soil properties and the properties of the stabilized ground. Two existing laboratory databases were acquired, one Norwegian and one Swedish. These were established under controlled conditions, making the results more reliable. The databases had only been analyzed using linear methods in previous studies, so there might have been correlations in the data that could be detected by using non-linear methods such as machine learning. With data from three different sources, this provides a reasonable basis for comparison, which means that it may be possible to detect reliable patterns.

1.2 Objectives

The objectives for this master's thesis are provided in Figure 1.1. A statistical approach was used to characterize the apparent correlation among the parameters. Furthermore, data mining techniques were utilized to reveal non-linear correlations.

In addition to the given objectives in Figure 1.1, it will be investigated whether there is a potential correlation between the strength of stabilized soil and the softness or sensitivity of the clay. The given hypothesis suggests that less energy is required for the mixing process, which improves the dispersion of the binder in the column. This can potentially increase strength.

Figure 1.1: Objectives Master's Thesis

1.3 Approach

In this master thesis, data from several DDM databases were used to investigate whether any variables correlate with the stabilized strength of the soil. Two databases were already established and consisted of laboratory-stabilized soils from Norway and Sweden. In addition, two further databases were created. These were based on CPTU and laboratory data from testing of the unstabilized soil from the E6 Kvithammar-Åsen project. The variables in the laboratory databases contained various index parameters and parameters related to the used binder agents. In the CPTU database, there were both normalized and non-normalized CPTU parameters. The laboratory and CPTU database from E6 Kvithammar included depth as a variable.

Both linear and non-linear methods were used to evaluate the correlations with the stabilized strength. These two non-linear methods were Gradient Boosting and Random Forest. Various machine learning models were created based on the different variables in the databases. A permutation importance analysis was conducted to determine which variables were most important for the different models. It was further investigated whether creating reliable models using only individual parameters was possible. These were used as a basis for comparison to see if it was possible to find correlations not captured by the linear methods.

The data was split into two sets, where 80% were used for training, while the remaining 20% were used for validating the models. Different evaluation metrics were used to evaluate the performance of the machine learning models. These were the R^2, Root Mean Square Error (RMSE), and Mean Absolute Error (MSE). The standard Pearson correlation coefficient gave linear correlations ranging from -1 to 1. By squaring these coefficients, they can be compared with the performance of the machine learning models. All machine learning models were evaluated using a 10-fold cross-validation technique.

1.4 Limitations

It can be challenging to predict the shear strength of stabilized soil. Additional uncertainty is associated with the Kalk Pelar Sondering (KPS) and Förinstallerad Omvänd Pelar Sondering (FOPS), two methods used to measure the shear strength of the stabilized soil. They are not optimal approaches for quality control, but they are the only ones available to characterize the

strength of the stabilized soil. Although the analyzes were carried out on different databases, it is not certain that the correlations are transferable to other databases. This applies especially to the databases from E6, where assumptions were made due to challenges with the distance between the data pairs and missing laboratory data. For both E6 databases, interpolating the CPTU and shear strength measurements was done to remove scatter and noise in the data. Nevertheless, it is not certain that all errors have been removed. All data used in this thesis are based on various laboratory and field tests conducted by someone else. It is, therefore, difficult to assess the accuracy and reliability of the testing process and results.

1.5 Structure of the Thesis

The structure of the thesis is given as follows. Section 2 introduces the theory behind DDM columns. The main mechanisms behind the strength development in DDM soils are presented. It also considers quality control and previous studies that have used machine learning to predict the strength of cement-stabilized soil. The literature review continues the work done in the project thesis. The different databases are presented in Section 3. For the E6 databases, it is explained how these were established. Furthermore, Section 4 briefly introduces Knowledge Development in Databases (KDD) and how this was implemented in this thesis. Section 5 shows the results from the different analyses. This section is divided into four main parts, where the different databases are presented in this order: CPTU E6 Kvithammar-Åsen, Laboratory E6 Kvithammar-Åsen, Norwegian and Swedish. The results are compared and discussed in Section 6. The key findings are summarized in the Section 7 where suggestions for further work are given.

2 Literature Review

The literature review is divided into five sections. Section 2.1 provides an introductory presentation of dry soil mixing and how it is performed. Section 2.2 summarizes the strength development mechanisms in stabilized soils. Each mechanism is presented with its influencing factors. Section 2.3 presents the current quality control methods used in the industry. Several studies where data mining has been applied to geotechnical engineering have been compared in Section 2.4. Section 2.5 highlights the literature review's research gaps and outstanding points.

2.1 Installation of DDM-columns

Dry soil mixing is an in-situ ground improvement technique where the soil is mixed with a binder. The method is referred to as "dry" because it involves the utilization of "dry binders," whereas, in wet mixing, a slurry is mixed into the soil. According to [3], dry soil mixing is mainly used to stabilize clay with a shear strength of 5-30 kPa. After stabilization, an improvement in shear capacity can be expected. Dry soil mixing is widely used in Norway and other Scandinavian countries. This is because the soil here is commonly loosely packed and has high water content. It will, therefore, not be necessary to add any extra water to the soil to start the chemical reactions with the binder.

According to [7], deep dry mixing is used to:

- Increase the bearing capacity.
- Lower the compressibility, leading to less settlements.
- Improve the stability of slopes.
- Improve vibration-prone places, such as next to railways.

The mixing is performed by pushing and rotating a drill string down through the soil, with a mixing tool attached at the end. When the mixing tool reaches the design depth, the machine pulls the drill string back toward the surface. At the same time, the nozzles in the mixing tool will open so that the binder is distributed into the soil. This process can be seen in Figure 2.1. The binder used in the stabilization process comes from a material tank. This can either be a separate carriage or a part of the machine.

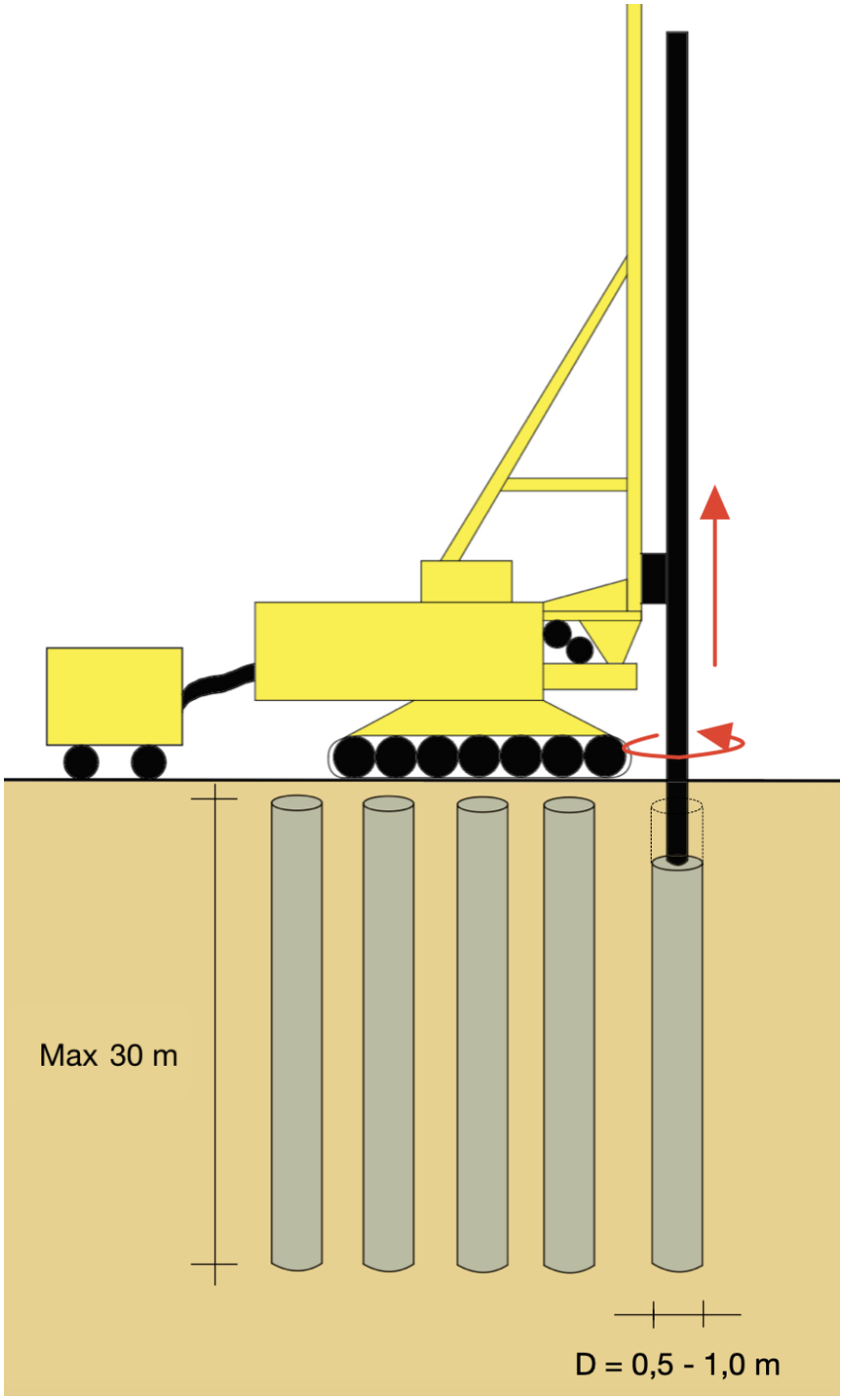

Figure 2.1: Illustration of DDM-column installation, inspired from [3].

In contrast to a similar soil stabilization technique, jet grouting, which can insert several drill strings during installation to increase the depth of the pile, deep dry mixing does not have this option. This means that the length of the drill string will give the column's maximum length. Standard lengths of drill strings are 15 m, 20 m, 25 m, and 30 m. The same applies to the diameter of the column, which is determined by the diameter of the mixing tool. Different mixing tools are used, as seen in Figure 2.2. The standard mixing tool was the first to be used, as illustrated Figure 2.2a. According to [3], it has been shown that it is more effective to use a mixing tool that has wings, shown in Figure 2.2b and Figure 2.2c.

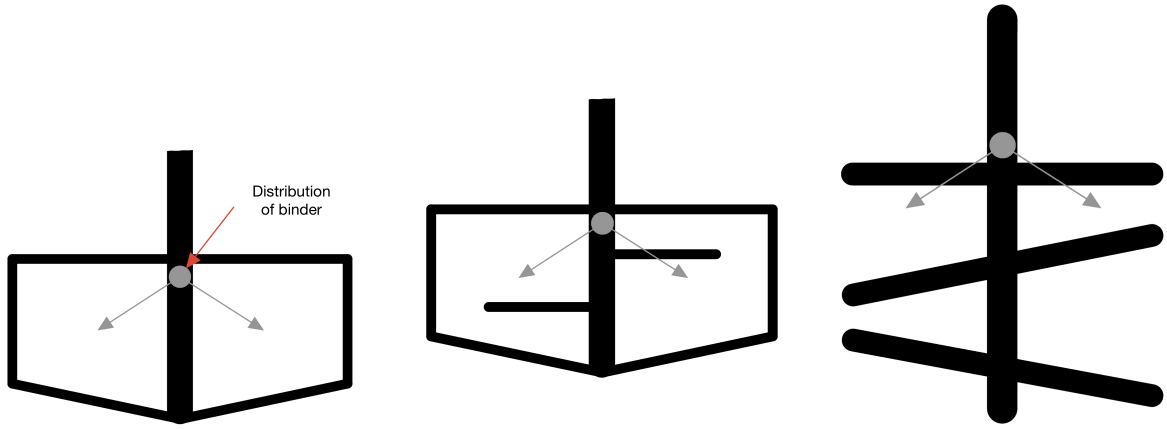

(a) Standard mixing tool **(b)** Standard mixing tool with wings **(c)** Pinnborr

Figure 2.2: Presentation of different mixing tools used for dry soil mixing, according to [3].

Different installation patterns exist for DDM columns, which can be seen in Figure 2.3. In Figure 2.3b, Figure 2.3c, Figure 2.3d, and Figure 2.3e, the columns are overlapped to make them coherent. How much overlap is needed depends on the diameter of the column, which is summarized in Table 2.1. To achieve the overlap between the columns, it is essential that the already installed columns have not hardened too much, as this will cause difficulties in connecting them.

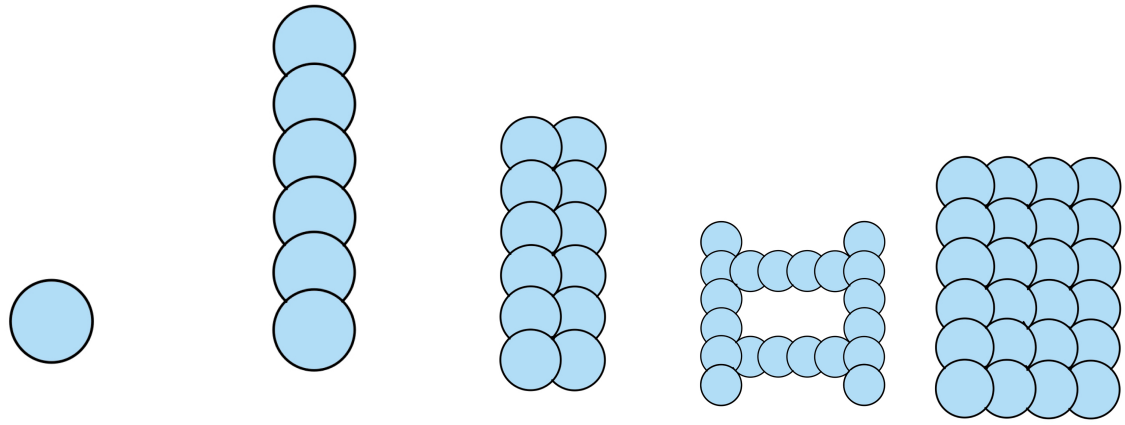

(a) Single column **(b)** Overlapped wall **(c)** Group columns **(d)** Lattice **(e)** Block

Figure 2.3: Illustration of common DDM column installation patterns, according to [3].

Column diameter [m]	Center distance[m]	Overlap [m]
0.5	0.4	0.10
0.6	0.45	0.15
0.7	0.55	0.15
0.8	0.65	0.15

Table 2.1: Recommended values for overlapping columns in continuous patterns, according to [7].

2.2 Strength Development of DDM Soils and Influencing Factors

The strength development in DDM columns is complicated and depends on several processes. [8] has divided this process into four main mechanisms: Characteristics of stabilizing agent, characteristics and conditions of soil, mixing conditions, and curing condition. Each class is then separated into several influencing factors, as seen in Table 2.2.

(I) Characteristic of stabilizing agent	1. Type of hardening agent 2. Quality 3. Mixing water and additives
(II) Characteristics and conditions of soil	1. Physical, chemical, and mineralogical properties of soil 2. Water content 3. pH of pore water 4. Organic content
(III) Mixing conditions	1. Degree of mixing 2. Timing of mixing / re-mixing 3. Quantity of hardening agent
(IV) Curing conditions	1. Temperature 2. Curing time 3. Humidity 4. Wetting and drying / freezing and thawing, etc.

Table 2.2: Factors affecting the strength increase according to [8].

2.2.1 Characteristic of Stabilizing Agent

In DDM, hydraulic binders are used. This means that the binder will be reactive with water. In Norway, three types of binder are typically utilized for DDM: Cement, Lime, and Multicem [3]. Multicem is the product name of Cement Kiln Dust. To get the full benefit from the chemical reactions between the binding agent and the soil, a mixture of cement and lime or cement and Multicem is used. According to [3], before 2005, it was standard to use a 50/50 mix between cement and lime. A mixing ratio of 75/25 of cement and lime was also used in some cases. In recent years, Multicem has been used as a substitute for lime, with a mix of 50/50 between cement and Multicem.

2.2.1.1 Cement

Cement is an essential part of the binder used for soil stabilization. According to [3], cement is usually the main part ($\geq 50\%$) in lime cement stabilization. Ordinary Portland Cement is the most common type of cement. This cement is made by burning limestone. Here, the crushed limestone is exposed to temperatures around 1450 degrees Celsius. The blend is then crushed before it is taken on to a new round of heating. The result of this process is clinker that is then grounded together with gypsum resulting in a cement powder. In Table 2.3, the mineral composition of a cement clinker is summarized, with the approximated content of each chemical component.

Notation	Formula	Name	Approximate content %
C_3S	$3CaO \cdot SiO_2$	Tricalcium silicate	57
C_2S	$2CaO \cdot SiO_2$	Dicalcium silicate	14
C_3A	$3CaO \cdot Al_2O_3$	Tricalcium aluminate	8
C_4AF	$4CaO \cdot Al_2O_3Fe_2O_3$	Tetracalcium aluminoferrite	7

Table 2.3: Mineral composition for cement according to [9]

The chemical reaction between water and cement is called primary hydration. In this reaction, Tricalcium silicate and Dicalcium silicate are central. They are the two most contributing chemical components in cement. Tricalcium is the best of the two since it is the most reactive. This means that it will take less time to set. Even though there are some differences in reactivity, both silicates can be categorized as highly reactive with water and will lead to the formation of cement paste. According to [9], the chemical reactions of the two components are given as Equation (2.1) and Equation (2.2). These equations can be simplified and summarized as shown in Equation (2.3). CSH is a notation for Calcium silicate hydrates, which is responsible for the strength increase in all materials based on cement, like concrete. The increase in strength comes from the cement paste that grows and fills out the voids between the particles, which reduces porosity. This process will typically take from 7-28 days.

$$2C_3S + 6H_2O \rightarrow C_3S_2 \cdot 3H_2O + 3Ca(OH)_2 \tag{2.1}$$

$$2C_2S + 4H_2O \rightarrow C_3S_23 \cdot 3H_2O + Ca(OH)_2 \tag{2.2}$$

$$Cement + H_2O \rightarrow CSH + Ca(OH)_2 \tag{2.3}$$

2.2.1.2 Lime

Lime is produced by burning limestone at around 1200 degrees Celsius. When the lime comes into contact with water, the lime will bind, forming calcium hydroxide. This is described in [9] and is visualized in Equation (2.4). The reaction will happen immediately after initiation, which leads to great heat generation. $Ca(OH)_2$ will not lead to increased strength development, but as seen in Equation (2.5), $Ca(OH)_2$ will increase the concentration of OH^-. This makes the pore water very basic, with a pH of around 13. Such a basic solution provides good conditions for the secondary hardening process. This process is called the secondary pozzolanic reaction and is referred to as the hardening that takes place after 28 days, i.e., long-term hardening. The high concentration of OH^- will dissolve silica and alumina in the soil. These will react with calcium hydroxide, resulting in secondary cementitious products, further increasing the strength of the stabilized soil. This reaction equation is given by [9] and shown in Equation (2.6).

$$CaO + H_2O \rightarrow Ca(OH)_2 \tag{2.4}$$

$$Ca(OH)_2 \rightarrow Ca^{2+} + 2(OH)^- \tag{2.5}$$

$$2Ca(OH)_2 + Al_2O_3 + SiO_2 \rightarrow C_2AS \cdot 8H_2O \tag{2.6}$$

2.2.1.3 Multicem

Multicem is another binder that is used in Norway. According to [10], it combines cement and CKD (Cement Kiln Dust). CKD is a by-product of the production of cement. To produce cement, many alternative fuels lead to chlorine and sulfur compounds. These are sucked out of the furnace system via a bypass system. Here the compounds will be cooled down, which will cause them to condense. In this solution, a lot of dust comes from the combustion process. This residual product is CKD, which is also called bypass dust. This would have been deposited in the past, but now it is used. This means Multicem will have a lower CO_2 profile than traditional lime cement. Multicem comes ready-made from the factory, where getting different amounts of bypass dust is possible.

2.2.1.4 Differences in Strength Increase due to Different Binders

[11] looked at the differences in the measured unconfined compressive strength obtained with different binders and binder combinations. Large differences were observed in the stabilized strength. The dataset consisted of clays from two places in Sweden, Löftabro, and Linköping. The different clay samples were stabilized with either cement, lime, slag, fly ash, or a pairwise combination. The binder quantity was the same for all samples at 100 kg/m^3. According to [11], it is typical for soils stabilized with cement to gain the most strength in the first three months. After this period, the strength increase will flatten out and move towards a constant value. For lime, on the other hand, the strength will normally not flatten out like for cement, so a long-term increase can be expected. However, this effect will depend on the soil conditions. This is explained in [11], where the clays from Löftabro, stabilized with lime, got a greater long-term increase in strength compared with the clays from Linköping, which did not get the same strengthening development.

2.2.2 The Impact of Unstabilized Soil Properties on Stabilized Ground Characteristics

2.2.2.1 Unstabilized Shear Strength of Soil

The undisturbed shear strength of the soil to be stabilized greatly impacts how effective the DDM will be. Less energy is required to stabilize low-strength soil compared to high-strength one. This is because it is more difficult to erode a strong type of soil sufficiently, facilitating good conditions for the spread of binder. According to [3], the non-stabilized soil's optimal in situ shear strength is between 5-30 kPa. When the shear strength exceeds 30 kPa, more mixing work will be required to ensure the same result as the weaker soil types.

In [12], the correlation between the shear strength in stabilized and unstabilized soil was examined. This was done by performing column penetration tests 12-16 days and 26-34 days after executing. This analysis showed that the shear strength of the stabilized and unstabilized soil was mainly dependent on the in-situ stress. When the results were corrected for the effect of the depth and the in-situ stress, the results showed no correlation between the stabilized and unstabilized soil.

2.2.2.2 Atterberg Limits

In the article [13], it was looked at the stabilization of soft clay or silt with lime and cement. It is explained that there is a connection between the relative increase in shear strength of the stabilized soil when the plastic limit is lowered. There was also a connection between increased optimum lime and cement content with increased water content and plasticity index of the unstabilized soil.

In Table 2.4, the linear correlations between the Atterberg limits and the ultimate compressive strength are summarized. Except for the plastic limit from [14], all results show a negative correlation. However, these correlations may not be valid for Norwegian ground conditions. This is because the cited articles in Table 2.4 are based on soil samples from Australia and Portugal. These countries have a completely different climate than Norway, with a different geological history. The number of data points in the different correlation analyses varies between 55-197. It is possible to get meaningful insight with valid results based on these data points. However, with only a limited number of values, this can lead to insufficient variation, making the results unrepresentative.

Refrence	Correlation with UCS			Data Point Count
	w_L	w_P	I_P	
Tran, 2022 [14]	-0.27	0.16	-0.34	197
Tinoco, 2021 [15]	-0.59	-0.53	-	121
Das, 2011 [16]	-0.50	-	-0.55	55

Table 2.4: Correlation between Atterberg limits and UCS.

2.2.2.3 Water Content

The initial water content of the soil has a major impact on the compressive strength of the stabilized soil. According to [17], a high initial water content will lead to a drop in ultimate compression strength compared to stabilized soil with similar properties except for lower water content. Increasing initial water content reduced the unconfined compressive strength for any given cement content. This also applies to Norwegian soils. Nevertheless, the water content must not be too low, resulting in insufficient water for the chemical processes between the binder and the soil. [3] states that an initial water content under 30%, in combination with high strength and low sensitivity, requires thorough follow-up of the mixing work to ensure that the stabilized column becomes homogeneous.

In Table 2.5, the linear correlation between the water content and the ultimate compressive strength is shown. As expected, all the cases show a negative correlation between the variables, but the correlations' strength varies. In [16], the water content showed a limited range from 5-19%. This can be explained by the fact that the soil samples were from Australia, and the warm climate will affect the water content. Conversely, the analyzed soil in [18] was Irish Moss Peat, with a water content ranging from 85-1000%. The last article dealt with soil from Portugal with a water content ranging from 14-113%. One major drawback with these articles is that the analyzed soils are not directly comparable with the Norwegian soil, which typically have a water content of around 20-60%. Further research will thus be needed to verify that these correlations are similar for Norwegian conditions. However, Swedish soils differ from Norwegian soils in that they can have a high organic content with correspondingly high water content. It is possible that

Swedish soils can be compared with [18] since this article explores soils with high water content and organic content. On the other hand, it cannot be guaranteed that the ground conditions are identical since the soil comes from two different countries. There is also a variation in the size of the data sets, from 55-1030 data points. This means there are differences in how much variation in water content the different databases can convey.

Reference	Correlation Water Content and UCS	Count Data Points
Tinoco, 2021 [15]	-0.62	121
Yousefpour, 2021 [18]	-0.09	1030
Das, 2011 [16]	-0.52	55

Table 2.5: Correlation between Water Content and UCS.

2.2.2.4 pH and Organic content

The soil's organic content can affect the soil's degree of stabilization. According to [3], a soil type with an organic content of a few percent needs a larger amount of binder than non-organic soil to obtain the same stabilized strength. Lime can be used to create the basis for the alkaline environment by making sure the pH is high enough. Once this is ensured, a further increase in the amount of lime will have little effect on the stabilization of the soil. The most effective binder for such soils is cement. [19] explains that this reduction in strength comes from the fact that there is a lot of microbial biomass in the organic content. This biomass activates decomposition rates when the soil is mixed with lime, which reduces the pore water's pH. The concentration of OH^-, determined by the pH, is essential for the secondary pozzolanic reaction. A higher pH, therefore, means better conditions for the pozzolanic reactions, which means an even greater increase in strength. So because the organic material lowers the pH, that results in a reduction in strength.

2.2.3 Mixing Conditions

2.2.3.1 The Mixing Energy

The Mixing Energy, or Blade Rotation Number (BRN), is calculated from the number of blades divided by the retrieval rate. This calculation is shown in Equation (2.7).

$$BRN = \sum Nr.\,blades * \frac{1}{Retrieval\,rate} \tag{2.7}$$

The article [20] states that the BRN plays a significant role in determining the stabilized soil's strength and coefficient of variation. It is stated that an increase in BRN leads to an improvement in strength while the coefficient of variation is lowered. On the other hand, it is not a given that an increase in mixing energy is the best solution for increased strength. [20] believes that an increase in the binder has a more reliable effect on increased shear strength in the soil, as the mixing process is complex.

2.2.3.2 Quantity of hardening agent

According to [21], the minimum binder quantity is the smallest amount of binder that provides a sufficient load-bearing skeleton. Up to this limit value of binder, no soil stabilization will occur. In table 2.6, the recommended quantities of the binder for different soil conditions are listed. The recommendations are more or less the same for all types of soil, except for some types of peat

with high water content, which demand a significantly higher binder content to stabilize the soil sufficiently.

Type of Soil	Type of Binder	Quantity of Hardening Agent $[kg/m^3]$	Remarks
Clay	Cement / Multicem	90 - 120	
	Cement / Lime	90 - 120	
Silty Clay	Cement / Multicem	75 - 110	If the silt content increases, increase the proportion of cement
	Cement / Lime	75 - 110	
Sensitive Clay	Cement / Multicem	80 - 110	
Peat	Cement / Lime	80 - 110	
	Cement	100 - >300	
	Cement / Multicem	100 - >300	Cement >75 %

Table 2.6: Recommended quantities of the binder for different soil conditions according to [3].

Due to a large climate footprint when producing the binder, it is desirable to be able to reduce the quantity. In [4], this was studied. The way this was done was to calculate the CO_2-equivalent per unit of shear strength. The lowest CO_2-eq/τ_{max} was found with a binder quantity of 30-50 kg/m^3. This interval was based on laboratory and field tests and is the lowest quantity that can be used without affecting the practical areas of use. If the binder content is lowered by more than 30 kg/m^3, this may lead to difficulties in the practical installation of the columns in the field.

2.2.4 Curing Conditions

2.2.4.1 Curing Temperature

The normal temperature of the soil in Scandinavia is around 8°C. This low temperature means the reaction between the cement and the soil particles will be slow. However, the reaction between lime and the soil particles will be slower. When the binder is mixed with water, an exothermic reaction is created, which leads to a high heat generation and an increase in the soil temperature. According to [9], cement can increase the soil temperature by around 5-10°C, whereas lime can increase the soil temperature by around 40-50°C. At its maximum, the lime can raise the temperature locally in the soil to up to 100°C. [22] describes the temperature increase as an accelerator to the hydration process, which thus leads to a higher strength. The high temperature causes a large concentration of reaction products from the cement to form. Furthermore, heat causes water to evaporate, accompanied by a lower water content, which in turn causes the pozzolanic reactions to start. According to [23], soil samples with different ages of up to 28 days and with different curing temperatures from 0-30°C was examined. These had an approximately linear correlation between the unconfined compressive strength and the curing temperature.

In [21], the difference in the curing temperature between laboratory and field testing is discussed. Since there is a difference in the temperature in the ground and laboratory, this results in a difference in reaction speed. This applies especially to the pozzolanic reactions, which are particularly dependent on temperature. At a temperature of ∼20°C in the laboratory compared to a temperature of ∼8°C in the ground, a more rapid increase in strength can be expected from the laboratory tests with binders containing lime.

On the other hand, the small laboratory samples, usually stored at ∼8°C to mimic the in-situ temperature in the ground, are cooled down much faster than the soil in the field. This is because the DDM columns are much larger than the cylinders used in the laboratory, which means they

will better retain heat. The available heat in the ground will lead to further development in strength.

2.2.4.2 Curing Time

As said in section 2.2.1, the strength development is divided into two phases, first the hydration and the pozzolanic reactions, also called the long-time hardening. This means the strength will continue to develop a long time after the column is performed and will not reach its final strength until months or years later.

2.2.4.3 Curing stress

According to [24], the influence of overburden pressure will increase strength. A linear relationship is described between the stabilized strength and the overburden stress. This is consistent with what is stated in [23], but here it is specified that the unconfined compressive strength only increased with confining stress if the stabilized soil was cured under drained conditions. On the other hand, if the soil had been cured under undrained conditions, a similar increase in compressive strength was not shown.

2.2.5 Water Binder Ratio

As described in the Section 2.2, the strength increase depends on several variables, two of which are the water content and the quantity of the hardening agent. In concrete, it is normal to express the ratio of the weight of the water and cement in the mixed slurry. This relationship is vital to the finished product's strength, durability, and workability. Since DDM columns are often produced using a combination of different binders, it is common to use the designation water binder ratio (wbr) instead. The equation for wbr is defined in [4] and shown in Equation (2.8).

$$wbr = \frac{m_{w,s} + m_{w,a}}{m_b} \tag{2.8}$$

Where:

$m_{w,a}$ = Mass of natural water content in the soil

$m_{w,s}$ = Mass of added water

m_b = Mass of dry binder

It is shown in [4] and [2] that there is a consistent correlation between the shear strength of the soil and the water binder ratio. [25] has formulated an equation for the unconfined compressive strength (q_u) of concrete, which has been found transferable to DDM columns, shown in Equation (2.9).

$$q_u = \frac{A}{B^{wbr}} \tag{2.9}$$

The constants A and B are empirical and will vary depending on many variables. According to [2], these influential variables are everything from the type of soil and binder, how the samples are tested, and the curing conditions. It is further explained in [2] that the expected values for the constant B typically vary from 1.1 to 1.3, although different binding agents, binding

quantities, and soils are used. On the other hand, the constant A will vary based on the unconfined compressive strength.

In Figure 2.4 and Figure 2.5, the relationship between the unconfined compressive strength and the water binder ratio for Swedish organic and inorganic clays is visualized. Here, the constant B is 1.24 for all cases, while the constant A varies from 800 to 2200.

In [4], a similar study has been carried out on the clay in Trondheim. The difference in this article is that the binder content has been corrected based on the content of CaO, which is the active ingredient in lime. The corrected binder quantity is calculated based on Equation (2.10). This further gives the corrected water binder ratio (wbr_{corr}).

$$\alpha_{corr} = \alpha \times K_{CaO,C} \times P_C + \alpha \times K_{CaO,QL} \times P_{QL} \tag{2.10}$$

Where:

α = Binder quantity

$K_{CaO,C}$ = Available CaO in Cement

$K_{CaO,QL}$ = Available CaO in Lime

P_C = Proportion of Cement in the binder

P_{QL} = Proportion of Lime in the binder

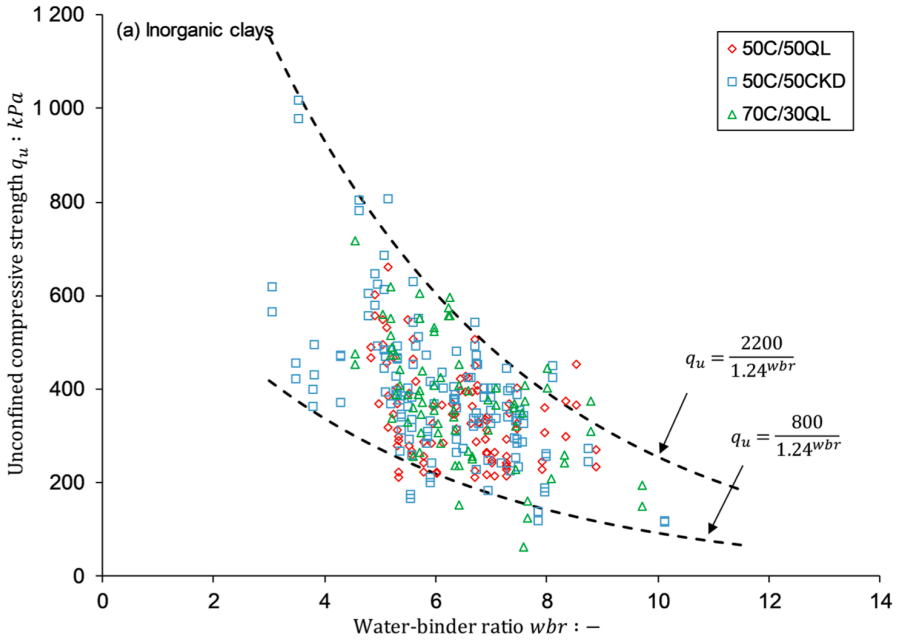

Figure 2.4: Relationship q_u and wbr for Swedish inorganic clays, from [2].

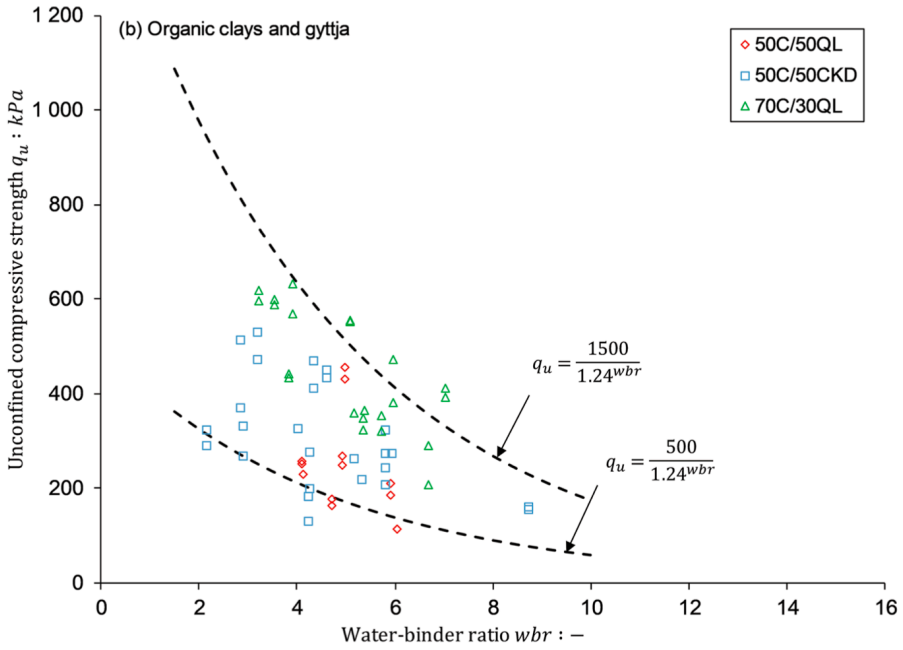

Figure 2.5: Relationship q_u and wbr for Swedish organic clays, from [2].

As seen in Figure 2.6, many different types of binders are used to stabilize the soil from six different sites in Trondheim. All of these are corrected, so they all have the same amount of CaO, meaning the binders will be equally reactive. From this, it is possible to see a consistent trend between the maximum shear strength and the corrected water binder number. This is expressed by the constants A = 950 and B = 1.09.

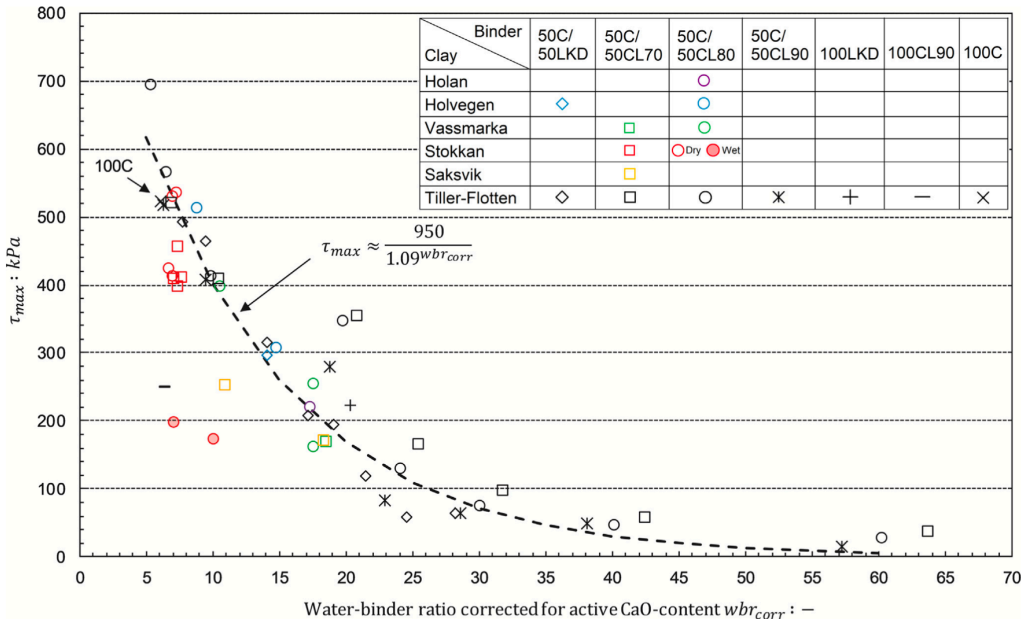

Figure 2.6: Relationship τ_{max} and wbr_{corr} for clays from Trondheim clays, from [4].

2.3 Quality Control

Due to the many factors (execution parameters, in-situ soil properties, curing conditions, etc.), the stabilized soil shows large spatial variations. According to [20], there are differences in what is common practice among engineers when it comes to selecting the nominal values of the stabilized soil's mechanical properties. Some use the average value, while others use a conservative assumption or the lowest value. This can lead to major differences in the various designs. Therefore, quality control is particularly important for DDM columns because it is difficult to determine the actual strength of the column.

The different parts of quality control are described in [20]. The first investigations are carried out on unstabilized soil. This is done to determine if the soil can be stabilized and which binders and quantities should be used. Based on the findings made in the laboratory, a test column can be established. The test column gives a more realistic picture of what mechanical properties can be achieved. If the results are within the design properties, production can start. The entire installation process is monitored and recorded. This data is referred to as the execution parameters. According to [26], the typical parameters are element identification, mixing tool details, mixing depth and time, binder specification and quantity, air pressure, rotation and speed of the drill string during penetration and withdrawal, and BRN. Based on these parameters, information is provided on whether the column has been installed correctly. The last part of quality control is the verification after execution.

2.3.1 Quality verification

Kalk-Pelar-Sondering (KPS) measures the shear strength in DDM columns. The method is similar to CPTU but uses a special probe with two wings, as seen in Figure 2.7. During the process, a probe is continuously pressed down through the column at a consistent speed of 20 mm/s. Simultaneously, the resistance encountered during penetration is carefully measured and recorded. The optimal dimension of the KPS probe is 100 mm less than the diameter of the column. It is common to pre-drill a center hole in the DDM column. This is done to ensure that the probe remains within the column so that the probe does not just follow the weakest path. Even if precautions are taken, there are often challenges with the probe coming out of the column. As a quality assurance of the KPS monitoring, measuring the angle of the probe when pressed down is common. This is done to detect if the probe has suddenly taken an unwanted change in direction. Another advantage of pre-drilling the column is that it will be easier to push the probe down when the column has high strength.

Förinstallerad Omvänd Pelar Sondering (FOPS) is another method to test the DDM columns' shear strength. The difference between FOPS and KPS is that the probe is installed during the execution of the column. Once the DDM column has cured, the probe is carefully extracted by pulling it out from the bottom and upwards. This process is illustrated in Figure 2.7. The problem with the FOPS method is that the steel wire used to extract the probe can affect the mixing process [20]. However, if the probe is installed after the column is manufactured, the results will be more valid.

According to [12], The shear strength (C_u) of the stabilized columns is calculated based on Equation (2.11).

$$C_u = \frac{1}{N_k} \times \frac{Q_{col}}{A_{probe}} \tag{2.11}$$

Where:

Q_{col} = The penetration force from FOPS or KPS

A_{probe} = The horizontal area of the wings of the probe

N_k = The cone factor, normally N_k is set to 10 for soft clays [12]

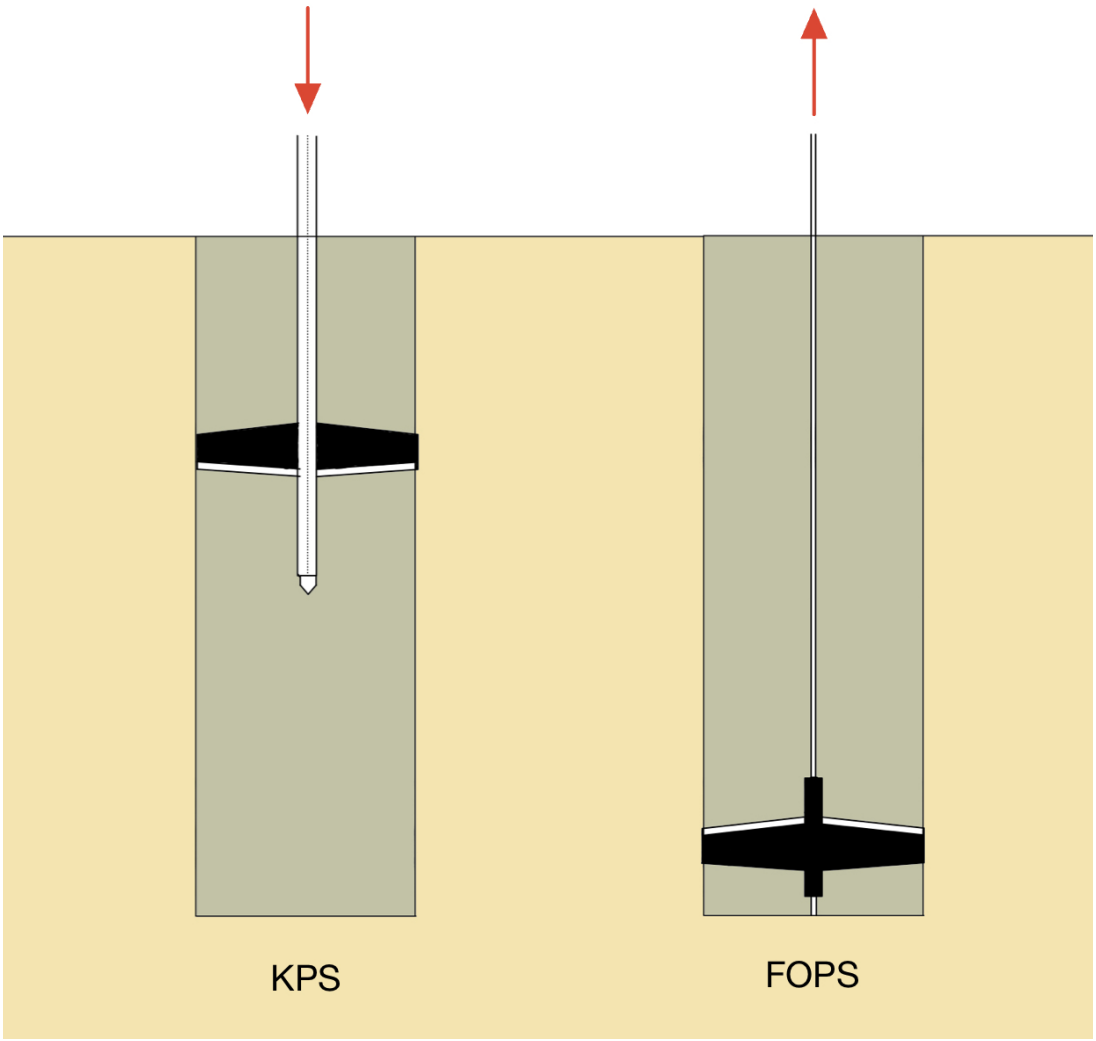

Figure 2.7: FOPS and KPS

2.4 Data Mining Applied to Geotechnical Engineering

Since it is very costly to perform various laboratory and in situ tests, finding other methods to predict the mechanical strength properties to reduce the number of tests is relevant. With the help of machine learning models, attempts have been made to determine various strength parameters.

2.4.1 Prediction of UCS from Laboratory Data

In Table 2.7, the performance of 10 different machine learning models is listed. These models are based on laboratory-stabilized soil from all around the world. Most of the listed studies are based on Australian and Asian soils, but some focus also on European soils. However, no machine learning models have been established on Scandinavian soil. Nor have any models been found that are based on field measurements from KPS/FOPS.

The different models are established to predict the strength of the laboratory-stabilized soil samples. The performance of the models is given in Table 2.7, where the R^2 ranges from 0.65 to 0.97. Based on these findings, it is possible to create well-functioning models that can predict the UCS of the stabilized soil with high accuracy. However, the performance of the models is only this accurate for the given data sets, so it is not certain that the models will be able to provide equally good predictions for unseen data.

Four different Data Mining algorithms have been used: Artificial Neural Networks (ANN), Support Vector Machines (SVM), Decision Trees (DT), and Multiple Regression (MR). The best-performing algorithm from each article is visualized with a red cross. Based on the results from the ten articles in Table 2.7, it may seem that ANN and DT provide the models with the highest R^2.

Reference	Data Mining Algorithm				UCS
	ANN	SVM	DT	MR	R^2
Eyo et al. (2022) [27]	X		X		0.90
Taffese et al. (2022) [28]	X		X		0.65
Tran (2022) [14]			X		0.97
Ngo et al. (2021) [29]	X	X	X		0.93
Taffese et al. (2021) [30]	X		X		0.69
Tinoco et al. (2021) [15]	X	X	X	X	0.95
Yousefpour et al. (2021) [18]	X			X	>0.9
Wang and Al-Tabbaa (2013) [31]	X				0.93
Das et al. (2011) [16]	X	X			0.92
Tinoco et al. (2011) [32]	X	X		X	0.94

Table 2.7: Summary of the R^2 of machine learning models from 10 different articles. The red cross represents the algorithm with the best performance. The abbreviations used: ANN = Artificial Neural Networks, SVM = Support Vector Machines, DT = Decision Trees, and MR = Multiple Regression.

In Table 2.8, the training features and the number of data points for the established models are summarized. The term training features are referred to the selected attributes used to train the machine learning model. As seen, most models are built on quite unique features, making most models not so user-friendly. However, in [30] and [28], the models are based on data from standard index testing. This is convenient as getting the features needed to use the models is relatively easy. However, these are the models with the lowest performance. This can be explained by the fact that the used training data have been obtained from soil samples worldwide.

Reference	Training Features	Count
Eyo et al. (2022) [27]	Liquid limit Plastic limit Plasticity index Curing duration Values of agro-based pozzolans Cementitious additives Soil class Strength class	392
Taffase et al. (2022) [28]	Liquid limit Plasticity index Plastic limit Soil Cement Lime Optimum moisture content Maximum dry density	162
Tran (2022) [14]	Liquid limit Plastic limit Plasticity index Linear shrinkage Clay content Sand content Gravel content Lime content Cement content Asphalt content Optimum moisture content Maximum dry density	197
Ngo et al. (2021) [29]	Soil type Water content Wet density of soil The soil sampling depth Cement content Specimen diameter Specimen length Specimen area Specimen volume Mass of specimen Density of specimen Curing condition Curing period Type of cement	216

Taffase et al. (2021) [30]	Liquid limit Plasticity index Plastic limit Soil Cement Lime Optimum moisture content Maximum dry density	190
Tinoco et al. (2021) [32]	Sand content Silt content Clay content Organic matter content Liquid limit Plastic limit Water content Cement content Cement dosage W/C ratio Age Length of the fiber Fiber content Fiber dosage Tensile strength of the fiber Deformability modulus of the fiber	121
Yousefpour et al. (2021) [18]	Organic content Water content The ratio of Portland Cement The ratio of Blast Furnace Slag The ratio of Pulverized Fuel Ash The ratio of Lime The ratio Magnesium Oxide The ratio Gypsum The quantity of binder Grout to soil ratio W/C ratio Sample size (diameter to height ratio) Age Temperature Relative humidity Carbonation	1030

Wang and Al-Tabbaa (2013) [31]	Gravel content Sand content Silt content Clay content Water content Liquid limit Plastic limit Plasticity index Liquidity index W/C ratio Curing time Curing stress	219
Das et al. (2011) [16]	Liquid limit Plasticity index Clay content Sand content Gravel content Water content Cement content	55
Tinoco et al. (2011) [32]	W/C ratio Type of cement Strength class of cement Cement dosage Age Specific weight of the sample Water content Sand content Silt content Clay content Organic matter content	175

Table 2.8: Comparison of training features with the corresponding number of data points. All models predicted the UCS and were based on soil stabilized, which were mixed and cured in the Laboratory.

2.4.2 Prediction of UCS from CPTU Data

Regarding the prediction of UCS from CPTU data, this is not as explored as for laboratory data. In [33], various combinations of CPTU data and their ability to predict the undrained shear strength of unstabilized soil were explored. The algorithm was Random Forest, and the database contained 250 data points. The best fit was found when combining the original CPTU parameters (q_c, f_s *and* u_2) with the depth. The R^2 value for this combination was 0.93, and even alone q_c managed to obtain an R^2 value > 0.8. The combination that included the normalized CPTU parameters (Q_t, F_r *and* B_q) showed a lower performance, with a maximum R^2 value of around 0.7.

2.5 Summary literature review

The literature review shows that in-situ parameters can significantly impact the quality of the stabilized soil. Ten studies were found where machine learning models were established based on laboratory mixed soil, which occurred under controlled conditions. However, it was not found any studies that were based on field data. There is no guarantee that a model based on laboratory data is comparable to what can be expected in the field. Therefore a model based on field data would have more industrial value because field conditions are highly variable and uncertain. Furthermore, no models have been found that are based on soil from Scandinavia.

3 Presentation of the Databases

In this chapter, the three sources of data are presented. Section 3.1 starts with a presentation of the E6 Kvithammar-Åsen project. An overview is given of the various tests that have been performed and how these are geographically located in relation to each other. Then follows the method for systematizing the KPS/FOPS, CPTU, and laboratory data into databases. In Section 3.2 and Section 3.3, the Norwegian and Swedish databases are presented. These databases were already established, but minor changes were made to make the data more usable for machine learning. Additional calculated variables were also introduced in the Norwegian database to provide a basis for comparing all databases.

3.1 E6 Kvithammar-Åsen

E6 Kvithammar-Åsen is a significant project to create a new transport corridor between Stjørdal and Åsen, which, as shown in Figure 3.1, is just north of Trondheim Airport. A new four-lane motorway with an estimated length of about 19 km is planned. Due to poor soil conditions, DDM columns have been utilized. 107,667 columns have been installed, corresponding to 1,315,268 meters in total length. As seen in Figure 3.1, five areas are marked. Tests have been carried out on the stabilized and unstabilized soil in the same construction sites. The data was gathered from several different tests, including 167 KPS or FOPS tests, 33 CPTU tests, and numerous laboratory tests performed on unstabilized soil samples obtained from 14 distinct locations.

The columns were designed with a BRN > 250 and a binder dosage of 50 kg/m^3. The used binder was a 50/50 mixture between standard cement FA CEM II and lime CL 70 Q. The diameter of the columns in P1, P9, and P11 was set to 0.8 meters, while in P3 and P7, it was 0.6 meters. The overlapping columns were done in the same shift to ensure that the columns were overlapped.

The shear strength testing of the stabilized columns was performed using KPS and FOPS tests. The top layer of soil above the columns was first excavated when carrying out the KPS. Then the columns were pre-drilled to provide a path for the probe.

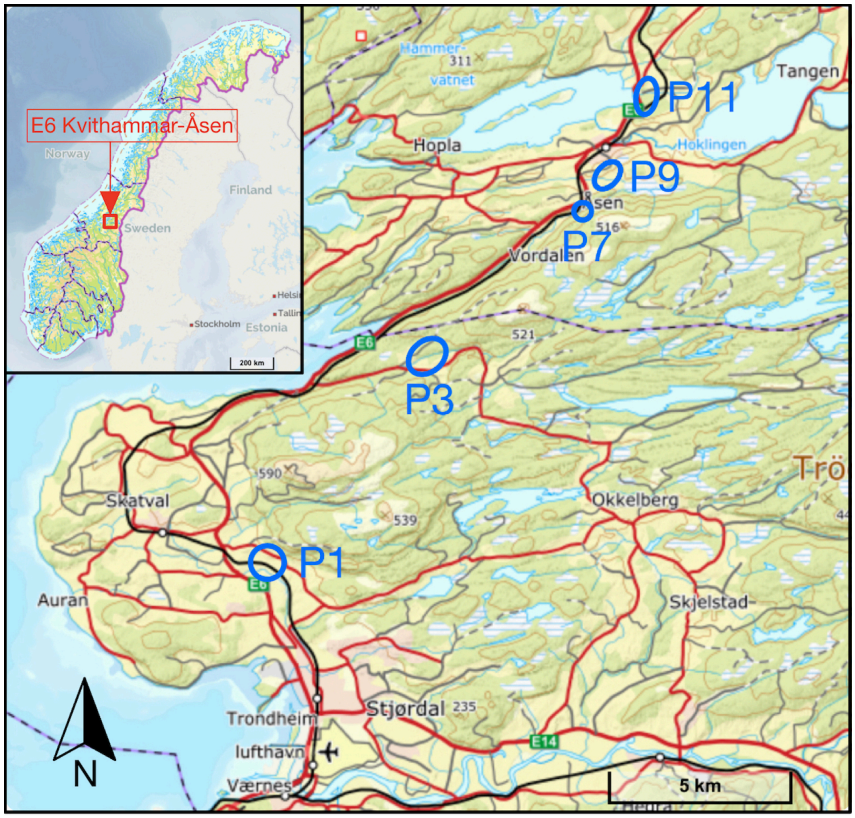

Figure 3.1: Location of the project site in Norway.

3.1.1 Presentation of the Five Areas

In Table 3.1, the essential soil parameters are listed. As seen, the various parameters have more or less the same range. However, this does not apply to the sensitivity in areas P3 and P7, which were much higher than in the other areas. Furthermore, area P11 had a higher water content. The following subsections will present the different areas in more detail. The shear strength of the stabilized columns is visualized as clusters, which are calculated based on the coordinates of the columns. This is done to display all columns in a more orderly way.

Parameter	Unit	P1	P3	P7	P9	P11
Intact shear strength	kPa	10-53	9-44	4-51	5-51	4-30
Remoulded strength	kPa	3-12	0.1-6	0.1-9	0.3-15	0.4-7
Sensitivity	-	3-11	5-440	4-210	1-28	2-40
Water content	%	25-39	23-44	23-32	22-38	28-59
Liquid limit	%	29-46	22-35	20-30	23-33	23-51
Plastic limit	%	18-22	17-22	14-18	6-20	15-23
Unit weight	kN/m^3	19-20	18-22	19-20	18-20	17-20

Table 3.1: Soil conditions in the different areas in E6 Kvithammar-Åsen.

3.1.1.1 P1 Kvithammar

In area P1 Kvithammar, there are a total of:

- 18 KPS
- 7 CPTU

- 1 Laboratory test point

This area is flat, with slight variations in soil conditions. The map over the area, Figure 3.2, shows that the stabilized columns are relatively close to the laboratory test point and some CPTUs. Although the remaining CPTUs are well away from the stabilized columns, they have similar measurements. All laboratory tests and CPTU readings for area P1 are visualized in Section A1.

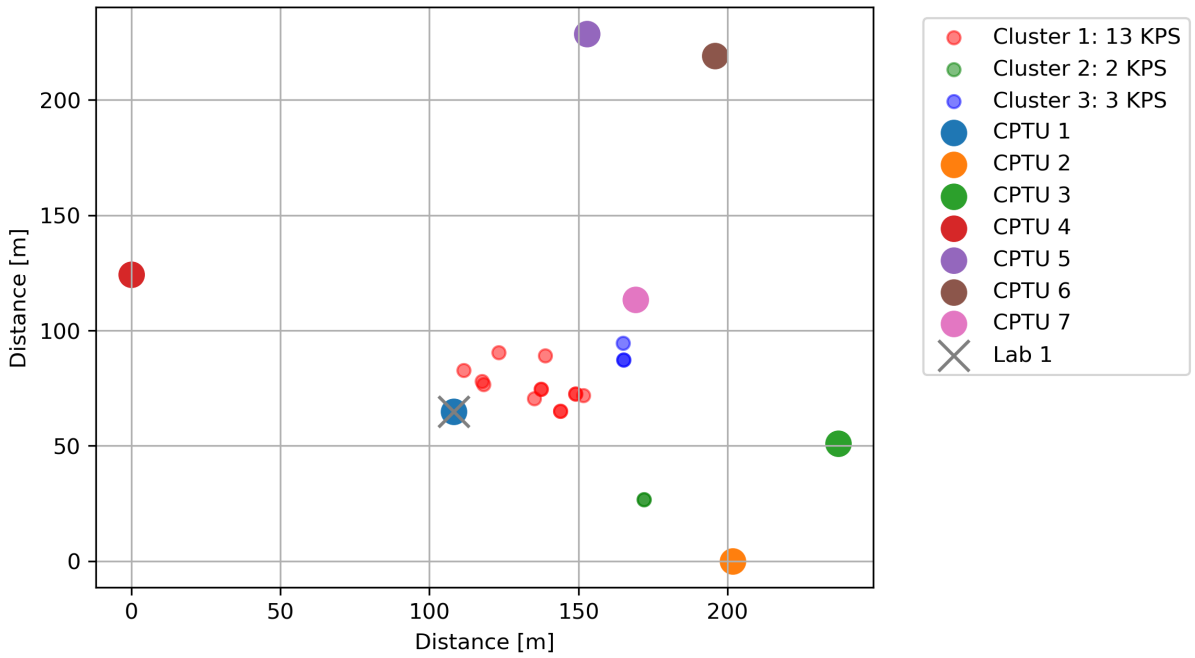

Figure 3.2: Map over area P1.

It is possible to see a correlation between the columns' shear strength and the unstabilized clay's index parameters. Figure 3.3a shows a marked reduction in shear strength from the top of the column down to an elevation of around 34 meters. With further reduction in elevation, the shear strength increased. The maximum water content, the water limit, and the plastic limit are all found at the same elevation, where the cluster indicates the lowest strength. When these index parameters are lowered, a corresponding increase in strength is seen.

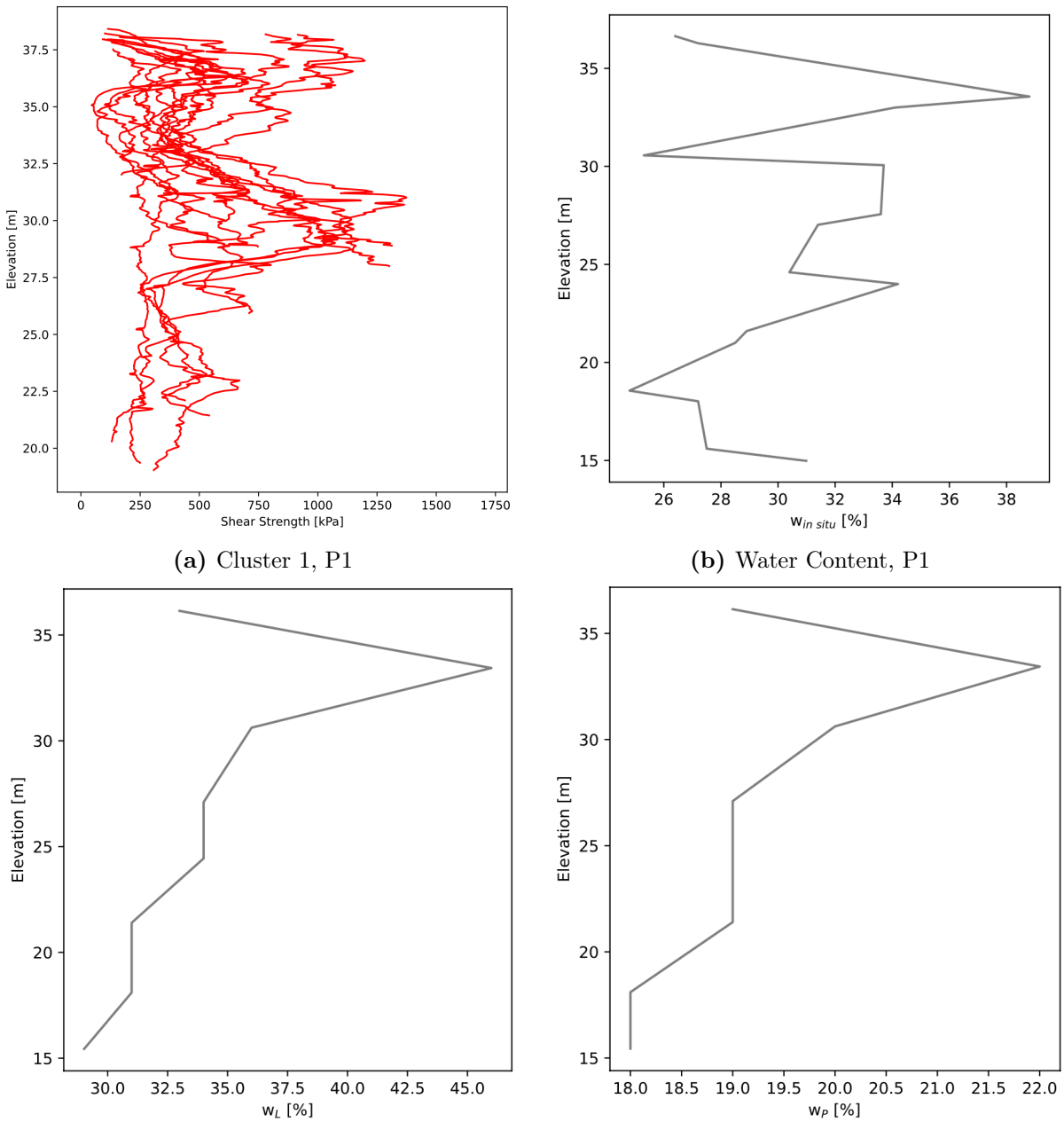

(a) Cluster 1, P1

(b) Water Content, P1

(c) Water Limit, P1

(d) Plastic Limit, P1

Figure 3.3: Correlation between column strength and index parameters in area P1.

3.1.1.2 P3 Langsteindalen

In area P3 Langsteindalen, there are a total of:

- 12 KPS
- 24 FOPS
- 9 CPTU
- 4 Laboratory test points

Of all the sites, P3 is the only one that has used FOPS. This was used due to problems excavating the top layer of soil above the columns. Compared to area P1, there is a more significant variation in elevation, soil conditions, and distance between the various tests. There is around 10 meters

difference between the highest and the lowest point and a distance of approximately 300 meters between the outermost stabilized column and its closest laboratory test point. However, there is a relatively small distance between the CPTUs and the stabilized columns. The CPTU data is highly variable for the area. The laboratory tests carried out in the center of the site (Lab 1, Lab 2, and Lab 4 from Figure 3.4) show soils with a sensitivity of over 400. In contrast, the soil from laboratory test 3 in the area at the bottom left in Figure 3.4 only has a sensitivity of around 50. The shear strength measurements of the columns in the same clusters seem consistent for the different groups. All plots are given in Section A2.

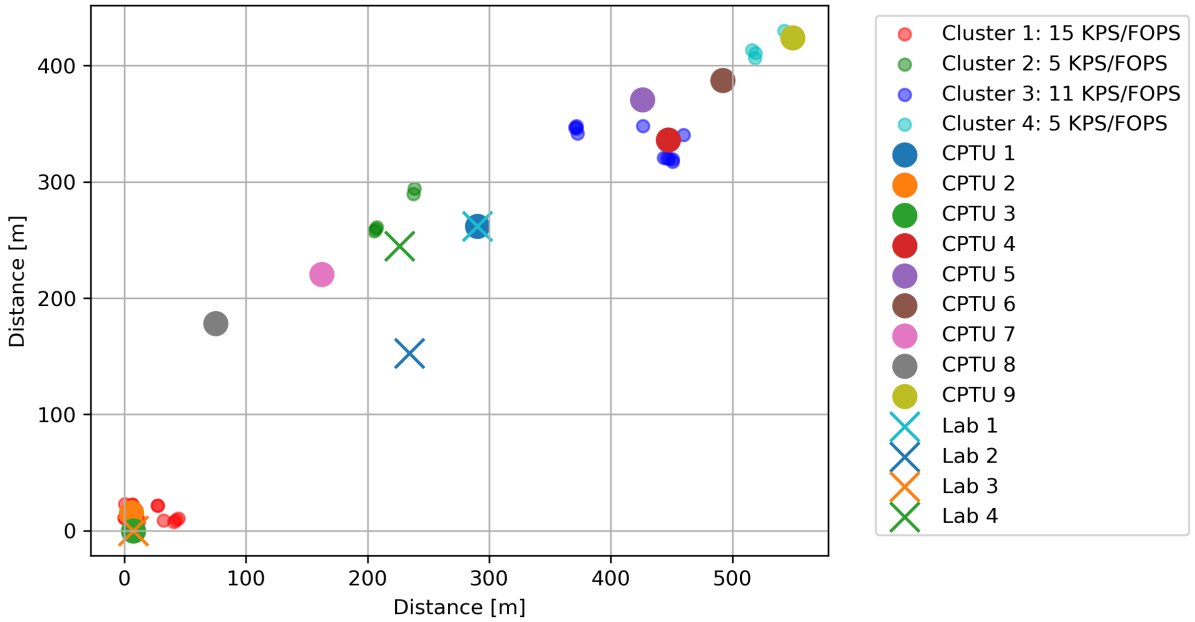

Figure 3.4: Map over area P3.

3.1.1.3 P7 Kleiva

In area P7 Kleiva, there are a total of:

- 39 KPS
- 7 CPTU
- 3 Laboratory test points

In Figure 3.5, the area is presented. In general, there is a slight variation in elevation. The measurements from the CPTU tests show some variation toward the depth, but they seem to follow the same trend. As seen in Table 3.1, there is little variation in the laboratory data, apart from the sensitivity. Laboratory tests 2 and 3, located at the top right in Figure 3.5, have a sensitivity of over 200. On the other hand, the sensitivity of laboratory test 1 is around 80. The different clusters show relatively clear trends in shear strength. However, this does not apply to clusters 1 and 4, where there are more significant deviations. See Section A3 for all the plots of the various data.

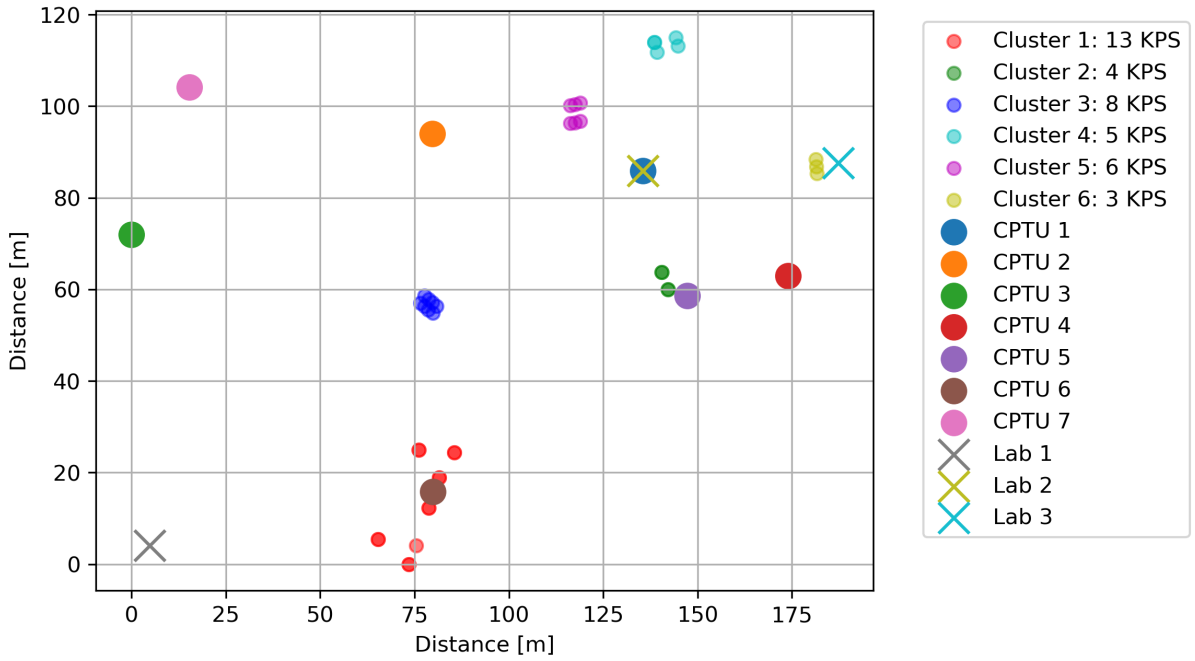

Figure 3.5: Map over area P7.

3.1.1.4 P9 Stokkan

In area P9 Stokkan, there are a total of:

- 37 KPS
- 7 CPTU
- 4 Laboratory test points

An overview of area P9 is given in Figure 3.6. As for area P3, there are challenges in terms of elevation. The difference in elevation for the various tests is shown in Section A4. Of the seven CPTUs, only one is comparable to the entire length of the stabilized columns. The remaining ones can only be compared with the deepest shear strength measurements. There are notable differences in the CPTU data, with CPTU 7 standing out. Similarly, the laboratory tests are localized at a lower elevation than the stabilized columns, which makes it difficult to create accurate data pairs.

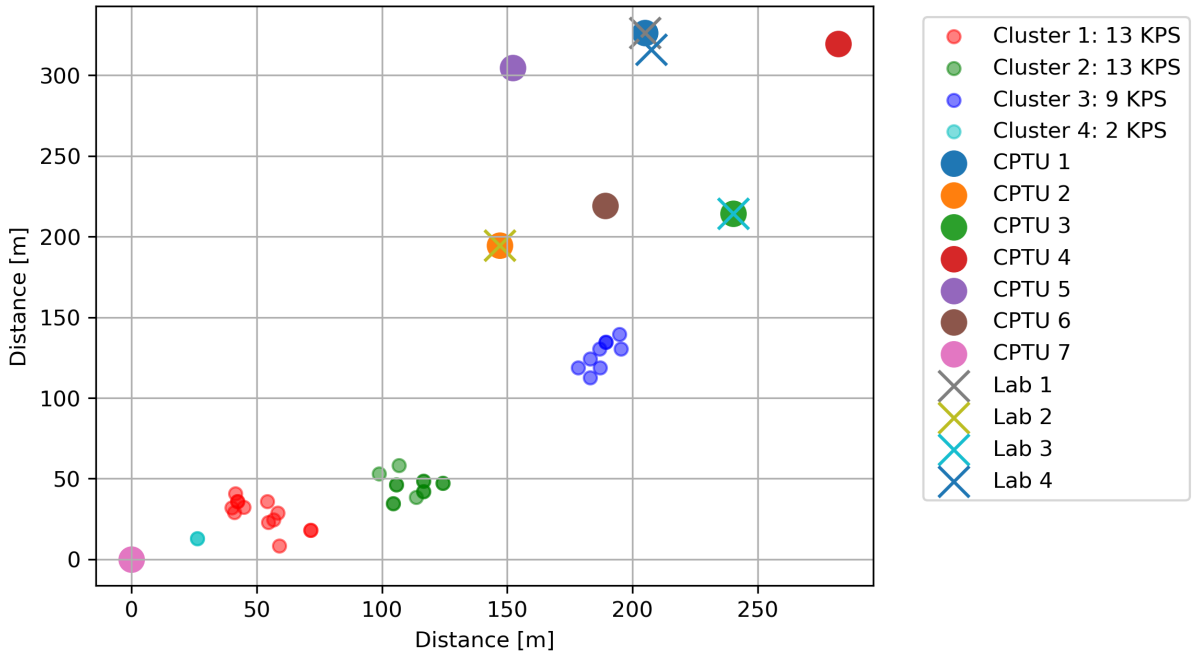

Figure 3.6: Map over area P9.

3.1.1.5 P11 Vassmarka

In area P11 Vassmarka, there are a total of:

- 37 KPS
- 3 CPTU
- 2 Laboratory test points

Area P11 is like P1 and P7, relatively flat, with only a few meters difference in elevation. The shear strength measurements of the different clusters, the CPTUs, and laboratory data all appear consistent with the same trends toward depth. These are shown in Section A5. Unfortunately, the only laboratory tests and CPTUs are conducted near clusters 1 and 2, as depicted in Figure 3.7. Consequently, large distances associated with the remaining clusters could result in uncertainties when comparing them.

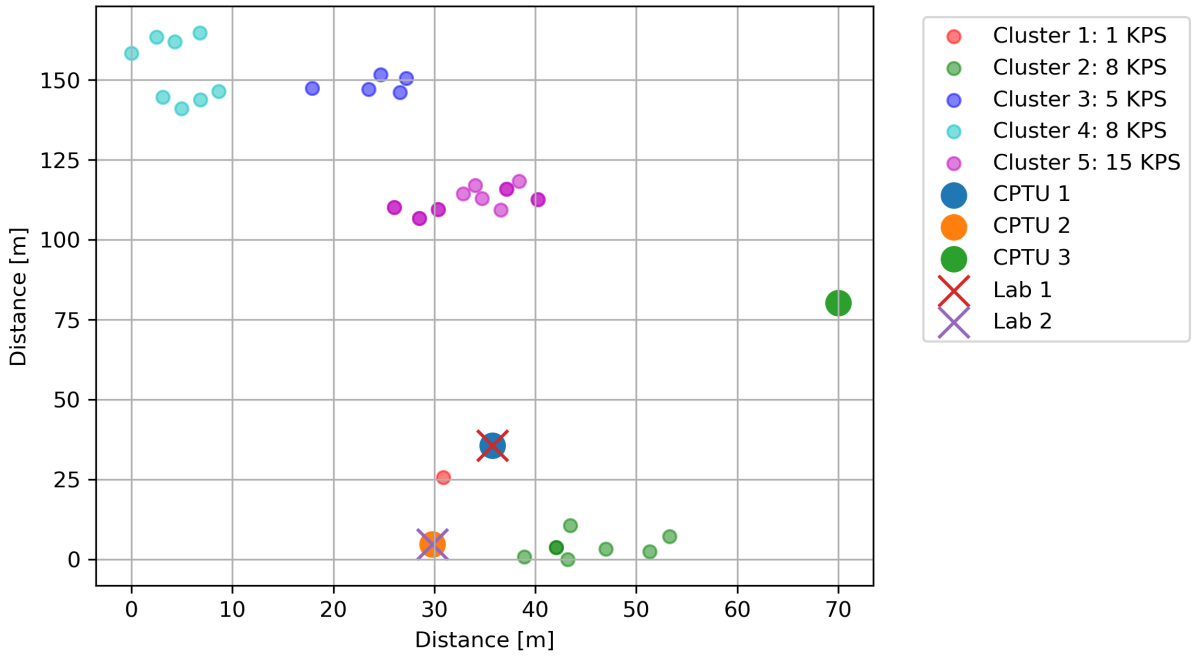

Figure 3.7: Map over area P11.

It is possible to see a correlation between the water content and the shear strength of the stabilized columns in cluster 2. In Figure 3.8, there is a drop in shear strength from the top of the column down to an elevation of around 34 meters. At this elevation, the clay has its highest water content. However, as the water content decreases, there is a corresponding increase in shear strength.

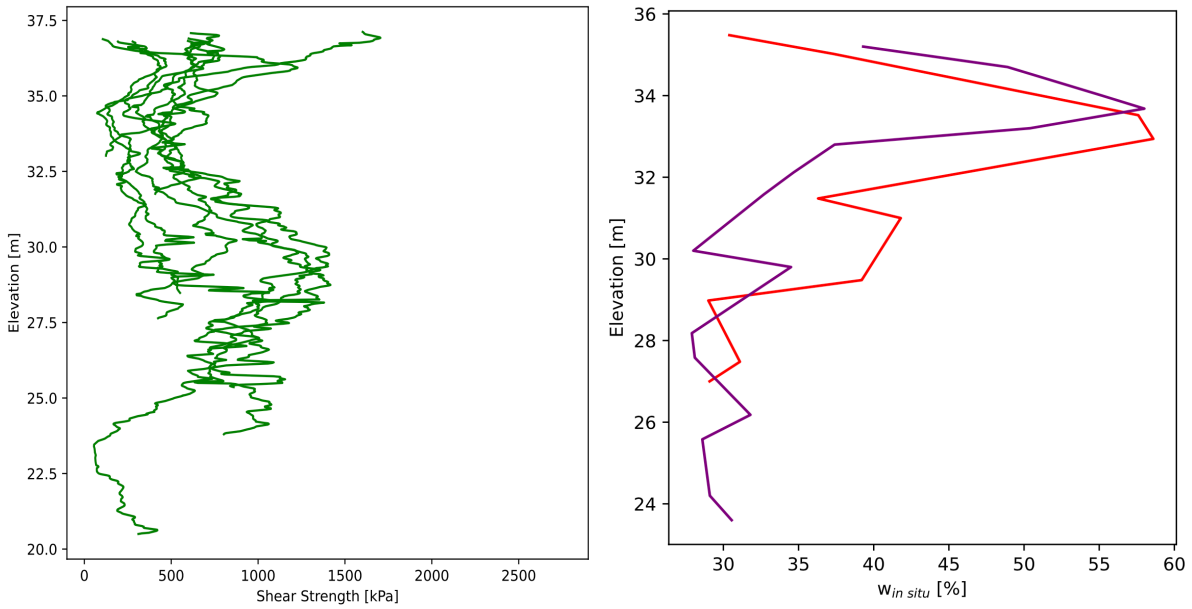

(a) Cluster 2, P11 **(b)** Water content, P11

Figure 3.8: Correlation between column strength and water content in area P11.

3.1.2 Development of the DDM Databases

3.1.2.1 KPS/FOPS Data

The shear strength of the stabilized columns was obtained from 167 FOPS and KPS tests. For each column, values for both depth and shear strength were recorded. All the data in the interval 0-1 meter below the surface were removed. This was done to eliminate outlier values due to the influence of the dry crust. Every single pile was assessed, whether or not the KPS probe had been pushed through the bottom of the column. In situations where this was obvious, where a constant low shear strength was observed, these values were removed. On the other hand, if it was uncertain whether the probe had gone through, the values were retained.

The values from the FOPS testing had to be put in reverse order due to the test starting at the bottom of the column and then being pulled up toward the surface. Another difference between the data from FOPS and KPS was the amount of data points per meter. FOPS gave 100 measurements per meter, while KPS gave half. Because the CPTU data also had measurements every 2 cm, it was decided to reduce the number of readings of the FOPS to the same interval as the others. During the KPS execution, it was first attempted to push down a 500x15 mm probe. Even though all columns were pre-drilled, some still had too high strength to push down the probe. Thus the procedure was changed to a smaller probe of 250x15 mm. To ensure that the smaller probe did not end up in the existing path from the previous attempt, it was rotated 90 degrees.

3.1.2.2 Laboratory Data

There were 14 different locations where laboratory tests were conducted in the E6 Kvithammar-Åsen project. Both cylinder and mini block samples were carried out. The data were given in individual Excel sheets for each specific test for the five areas. All test points contained data from fall cone, water content, and Atterberg limits. Unit weight and uniaxial compression tests were conducted in all points except one from P3 and another from P7. The data from the various areas were put together in databases based on the tests. The corresponding depth of the results was also given in the databases.

The greatest challenge with the laboratory database was the lack of data compared to measurements from KPS/FOPS. Several methods were evaluated to create more data. It was first considered to use the Kriging algorithm, also called the Gaussian process regression, which can be used for interpolation. But this method produced unrealistic trends, and it was difficult to assess which Variogram models were the most correct. Therefore, it was decided to use ordinary linear interpolation between the various laboratory tests conducted within the same borehole. An interval of 2 cm between the new data points was chosen, resulting in the same number of values as for the KPS and FOPS tests.

Based on the interpolated laboratory data, new variables were calculated. These new variables were:

- The Liquidity Index
- Porosity
- The Corrected Water Binder Ratio

The Liquidity Index (I_L) was calculated using Equation (3.1).

$$I_L = \frac{w - w_P}{w_L - w_P} \ [-] \tag{3.1}$$

Where:

w_P = Plastic limit [%]

w_L = Liquid limit [%]

w = Water content [%]

The porosity (n) was calculated using a slightly modified equation from [34]. The porosity is given by the pore volume divided by the soil sample's total volume, which is seen in Equation (3.2).

$$n = \frac{V_p}{V} = 1 - \frac{\rho_b}{\rho_s(1 + \frac{w}{100})} \ [-] \tag{3.2}$$

Where:

V_p = Volume of pores [m^3]

V = Volume [m^3]

ρ_b = The bulk density [g/cm^3]

ρ_s = The grain density [g/cm^3]

w = Water content [%]

The bulk density and the water content were available data. However, no tests were carried out to determine the grain density, so in the porosity calculation, it was assumed a grain density of 2.75 g/cm^3, which is the typical value for Norwegian clays, according to [34].

The water binder ratio, as seen in Equation (2.8), is given by water content [L/m^3] divided by the quantity of binder [kg/m^3]. The total volume of the natural water content per cubic meter was calculated based on the porosity of the soil. Since there are 1000 liters of water per cubic meter, the amount of water was found by multiplying the porosity by 1000. This product divided by the binder quantity resulted in the water binder ratio. Correcting this variable according to the amount of CaO in the binder is possible. For the correlation analysis, it would not have mattered which of the two versions of the water binder ratio was used. Due to the desire to see if the soil from E6 Kvithammar-Åsen could reproduce the same relationships described in [4], it was decided to use the corrected water binder ratio. This variable is calculated using the corrected binder quantity, which is based on how much CaO the binder has. The binder used in the E6 Kvithammar-Åsen project was 50C/50CL70 with a binder quantity of 50 kg/m^3. This means there was a 50/50 mix between lime and cement, where the lime had an active CaO-content of more than 70 percent. According to [4], Quicklime CL70 typically has a CaO active of $\sim 75 \pm 5\%$. The corrected binder quantity can be calculated using Equation (2.10) according to [4].

The corrected binder content for the E6 project was calculated to be ≈ 44 kg/m^3 found from Equation (3.3).

$$wbn_{corr} = \frac{n \times 1000\,L/m^3}{\alpha_{corr}} = \frac{n \times 1000\,L/m^3}{44\,kg/m^3} \tag{3.3}$$

3.1.2.3 CPTU Data

In total, 33 different CPTUs from the E6 Kvithammar-Åsen project were analyzed. The data were provided as raw data files, so the first step was the interpretation. Based on the CPTU parameters, the normalized CPTU parameters B_q, F_r, and Q_t were calculated. This was done according to the equations Equation (3.5), Equation (3.6), and Equation (3.7). These calculations assumed hydrostatic water pressure with a groundwater level one meter below the surface and a unit weight of the soil of 20 kN/m^3.

$$q_t = q_c + (1 - a) \times u_2 \tag{3.4}$$

$$Q_t = \frac{q_t - \sigma_{v0}}{\sigma'_{v0}} \tag{3.5}$$

$$F_r = \frac{f_s}{q_t - \sigma_{v0}} \tag{3.6}$$

$$B_q = \frac{u_2 - u_0}{q_t - \sigma_{v0}} \tag{3.7}$$

Where:

q_t = Corrected cone resistance [kPa]

q_c = Recorded cone resistance [kPa]

f_s = Sleeve friction [kPa]

u_2 = Total pore pressure in the probe [kPa]

u_0 = In situ pore pressure [kPa]

σ_{v0} = Total vertical overburden stress [kPa]

σ'_{v0} = Effective vertical overburden stress [kPa]

a = Net area ratio of the given probe [-]

Q_t = The cone resistance number [-]

F_r = The friction ratio [%]

B_q = The pore pressure ratio [-]

3.1.2.4 Interpolation and Adjustment of Shear Strength and Depth Values in the Databases

In this master's thesis, a conscious decision was made to use elevation instead of depth values. This was because the analyzed areas were not flat but had varying elevations. These variations would not be captured by using depth below ground, which could have led to misleading results. For each test performed, x, y, and z coordinates were provided. The used z-coordinate referred to the ground surface where the tests were performed. The elevation was calculated by subtracting the different depth values from the z-coordinate. This is shown in Equation (3.8), where a given

test is performed at a ground level of 30 m. In this case, the data at a depth of 20 m would correspond to an elevation of 10 m.

$$Elevation = z - Depth = 30 - 20 = 10\,m \tag{3.8}$$

The next challenge was that the columns had not been tested the same number of days after being performed. This meant the columns with the most curing days had gained the most strength. To consider the effect of curing time, the shear strength for all columns was calculated to be 28 days after execution. [11] has proposed an equation to calculate the strength at 28 days, seen in Equation (3.9). The problem with this equation is that it assumes the columns to have zero strength on day 1, which results in a rapid increase in strength in the first days. Due to the stated reason, it was chosen to use a more conservative formula to calculate the estimated shear strength at 28 days. This is shown in Equation (3.10) and was provided by [35].

$$c_{u(28)} = \frac{c_{u(t)}}{0.3 \times ln(t)} \tag{3.9}$$

$$c_{u(28)} = \frac{0.3 + 0.21 \times ln(28)}{0.3 + 0.21 \times ln(t)} \times c_{u(t)} \tag{3.10}$$

The raw data had challenges related to noise or scatter in the data. This was seen especially in the CPTU data, where the signal was occasionally interrupted by far too-high values. The data from FOPS also had challenges related to noise or scatter, which can be seen in Figure 3.9a. Two different types of techniques were used to reduce the noise in the data: Moving average and moving median. They calculated the average or median over a given window of points that moved through the dataset. For every step this window takes, a new average or median is calculated that smoothes out the data. The KPS and FOPS data have been interpolated using the moving average. A window size of 5-15 data points was used, corresponding to approximately 20 cm. The before and after are shown in Figure 3.9. However, the CPTU data had too much scatter, where the moving average was insufficient. Hence, the moving median was employed as it is less influenced by significant deviations than the average. In Figure 3.10, the originally recorded cone resistance from area P3 is shown with the moving average and median results. As seen in the figures from left to right, the noise is reduced, with the moving median giving the result with the least noise. The window size was the same as for the KPS and FOPS data.

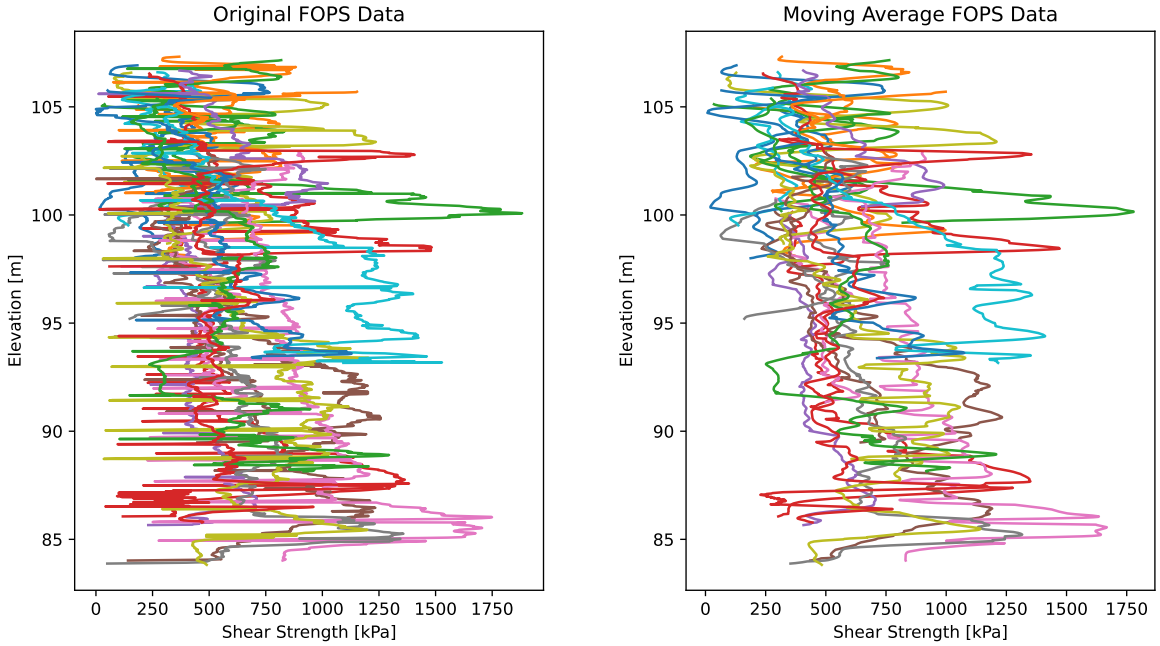

(a) Original FOPS data. **(b)** Moving average.

Figure 3.9: The figures show the difference in the original and the interpolated values, where the noise is decreased.

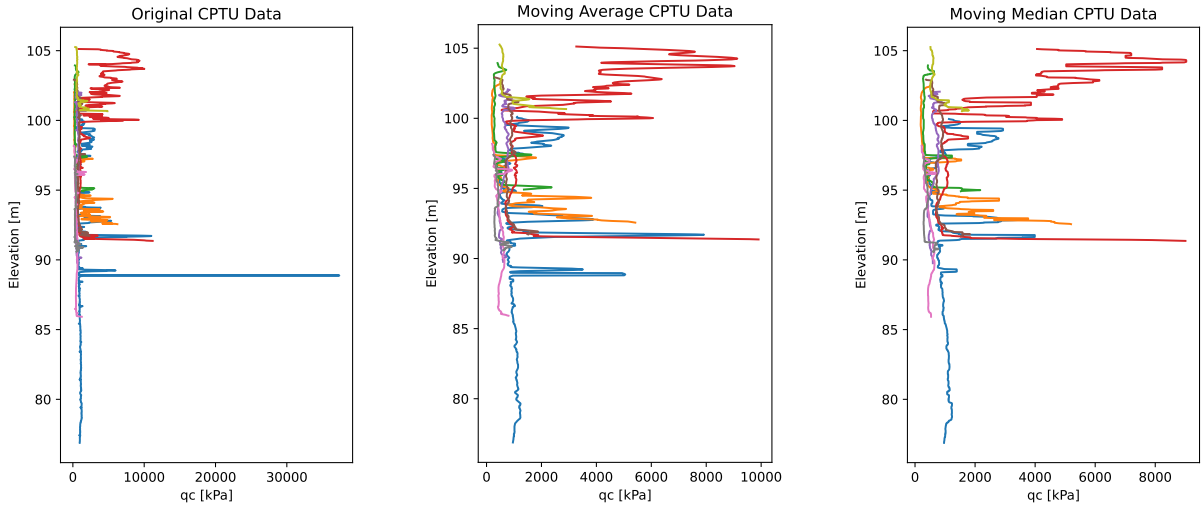

(a) Original CPTU data. **(b)** Moving average. **(c)** Moving median.

Figure 3.10: The figures show the difference between the original and the interpolated values, where the noise is decreased.

3.1.2.5 Completion of the Laboratory and CPTU Databases

The most significant challenge in the analyzed data was that the laboratory and CPTU data were not in the exact same coordinate as the KPS/FOPS data. To make the most reliable pars of data, each KPS or FOPS was assigned the data from the closest laboratory and CPTU test. This process is shown in Figure 3.11. In this case, the shear strength values from the KPS will only be linked with the values from CPTU 1 since its the closest CPTU. The distance (D) has been

found using the Equation (3.11), calculated from the coordinates of the tests.

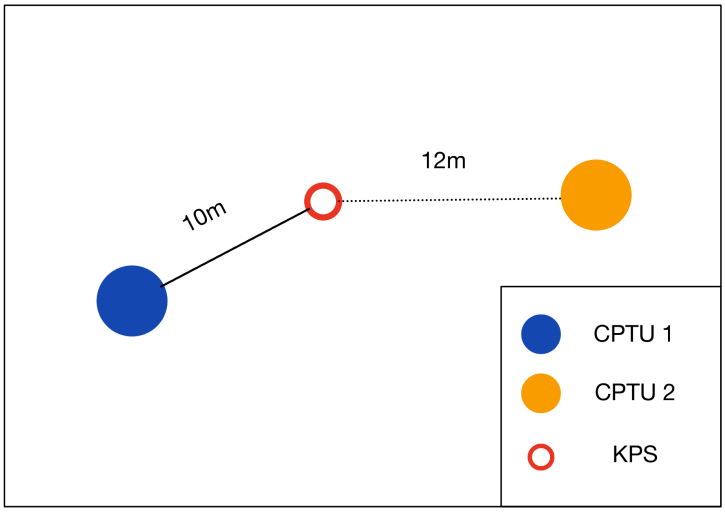

Figure 3.11: The method for selecting which CPTU should be linked with each KPS.

$$D = \sqrt{(x_{(CPTU/Lab)} - x_{(KPS/FOPS)})^2 + (y_{(CPTU/Lab)} - y_{(KPS/FOPS)})^2} \tag{3.11}$$

As seen in Figure 3.12, the distances from the KPS/FOPS to the nearest CPTU varied from 3 m to 133 m. The distances between the KPS/FOPS and the nearest Laboratory test were even bigger. This is seen in Figure 3.13. Here the distances were from 6 m to 300 m. The different colors in the two plots represent each area from the E6 Kvithammar-Åsen project. For the CPTU data, areas P9 and P11 had large distances between the CPTUs and the KPS/FOPS tests, whereas, for the laboratory data, areas P3 and P9 were the areas with the largest distances. The cumulative distribution function is the total for all areas in both plots. In Figure 3.12, it can be seen that around 50% of the data had distances less than 30 m. The distance had to be increased to just over 50 m for the same percentage share of laboratory data. Even if there were large distances between some of the data pairs, a large proportion of data were reasonably close to each other.

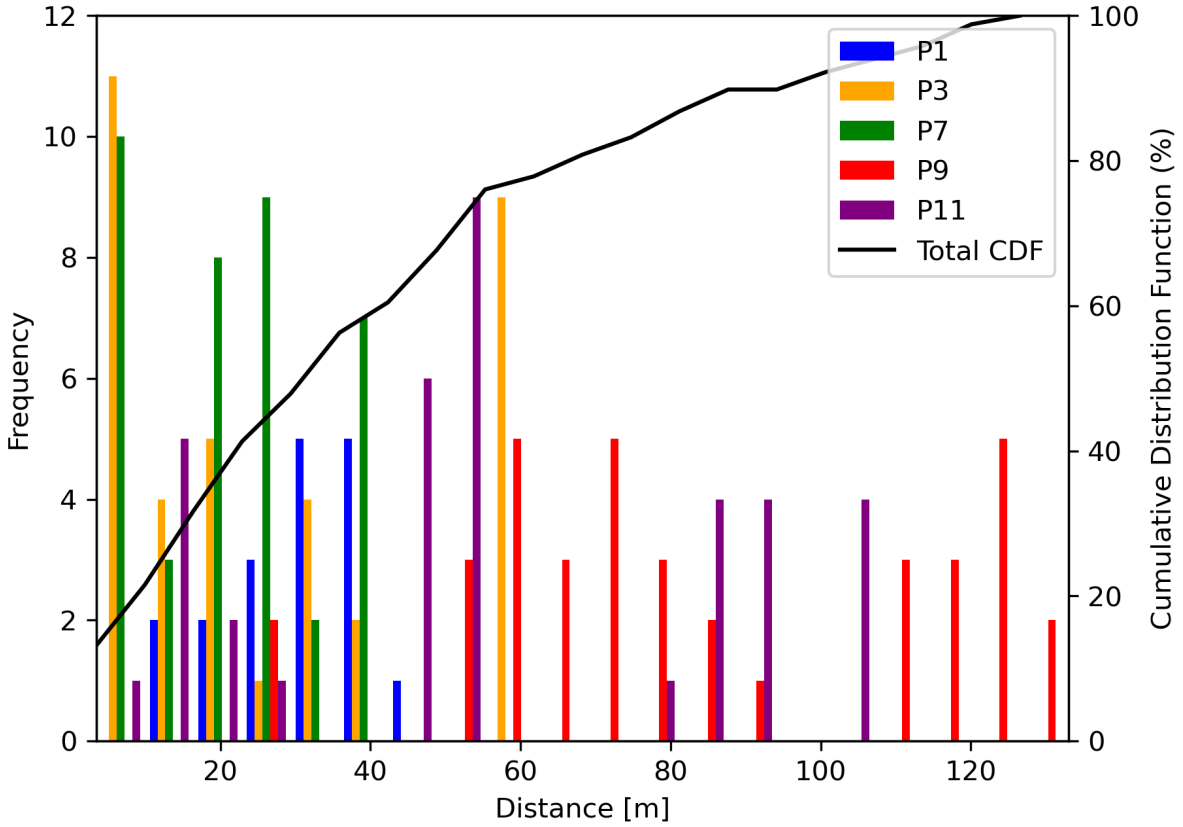

Figure 3.12: The distance between the CPTUs and the nearest KPS/FOPS test.

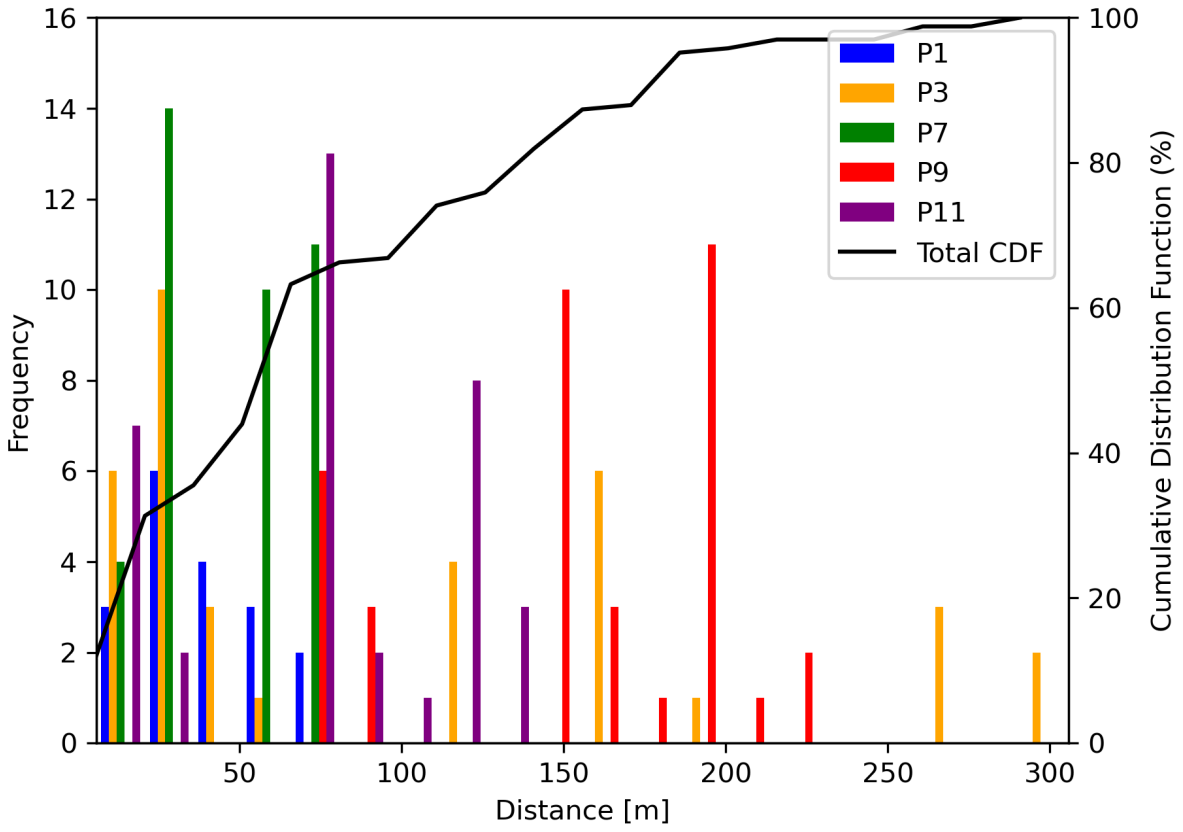

Figure 3.13: The distance between the Lab tests and the nearest KPS/FOPS test.

When each stabilized column was assigned the nearest CPTU and Laboratory data, a data pairing against elevation was performed. The combined data consisted only of data pairs with exactly the same elevation, meaning any extra data that did not have a corresponding value to be paired with was removed. This process is seen in Figure 3.14. All laboratory tests from area P9, as stated in **??** 3.1.1.4, had a top elevation of around 85 m. Since all KPS tests were conducted at a higher altitude (approx. 90-96 m), this would have made it difficult to form reliable pairs. It was therefore decided to remove the entire area P9 from the laboratory analysis. The finished CPTU database can be seen in Section 5.1.1 and the Laboratory database in Section 5.2.1.

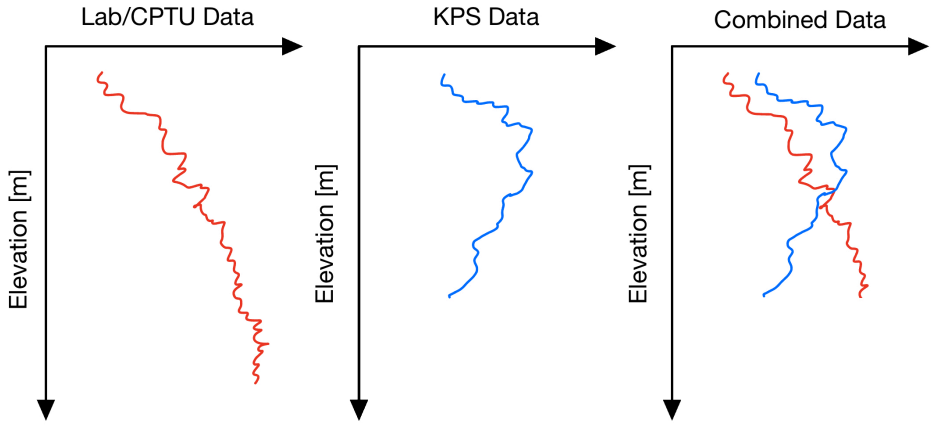

Figure 3.14: The slicing process when combining data.

3.1.2.6 Machine Learning Database: CPTU Data

The established database contained similar data since several stabilized columns used the same CPTUs. This database could have created potential problems for the performance of the machine learning models. Repeating the CPTU data, in combination with varying shear strength in the different columns, could have presented challenges for the machine learning models and affected the accuracy of the predictions. A new database was created, where instead of creating a data pair between each stabilized column and the closest CPTU, pairs were made between each CPTU and its nearest stabilized column. The process is shown in an example in Figure 3.15. It was assumed that the values from the shear strength measurements carried out closest to each CPTU were the most correct, meaning that all stabilized columns further away were removed. Given the example in Figure 3.15, none of the CPTUs have been linked to the values from KPS 3.

There were 33 CPTUs from the E6 Kvithammar-Åsen project. Some CPTUs had the same KPS/FOPS as their nearest shear strength measurement. Therefore, the pairs that were the furthest from each other were removed to avoid equal shear strength values. An upper limit was used for the distance to reduce the uncertainty associated with large distances between the stabilized columns and the performed CPTUs. This was set to 60 meters. After the target data was selected, 18 pairs were left between different CPTUs, and stabilized columns in the database. The completed database is shown in Section 5.1.3.

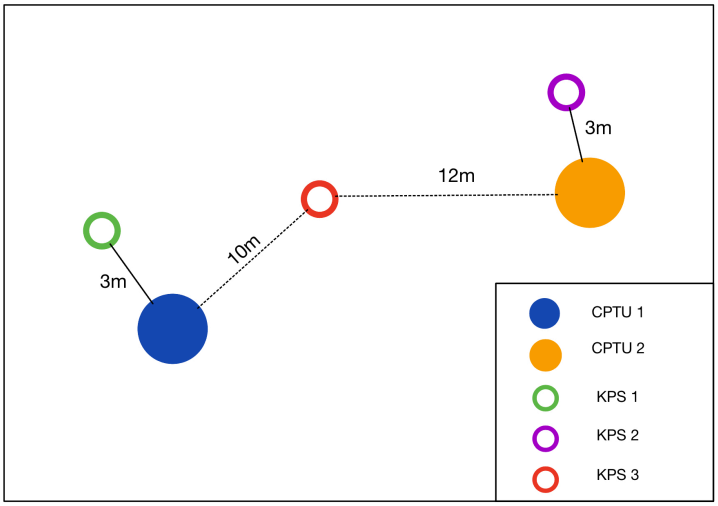

Figure 3.15: The method for selecting which KPS should be linked with each CPTU.

3.1.2.7 Machine Learning Database: Laboratory Data

The laboratory database had the same problems as the original CPTU database, where the same laboratory tests were connected with multiple stabilized columns. A new laboratory database had to be made to get reliable results and performance from the machine learning models. A total of 14 Laboratory test points were conducted in the five areas in the E6 Kvithammar-Åsen project. Due to differences in elevation, all the laboratory test points from area P9 were removed, which left ten laboratory test points for further analysis. To minimize the risk of the shear strength measurement closest to the remaining laboratory test points deviating, precautions were taken. This was done using the average shear strength of all the stabilized columns in the laboratory test points nearest cluster, compared to just the nearest stabilized column. The clustering was performed using the open-source library from Scikit-Learn called DBSCAN. This package sorted the various KPS/FOPS tests into clusters based on their coordinates. The selection of which clusters were closest to each laboratory test point was made manually. The chosen combinations are shown in Figure 3.16.

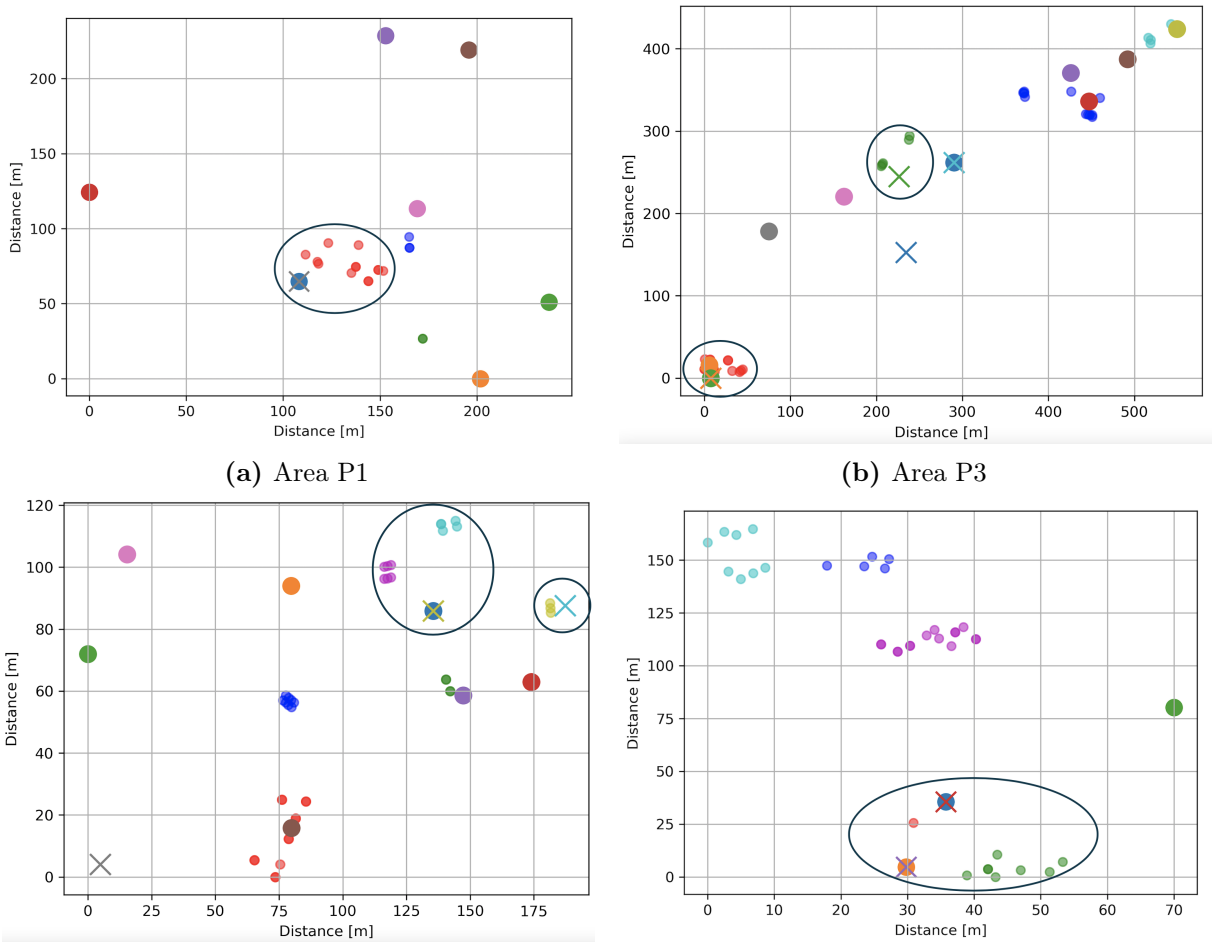

(a) Area P1

(b) Area P3

(c) Area P7

(d) Area P11

Figure 3.16: The chosen combinations of laboratory test points and clusters of stabilized columns in areas P1, P3, P7, and P11. The laboratory tests are illustrated with crosses, while the different clusters are given as small circles of the same color. For naming the different tests, see section 3.1.

Referring to Figure 3.16c and Figure 3.16d, the circles in these figures represent combinations of multiple clusters. For such cases, an average value was calculated by considering both clusters. Similarly, an average value was computed when analyzing the two laboratory tests in P11. It was decided to remove the laboratory test points the furthest away from the stabilized columns. This left a database of six laboratory test points with corresponding shear strength measurements. The calculated averages of the stabilized columns are shown in Figure B5.8 and Figure B5.9. The moving average was used to interpolate these values as the calculated averages exhibited some scatter. The window size for the interpolation analysis was set to 20 cm or 10 data points.

During the establishment of this machine learning database, another challenge encountered was the lack of laboratory tests performed in laboratory point number four in area P3. No tests were performed from Uniaxial compression, Unit weight, and bulk density in this point. Although all points had Atterberg limits data, the total amount of data points was less than the other variables. Missing data is a problem for most machine learning models resulting in difficulties with training them. However, there are several methods for dealing with this, like inserting the mean or median of the missing variable. These methods were assessed as not appropriate for this thesis. The only sensible approach was removing features and any row with a missing value.

This also has its disadvantages, in that critical information may be erased. Instead of removing all the Atterberg limit variables, it was deemed preferable to eliminate the features explicitly missing from the laboratory test point in area P3. Retaining more laboratory test points ensure a more comprehensive data set, increasing the reliability of the machine learning models. The established database is given in Section 5.2.4.

3.2 The Norwegian Database

The Norwegian database consists of 325 clays samples stabilized in the laboratory and was established for the article [1]. The clay was stabilized using different binder combinations. Mostly a 50/50 combination of lime and cement or CKD and cement was used, with a binder amount of 100 kg/m^3. The strength was measured using uniaxial compression. Correlations were identified between the water content and the plasticity index with the stabilized strength. Furthermore, higher strength was observed at increased amounts of binder. The stabilized soil samples with the highest strength were given by a combination of cement/CKD, long curing time, and water content below 30 percent. There was also a noticeable correlation between an increase in the water binder ratio and a decrease in the stabilized strength. Correlation coefficients have not been calculated in [1], nor have machine learning models been used to investigate whether there are undiscovered non-linear relationships in the database.

As for the established E6 Kvithammar-Åsen databases, the samples had different curing days. For the Norwegian database, the differences were significant, with curing days ranging from 1-60 days. To make the shear strengths comparable, all have been converted to 28 days strength, as explained in Section 3.1.2.4.

For the Norwegian database, there was little variation in the total binder amount and the percentages of the individual binders in the total mix. Getting useful knowledge from a low-variety database is demanding. Therefore, an attempt was made to create a greater variation by using the quantity of each binder instead of the total.

The Norwegian database contained many variables, of which the nine most relevant were selected for further analysis. These were the water content, sensitivity, unit weight, plastic limit, liquid limit, plasticity index, lime content, cement content, and CKD content. It was also decided to calculate three additional variables, the liquidity index, the porosity of the unstabilized soil, and the water binder ratio. These were calculated according to Section 3.1.2.2. The Norwegian database consists of many of the same variables as the laboratory database from E6 Kvithammar-Åsen. Comparing the field and laboratory results will be possible based on these two.

3.3 The Swedish Database

The Swedish database contains a total of 877 stabilized soil samples and was established for [2]. The soil samples were mostly taken from the area around Stockholm. They were stabilized with the same binders used in the Norwegian database, but there was a wider variety of binder contents and the mixing ratio between them. There were major differences in the water content for the Swedish soils ranging from 34 to 270 percent. This interval is deviant compared to the Norwegian soils, which only range from around 20 to 60 percent.

Uniaxial compression was used to determine the shear strength of the soil samples. The shear strengths of the stabilized soil samples were converted to 28 days strength, as for the other

databases. Even though there were larger variations of the different binder contents, it was decided to use the same methodology as for the Norwegian database. Meaning the amount of the individual binders in kg/m^3 was used instead of just a percent of the total binder amount.

There are fewer variables in the Swedish database, but on the other hand, there are more data points than in the Norwegian database. The used variables were water content, bulk density, lime content, cement content, CKD content, porosity, dry weight clay, and water binder ratio. From the common variables in the laboratory databases, it will be possible to compare whether any of the variables show consistent results.

4 Methodology

This chapter is divided into three sections. Section 4.1 presents how the Knowledge Development in Databases process has been implemented into this thesis. Further in Section 4.2, the different evaluation metrics used to validate the performance of regression models are addressed. Finally, a brief introduction to cross-validation is given in Section 4.2.4.

4.1 Implementation of the KDD Process to the Databases

Knowledge Development in Databases is a process of finding patterns in large amounts of data, which can be turned into useful knowledge. This process consists of six predetermined steps, which can be seen in Figure 4.1.

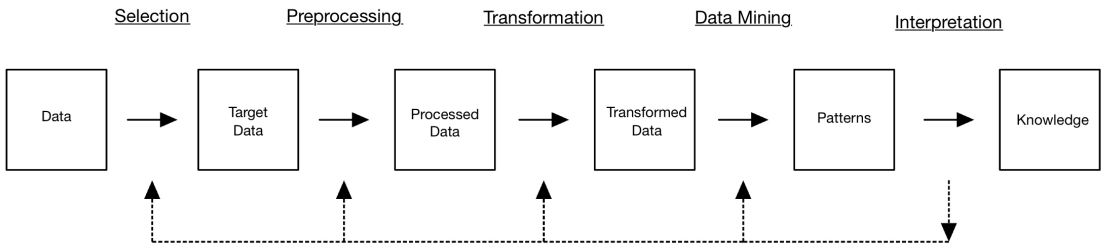

Figure 4.1: The KDD process according to [5].

The methodology for this master's thesis has followed the KDD process. In Section 3.1.2, Section 3.2 and Section 3.3, the two first steps of the KDD are described. In the first step, the data considered to be of interest were selected. In the second step, actions were taken on the target data to reduce the number of outliers and scatter in the data.

Before more advanced nonlinear machine learning methods were used, the linear correlations for all databases were calculated. This was done using the built-in function in the Pandas library. The function returns a number between -1 and 1, representing the linear relationship between two variables. The method of correlation from Pandas is Pearson, the standard correlation coefficient. In the calculation of the correlations, the NaN values were excluded.

The next step in the KDD process is transforming the processed data into transformed data. This is done to improve the performance of the machine learning models. All features used in this thesis's various machine-learning models have been normalized to a common scale between 0 and 1 using the MinMaxScaler from the Scikit Learn library. The features have been normalized because the different variables had different ranges, which could have resulted in some variables having a more significant impact on the model than others.

To perform Data Mining, the appropriate method and algorithm must be selected. It was decided that the most considerate approach for this task was regression. However, the choice of which algorithm to use was not as obvious. As seen in Table 2.7, four different algorithms were used: Artificial Neural Networks, Support Vector Machines, Decision Trees, and Multiple Regression. In this thesis, two types of Decision Trees have been used: Gradient Boosting and Random Forest.

The two models' differences are visualized in Figure 4.2. Random Forest uses the bagging

method [36]. This is based on splitting the training data into multiple bootstrap samples, where independent decision trees are made. The output comes from averaging the predictions from the models. Gradient Boosting, on the other hand, is different from Random Forest in that the decision trees are not independent but connected sequentially. Each time a new decision tree is formed, it tries to correct the error of the previous tree.

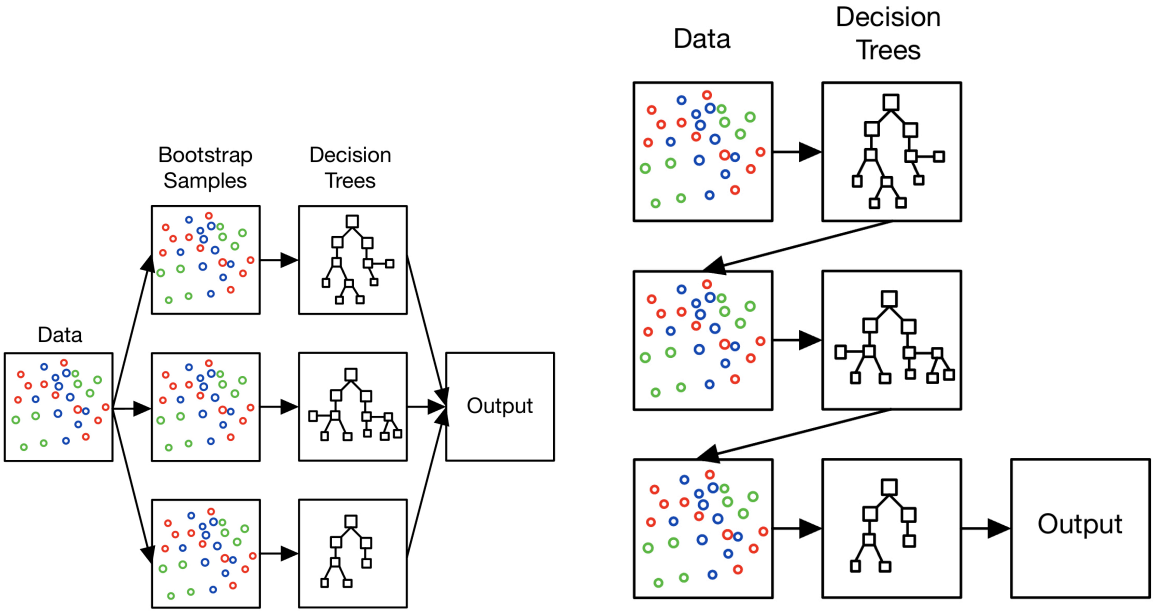

(a) The Bagging method **(b)** The Boosting method

Figure 4.2: Visual presentation of the difference in the bagging and boosting method, inspired by [6].

To assess how well the established models work, the model needs to be tested on data on which it has not been trained. Thus the data were divided into a training set and a test set, where 80 % of data were allocated for training, and the remaining 20 % were for testing purposes. This was carried out by the Train Test Split function from the Scikit Learn library, which randomly shuffled the data into two sets. However, this way of splitting the data did not work for the machine learning databases from E6 Kvithammar-Åsen since the data were continuous with depth. That would have meant that the test data contained values almost identical to what the model was trained on, leading to an artificially good result. Instead, the solution was to split the data based on the names of the stabilized columns, meaning that the model would be tested on a new column on which it was not trained.

All Random Forest and Gradient Boosting models in this master's thesis have been established using the Scikit Learn library with default hyperparameters.

4.2 Evaluation Metrics

Three different evaluation metrics have been used to measure how well the different regression models perform.

4.2.1 Coefficient of Determination, R^2

The coefficient of determination is according to [37] found from subtracting 1 with the quotient of the mean square error and the mean total sum of squares, as seen in Equation (4.1). The mean square error is found by taking the sum of the squared residuals between the predicted and actual values. The mean total sum of squares is found by subtracting the actual values from the mean of the actual values.

The coefficient of determination range from $(-\infty, 1]$, where 1 indicates a perfect fit. If the R^2 value is between 0 and 1, it will be the same as the squared correlation coefficient. According to [38], if the R^2 value is between 0-1, it corresponds to how much of the variation in output of the dependent variable that the independent variables can represent. If a model has a R^2 of 1, it can predict 100 % of the variation of the dependent variable. On the other hand, if the $R^2 = 0$, the model cannot predict any of the variations of the dependent variable, which happens when MSE = MST. As stated by [37], a R^2 of 0 will result in the fitted line being horizontal. The R^2 can be negative when performing nonlinear regression. This happens when the best fit from the model performs worse than the horizontal line.

$$R^2 = 1 - \frac{MSE}{MST} = 1 - \frac{\sum_{i=1}^{m}(X_i - Y_i)^2}{\sum_{i=1}^{m}(\bar{Y} - Y_i)^2} \tag{4.1}$$

Where:

MSE = The mean square error

MST = The mean total sum of squares

X_i = The predicted values

Y_i = The actual values

$\bar{Y}$ = The mean of the actual values

4.2.2 The Root Mean Square Error, RMSE

The root mean square error is another performance measure for machine learning models. It is the same expression as the mean square error, which is then taken the square root of, as seen in Equation (4.2). The model is quite sensitive to outliers since the residuals are squared. The RMSE is given in the same unit of measurement as the dependent variable, where the best value is given as 0 and the worst as $+\infty$.

$$RMSE = \sqrt{\frac{1}{m}\sum_{i=1}^{m}(X_i - Y_i)^2} \tag{4.2}$$

4.2.3 The Mean Absolute Error, MAE

The mean absolute error model will be less sensitive to outliers since the residuals are not squared as in the RMSE. On the contrary, it is the absolute value of the residuals instead, as seen in Equation (4.3). Like the RMSE, the MAE is also expressed with the same designation as the dependent variable and the same limits on the best and the worst values.

$$MAE = \frac{1}{m} \sum_{i=1}^{m} |X_i - Y_i| \tag{4.3}$$

4.2.4 10-Fold Cross-Validation

According to [39], 10-fold cross-validation is a method used to assess the actual generalization capabilities of a machine learning model. It can also be used to avoid overfitting. The method is based on splitting the data into ten different folds. Furthermore, the model is trained ten times, where each time a new model is trained, a different fold is used for validation. This results in a more robust estimate of the model's actual performance.

5 Results

The results chapter consists of four main sections, one for each analyzed database. The different databases are presented in the following order: CPTU Data E6 Kvithammar-Åsen, laboratory Data E6 Kvithammar-Åsen, Norwegian Database, and Swedish Database. The findings are presented in the same sequence, beginning with the descriptive information of the databases accompanied by correlations, histograms, and scatter plots. For the E6 Kvithammar-Åsen databases, one additional linear correlation analysis has been performed to reduce the uncertainty related to the distance between the performed tests. Regression has been carried out with Gradient Boosting and Random Forest for all databases. Furthermore, curve fitting has been executed for the water binder ratio in the laboratory databases, which have been compared with the already established relationships in the literature.

5.1 CPTU Data E6 Kvithammar-Åsen

5.1.1 Correlation Analysis with All CPTU Data

In Table 5.1, the descriptive statistics of the CPTU database are given. It contains eight variables, the original CPTU parameters, the normalized CPTU parameters, the depth, and the shear strength of the stabilized columns (from KPS and FOPS). In this analysis, depth under terrain was used and not elevation. From the percentiles as well as the histograms along the diagonal in Figure 5.1, it can be seen that there is a strong skew toward the lower values in the interval of q_c, f_s, Q_t, and F_r. On the other hand, there is a more even distribution of the depth, the shear strength of the stabilized columns, u_2, and B_q. All variables have the same number of data points of 58,166.

The linear correlation coefficients (R) are summarized in Table 5.2. They range from -0.18 to 0.18, and the R^2 values from 0.00 to 0.03.

The bottom row in Figure 5.1 shows the scatter plots between the various variables and the shear strength of the stabilized columns. While these scatter plots show the trends between various data combinations, it can be challenging to identify clusters with a higher density of points. Therefore, scatter plots with heat plots have been used, given in Figure C6.1 and Figure C6.2. The stronger the color, the greater the density of points.

	Depth $[m]$	q_c $[kPa]$	u_2 $[kPa]$	f_s $[kPa]$	Q_t $[-]$	F_r [%]	B_q $[-]$	C_u Column $[kPa]$
count	58166	58166	58166	58166	58166	58166	58166	58166
mean	6.22	580.63	354.53	7.35	7.41	1.89	0.95	740.00
std	3.49	815.39	145.21	8.19	15.38	1.44	0.46	404.58
min	1.00	189.00	15.00	0.00	1.20	0.00	-0.05	4.39
25 %	3.48	341.00	254.00	3.00	2.35	0.90	0.67	430.91
50 %	5.70	415.00	359.00	5.00	3.86	1.43	0.92	641.95
75 %	8.24	550.00	427.00	8.00	6.62	2.91	1.22	1017.47
max	19.90	9033.00	927.00	143.00	354.00	18.32	2.59	2777.88

Table 5.1: Descriptive statistics of the CPTU data. For each variable, the number of data points, the mean, the standard deviation, the minimum value, the maximum value, the 25^{th}, 50^{th}, and 75^{th} percentile are provided.

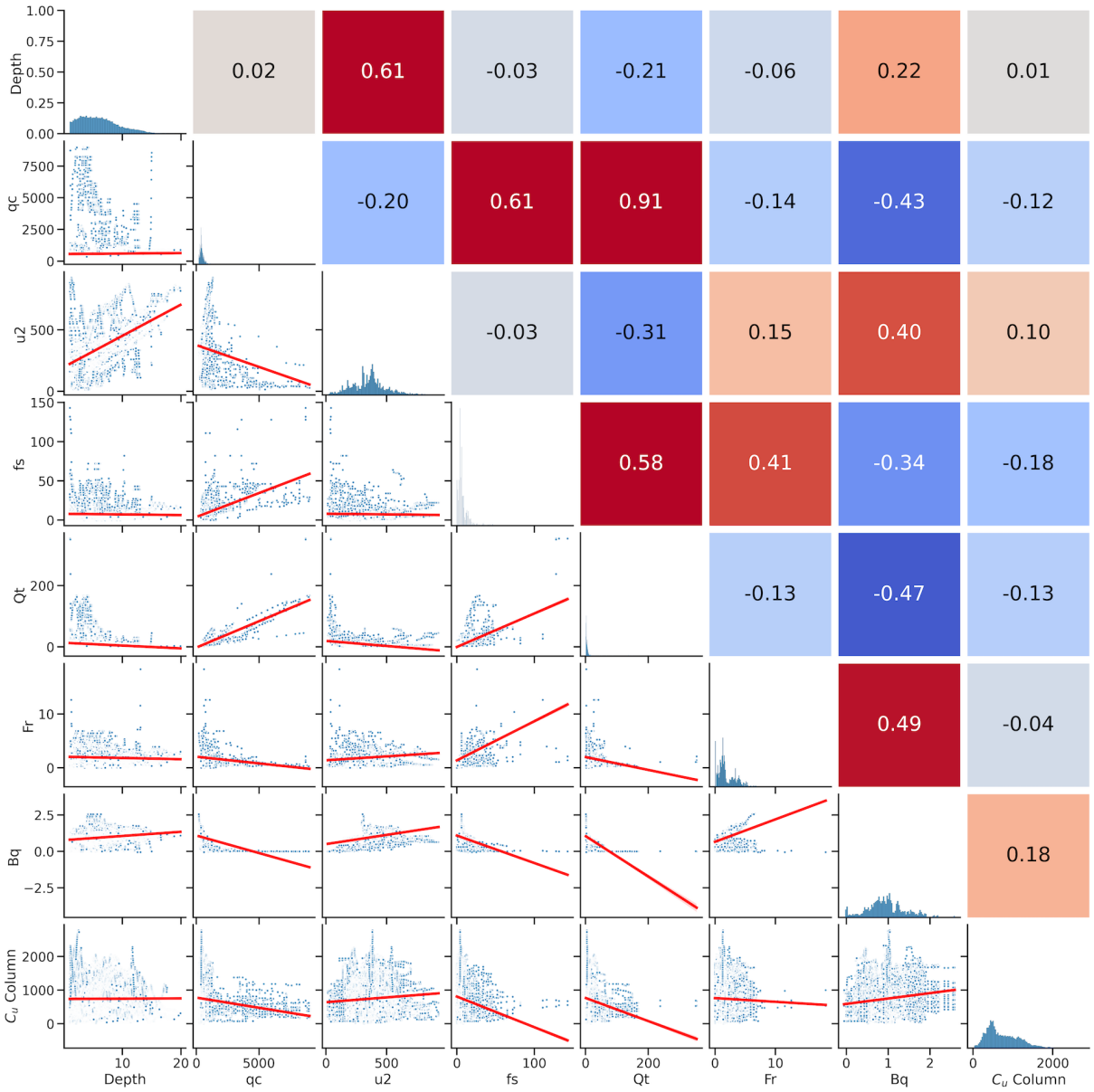

Figure 5.1: The Scatter Plot Matrix for the CPTU database. The lower triangle shows scatter plots with the corresponding regression line, the diagonal shows the histograms, and the upper triangle shows the correlations.

Variable	Symbol	Count	R	R^2
Cone resistance	q_c	58166	-0.12	0.01
Pore pressure	u_2	58166	0.10	0.01
Sleeve friction	f_s	58166	-0.18	0.03
Cone resistance number	Q_t	58166	-0.13	0.02
Friction ratio	F_r	58166	-0.04	0.00
Pore pressure ratio	B_q	58166	0.18	0.03
Depth	-	58166	0.01	0.00

Table 5.2: Summary of the linear correlations between the CPTU data and the column strength.

5.1.2 Correlation Analysis Regarding the Distance between CPTUs and Stabilized Columns

In the correlation analysis carried out in Section 5.1.1, all CPTU data were used. In this analysis, spatial variability was not taken into account. Therefore, a new analysis was performed where the data from the CPTU database were divided into groups based on the given distance between the CPTUs and the stabilized columns. As mentioned earlier, this distance ranged from 3-133 m. The data were therefore divided into 20 m intervals, where subsequent correlation analyses were performed. The results from the analysis regarding the spatial variability are shown in Figure 5.2. The correlations varied greatly, especially when the distance was increased above 80 m. There was a significant decrease in the number of data points from distances over 60 m, which can be seen in Figure D10.1.

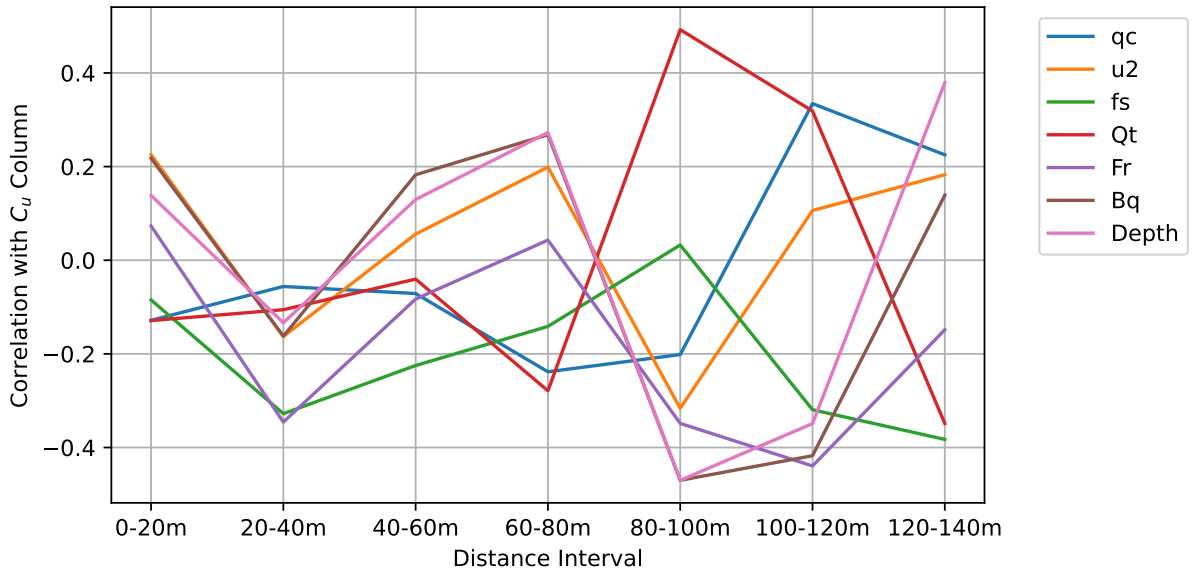

Figure 5.2: The correlation of the CPTU data and C_u Column at different distances. The different correlations are calculated based on 20 m intervals.

The scatter plots for the data in the innermost interval are shown in Figure C7.1 and Figure C7.2, with the summary of the correlations in Table 5.3. There was only a minimal change in the correlations, from -0.13 to 0.23, while the R^2 values ranged from 0.01 to 0.05.

Variable	Symbol	Count	R	R^2
Cone resistance	q_c	17071	-0.13	0.02
Pore pressure	u_2	17071	0.23	0.05
Sleeve friction	f_s	17071	-0.09	0.01
Cone resistance number	Q_t	17071	-0.13	0.02
Friction ratio	F_r	17071	0.07	0.01
Pore pressure ratio	B_q	17071	0.22	0.05
Depth	-	17071	0.14	0.02

Table 5.3: Summary of the linear correlations between the CPTU data and the column strength, where all the data where the distance between the CPTU and the nearest stabilized column is more than 20 m are removed.

5.1.3 CPTU Machine Learning Database

In Table 5.4, the descriptive statistics for the data in the CPTU machine learning database are summarized. The largest difference between the two CPTU databases is the number of data points, which has been reduced from 58,166 to 8,691. The number of data points was reduced because this particular database was made by pairing each CPTU test with its nearest KPS or FOPS test, which was the opposite of how the original CPTU database was made. It was desirable not to have repeated CPTU data since this may have influenced the accuracy of the machine learning models in predicting the shear strength of the columns. The correlations, as given in the upper triangle in Figure 5.3, are more or less the same as in the calculation for the original CPTU data.

	q_c $[kPa]$	u_2 $[kPa]$	f_s $[kPa]$	Q_t $[-]$	F_r [%]	B_q $[-]$	C_u Column $[kPa]$
count	8691	8691	8691	8691	8691	8691	8691
mean	716.42	380.28	7.42	8.93	1.40	0.79	722.01
std	898.00	177.89	8.54	15.68	1.24	0.37	354.29
min	189.00	15.00	0.00	1.20	0.00	-0.05	29.68
25 %	378.00	250.00	3.00	2.77	0.62	0.61	463.43
50 %	499.50	359.00	5.00	4.67	1.13	0.81	634.91
75 %	699.00	503.00	8.00	8.28	1.62	1.00	958.52
max	9033.00	927.00	82.00	167.04	18.32	2.59	1973.15

Table 5.4: Descriptive statistics of the CPTU data for machine learning. For each variable, the number of data points, the mean, the standard deviation, the minimum value, the maximum value, the 25^{th}, 50^{th}, and 75^{th} percentile are provided.

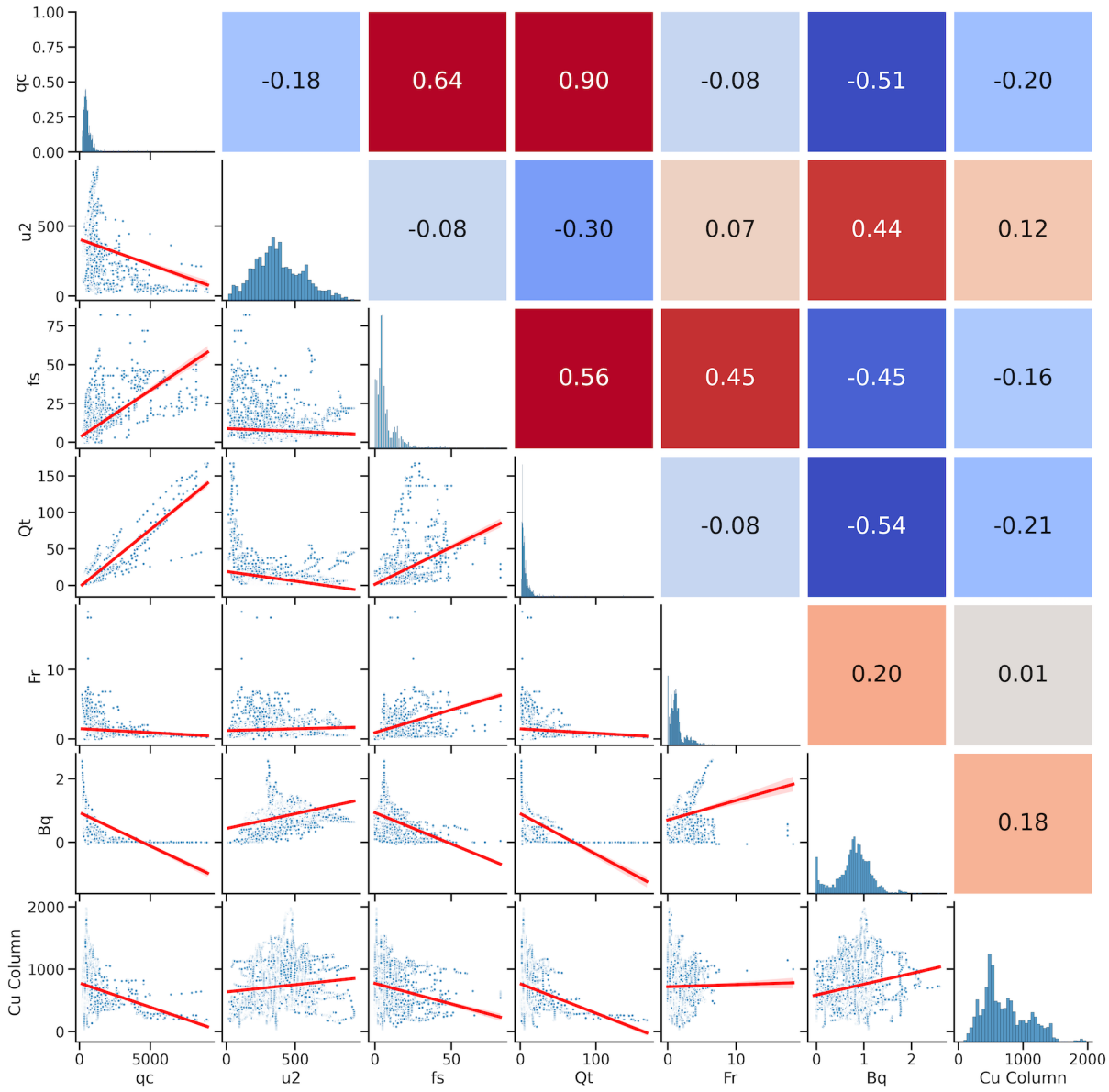

Figure 5.3: The Scatter Plot Matrix for the CPTU machine learning database. The lower triangle shows scatter plots with the corresponding regression line, the diagonal shows the histograms, and the upper triangle shows the correlations. The shaded areas around the regression lines represent the uncertainty in the estimation.

5.1.3.1 Regression with Gradient Boosting and Random Forest

In Table 5.5, the performance from the Gradient Boosting and Random Forest models are summarized. The Random Forest model seems to be better at predicting shear strength based on the data it is trained on. However, the models have more or less the same performance based on the testing data. The performance plots for the Gradient Boosting and Random Forest models are given in Figure 5.4 and Figure 5.5.

Model	Training			Testing		
	R^2	RMSE	MAE	R^2	RMSE	MAE
Gradient Boosting	0.82	152.75	115.48	-0.70	449.16	377.44
Random Forest	1.00	16.93	7.14	-0.84	467.53	385.18

Table 5.5: Summary of the performance from the CPTU machine learning models.

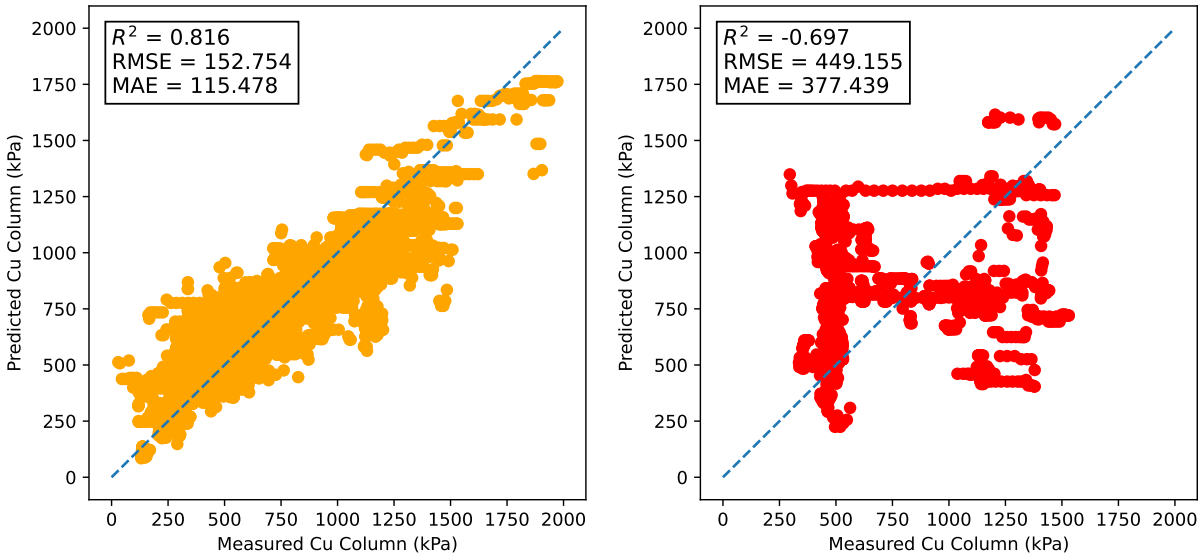

(a) Training data CPTU E6. **(b)** Testing data CPTU E6.

Figure 5.4: The difference in performance for training and testing data from Gradient Boosting.

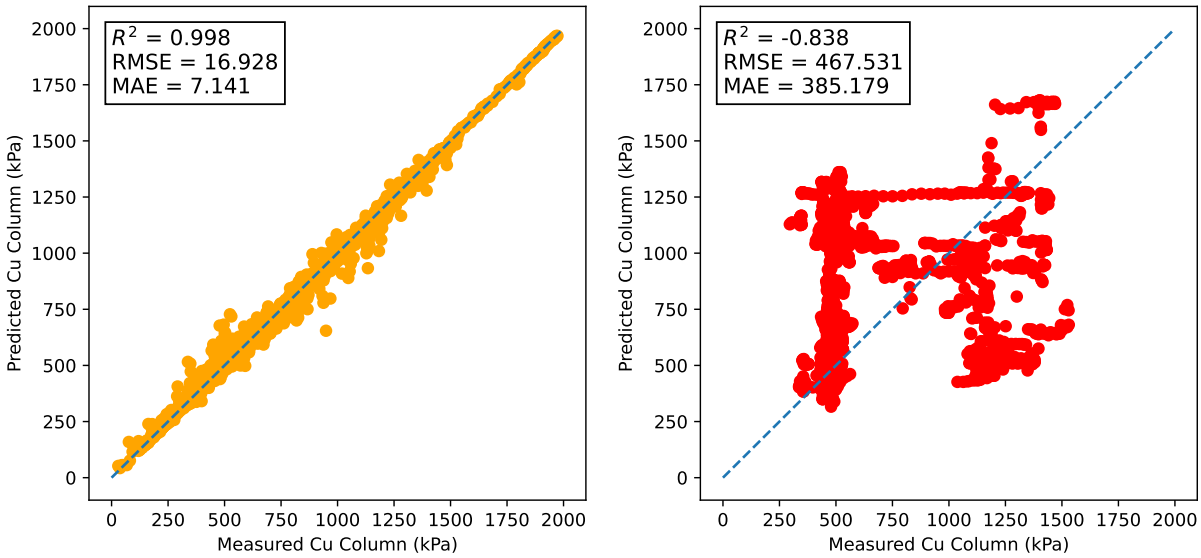

(a) Training data CPTU E6. **(b)** Testing data CPTU E6.

Figure 5.5: The difference in performance for training and testing data from Random Forest.

The testing data consisted of four columns on which the model had not been trained. In Figure 5.6, the predicted and measured shear strength are plotted against elevation. Based on the plots, the output from the models was more or less the same. It can be seen that there are quite large deviations between the actual and predicted shear strength. On average, the models missed by about 400 kPa, based on the values from RMSE and MAE. The given models underestimated and overestimated the strength of the columns. However, in Figure 5.6a and Figure 5.6c, the models were more in agreement with the actual strength.

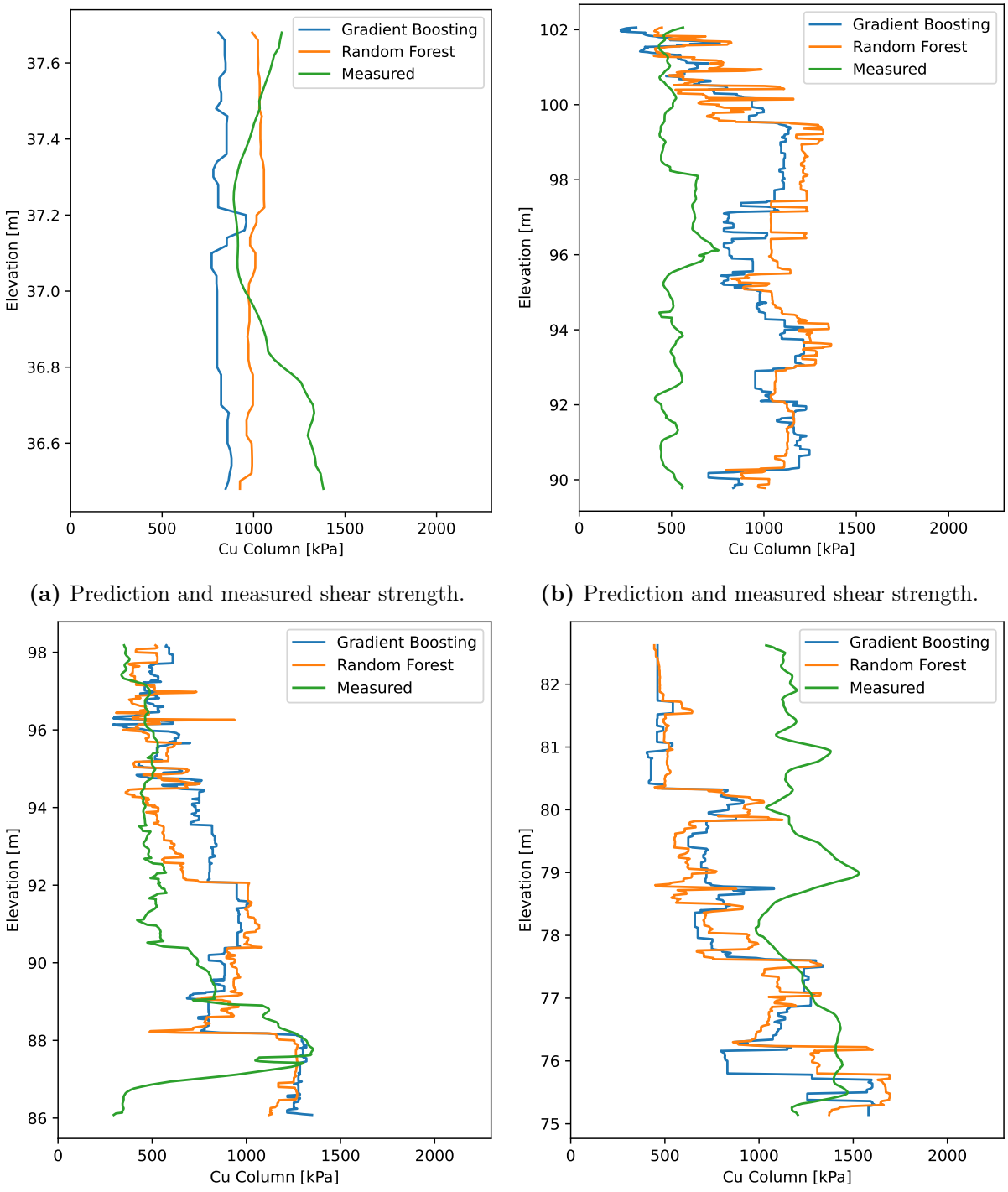

(a) Prediction and measured shear strength.

(b) Prediction and measured shear strength.

(c) Prediction and measured shear strength.

(d) Prediction and measured shear strength.

Figure 5.6: The predicted shear strength from Gradient Boosting and Random Forest compared with the actual shear strength.

5.2 Laboratory Data E6 Kvithammar-Åsen

5.2.1 Correlation Analysis with all the Laboratory data

The descriptive statistics of the laboratory data from E6 Kvithammar-Åsen are given in Table 5.6. In total, 15 variables are listed. Most of the variables were from various laboratory tests performed on the unstabilized clay from the project. The porosity, the water binder ratio, and the liquidity

index were calculated based on the laboratory results, as seen in Section 3.1.2.2. All non-calculated variables were linearly interpolated between each test performed in the same borehole to obtain continuous results with depth. An equal number of recordings per meter, corresponding to the number from the shear strength measurements, were used for the interpolated values. The number of data points varied from 24,194 to 41,314.

Based on the percentiles in Table 5.6 and the histograms in Figure 5.7, the variables generally had a small range. From the 25^{th} to the 75^{th} percentile, there were only a few units of difference for the variables. In contrast, the range of shear strength was wider, with a more even distribution between the minimum and maximum values.

	Depth $[m]$	$w_{in\,situ}$ [%]	Porosity unstab. [−]	C_u (Uniaxial) $[kPa]$	C_u (Fall cone) $[kPa]$	C_{ur} $[kPa]$	S_t [−]	w_P [%]	w_L [%]	I_P [%]	I_L [−]	γ $[kN/m^3]$	ρ $[Mg/m^3]$	wbr_{corr} [−]	C_u Column $[kPa]$
count	41314	41314	39472	34881	41131	41131	41131	24194	24194	24194	24194	39472	39472	39472	41314
mean	6.67	33.18	0.46	20.16	22.62	2.47	49.96	18.24	31.72	13.48	1.18	19.33	1.97	10.50	752.50
std	3.95	8.15	0.05	9.71	11.86	2.65	91.30	2.24	6.42	4.38	0.51	0.82	0.08	1.15	416.69
min	1.00	22.70	0.35	8.00	3.60	0.10	2.00	14.00	20.00	5.00	0.33	16.90	1.72	7.89	19.19
25 %	3.74	27.61	0.42	13.00	11.80	0.47	6.92	16.00	27.25	10.80	0.75	18.93	1.93	9.65	424.97
50 %	5.90	30.68	0.45	17.34	20.00	0.97	16.42	18.75	29.80	12.00	1.01	19.49	1.99	10.26	668.75
75 %	8.44	37.12	0.48	23.87	31.87	4.43	30.00	19.90	35.45	15.69	1.59	19.90	2.03	11.03	1035.19
max	19.90	58.60	0.60	55.32	53.00	12.00	440.00	23.00	51.00	29.00	2.86	21.70	2.21	13.76	2777.88

Table 5.6: Descriptive statistics of the laboratory data. For each variable, the number of data points, the mean, the standard deviation, the minimum value, the maximum value, the 25^{th}, 50^{th}, and 75^{th} percentile are provided.

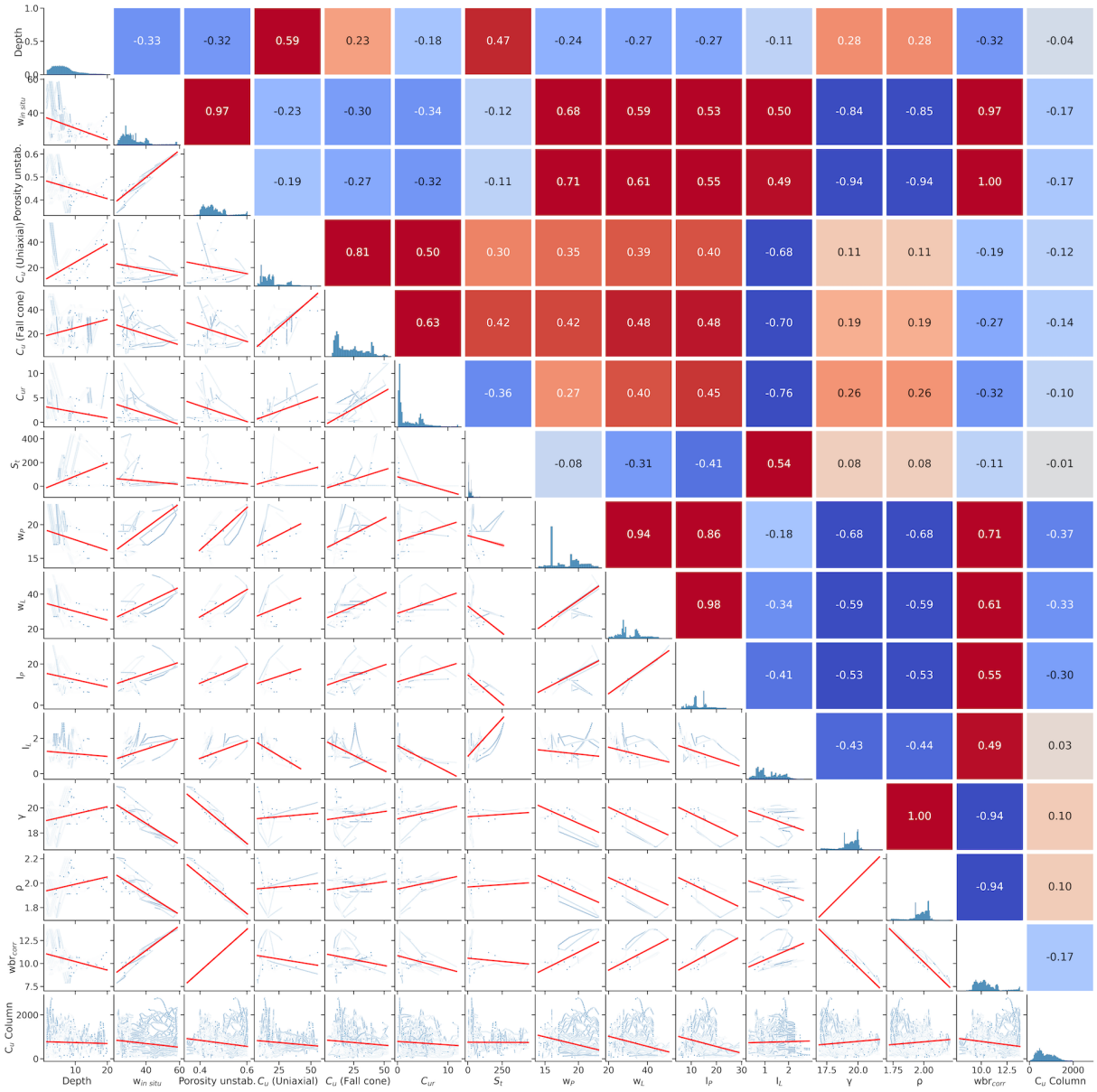

Figure 5.7: The Scatter Plot Matrix for the laboratory database. The lower triangle shows scatter plots with the corresponding regression line, the diagonal shows the histograms, and the upper triangle shows the correlations.

The linear correlations between the laboratory data and the shear strength of the columns are summarized in Table 5.7. The correlations ranged from -0.37 to 0.10. The plastic limit was the parameter with the strongest correlation with the shear strength of the column. The R^2 values ranged from 0.00 to 0.14. The scatter plots with heat plots are shown in Figure C8.1, Figure C8.2 and Figure C8.3.

Variable	Symbol	Count	R	R^2
Water content	$w_{in\,situ}$	41314	-0.17	0.03
Porosity unstab.	-	39472	-0.17	0.03
Shear Strength (Uniaxial)	C_u	34881	-0.12	0.02
Shear Strength (Fall cone)	C_u	41131	-0.14	0.02
Remolded shear strength	C_{ur}	41131	-0.10	0.01
Sensitivity	S_t	41131	-0.01	0.00
Plastic limit	w_P	24194	-0.37	0.14
Liquid limit	w_L	24194	-0.33	0.11
Plasticity index	I_P	24194	-0.30	0.09
Liquidity index	I_L	24194	0.03	0.00
Unit weight	γ	39472	0.10	0.01
Bulk density	ρ	39472	0.10	0.01
Corrected water binder ratio	wbr_{corr}	39472	0.17	0.03
Depth	-	41314	-0.04	0.00

Table 5.7: Summary of the linear correlations between the laboratory data and the column strength.

5.2.2 Correlation Analysis Regarding the Distance between Laboratory Tests Points and the Stabilized Columns

As for the CPTU data, a new analysis was carried out where the spatial variation was considered. The data were grouped into intervals based on the distance between the stabilized columns and their nearest laboratory test point. For distances below 100 m, the interval between the groups was set to 20 m. A collection group was created for the remaining data with distances over 100 m. The results are shown in Figure 5.8. The correlations seemed to be more or less consistent within 40 m. For distances larger than this, the correlations varied. There were fewer data points in the interval between 40-60 m as well for distances over 80 m, which can be seen in Figure D12.2 and Figure D12.1.

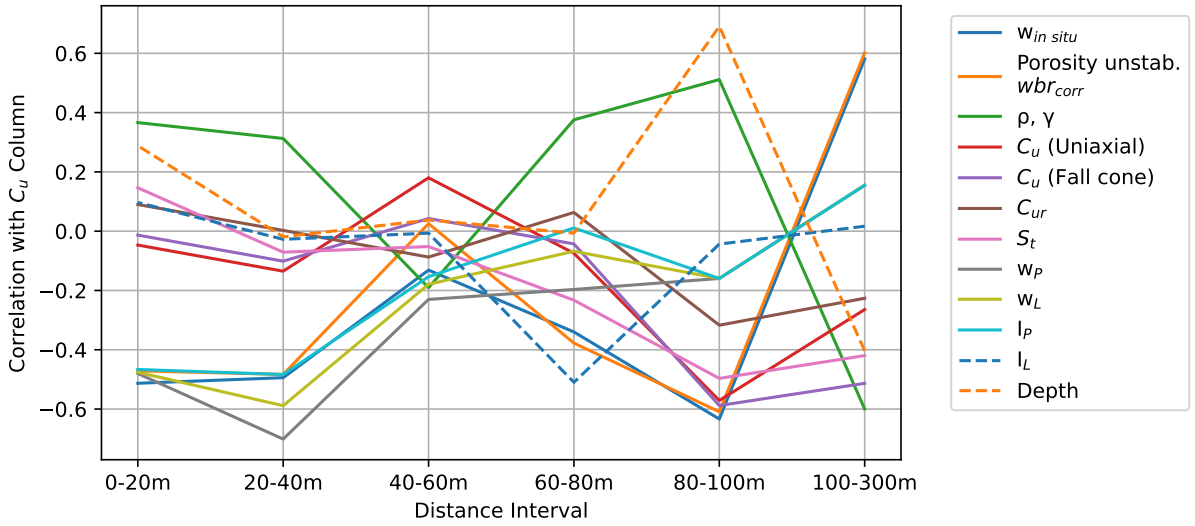

Figure 5.8: The correlation of the Lab data with C_u Column at different distance intervals.

The correlations within 0-40 m between the laboratory data and the column strength are summarized in Table 5.8. The table further provides the corresponding R^2 values and the number

of data points used in the analyses. The correlation coefficients were increased by removing the data pairs with the greatest distances and ranged between -0.60 and 0.32. The plastic limit showed the strongest relationship, with the R^2 value given by 0.32. On the other side, the parameters: Depth, liquidity index, in-situ shear strength from both fall cone and uniaxial compression, remolded shear strength, and sensitivity all showed an R^2 value equal to 0. In Figure C9.3, Figure C9.1 and Figure C9.2, the scatter plots with heat plots are provided.

Variable	Symbol	Count	R	R^2
Water content	$w_{\text{in situ}}$	18137	-0.49	0.24
Porosity unstab.	-	17099	-0.47	0.22
Shear Strength (Uniaxial)	C_u	18042	-0.07	0.01
Shear Strength (Fall cone)	C_u	18042	-0.04	0.00
Remolded shear strength	C_{ur}	18042	0.05	0.00
Sensitivity	S_t	18042	-0.03	0.00
Plastic limit	w_P	12706	-0.60	0.36
Liquid limit	w_L	12706	-0.52	0.27
Plasticity index	I_P	12706	-0.46	0.21
Liquidity index	I_L	12706	0.01	0.00
Unit weight	γ	17099	0.32	0.11
Bulk density	ρ	17099	0.32	0.10
Corrected water binder ratio	wbr_{corr}	17099	-0.47	0.22
Depth	-	18137	0.08	0.01

Table 5.8: Summary of the linear correlations between the laboratory data and the column strength.

5.2.3 Curve Fitting Water Binder Ratio

As provided in Section 2.2.5, there are established relationships between the corrected water binder ratio and the shear strength of the stabilized soil. The relationship is expressed using the equation proposed from [25]. In [4], the established relationship for the clays in Trondheim was described. In Figure 5.9 and Figure 5.10, curve fittings were performed on the laboratory database with two different distance intervals. For the curve fitting, an open-source package in Python named Skipy was used. This was presented with the formula from [25], and the most correct A and B constants were calculated. The analyses used two intervals: 0-20 m and 0-40 m. By only using the innermost 20 m of the data set, the established formula for the shear strength seemed less aggressive.

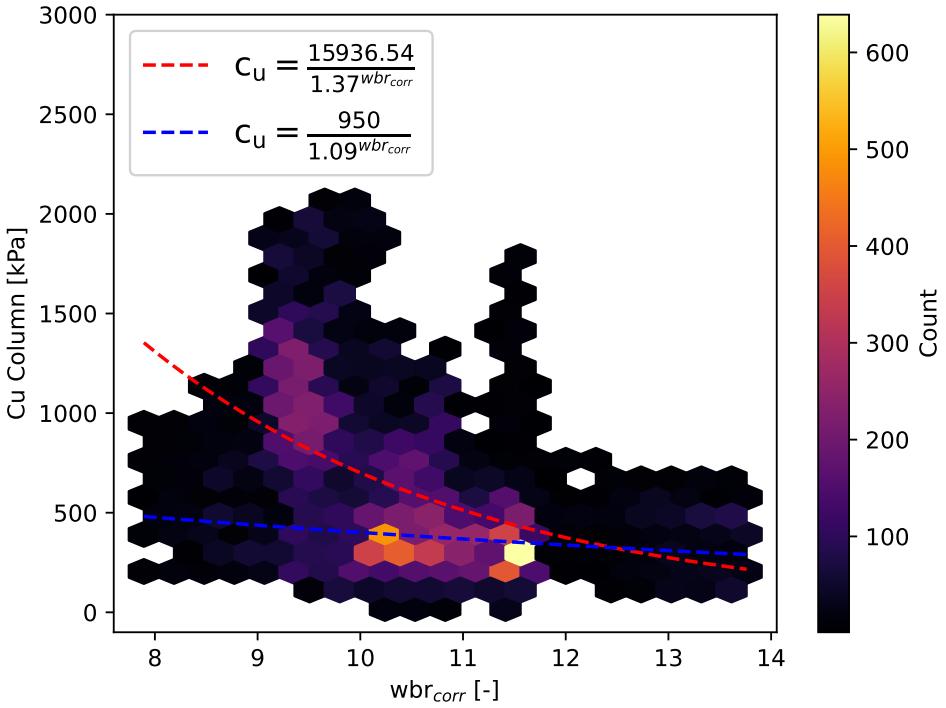

Figure 5.9: Scatter plot for the C_u column with the water binder ratio. Only data within the 0-40 m interval between the stabilized columns and the laboratory tests were used. The red dotted line shows the equation found by curve fitting, the blue is from [4].

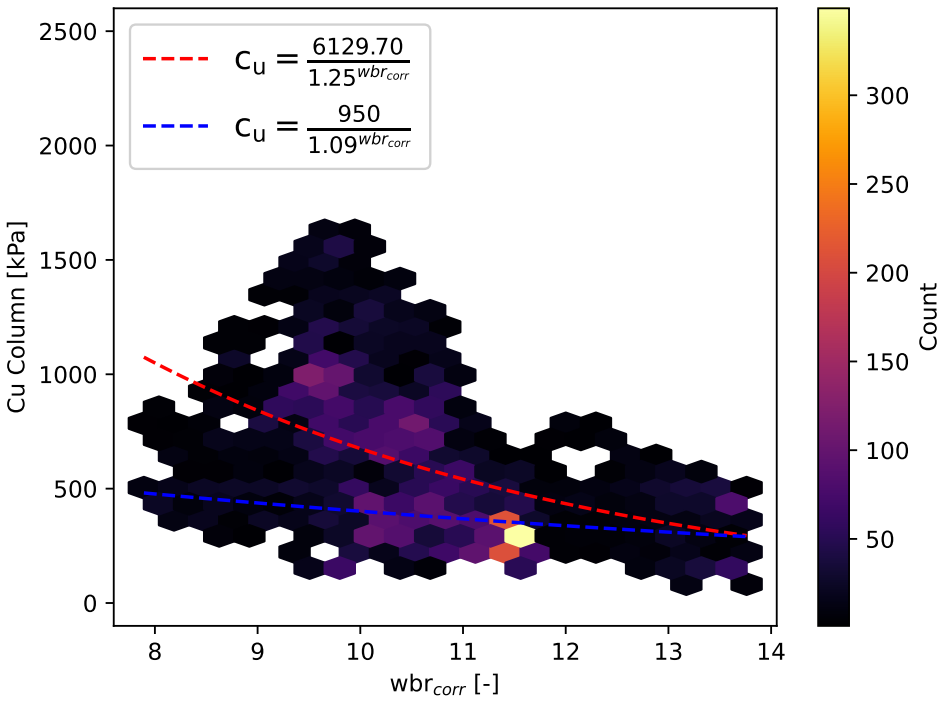

Figure 5.10: Scatter plot for the C_u column with the water binder ratio. Only data within the 0-20 m interval between the stabilized columns and the laboratory tests were used. The red dotted line shows the equation found by curve fitting, the blue is from [4].

5.2.4 Laboratory Machine Learning Database

In Table 5.9, the descriptive statistics of the laboratory database used for machine learning are shown. The database was established as described in Section 3.1.2.7. The database consisted of six data pairs between laboratory test points and shear strength measurements of the stabilized columns. The training of the models was based on five of these pairs, whereas the last one was used for testing.

The correlations between the selected parameters and the shear strength of the columns are given in the rightmost column in Figure 5.11. Apart from the sensitivity, all parameters showed negative correlations.

	$w_{\text{in situ}}$ [%]	C_u $[kPa]$	C_{ur} $[kPa]$	S_t $[-]$	w_P [%]	w_L [%]	I_P [%]	C_u Column $[kPa]$
count	2224	2224	2224	2224	2224	2224	2224	2224
mean	31.79	21.53	2.81	28.11	18.17	30.91	12.74	698.28
std	6.21	10.81	2.63	43.98	2.05	6.28	4.54	369.32
min	23.10	3.60	0.10	2.00	15.00	21.00	5.00	252.02
25 %	27.90	10.65	0.51	6.42	16.00	25.83	9.09	391.59
50 %	30.44	21.08	2.00	8.94	18.95	31.00	12.13	609.66
75 %	33.69	30.97	4.59	23.47	19.55	34.46	15.00	882.10
max	56.72	51.38	11.60	260.00	23.00	51.00	29.00	1609.14

Table 5.9: Descriptive statistics of the laboratory data for machine learning. For each variable, the number of data points, the mean, the standard deviation, the minimum value, the maximum value, the 25^{th}, 50^{th}, and 75^{th} percentile are provided.

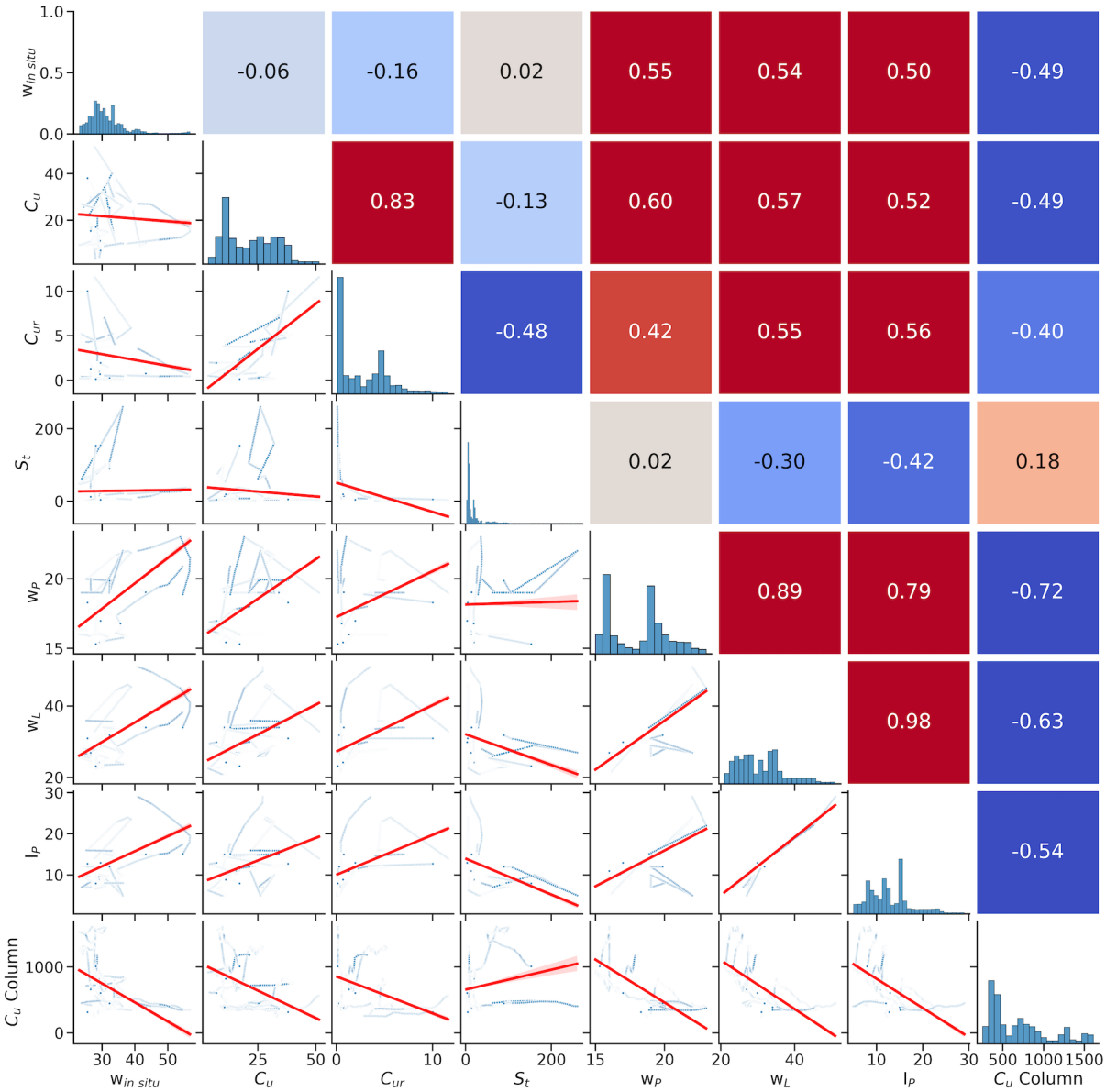

Figure 5.11: The Scatter Plot Matrix for the laboratory database for machine learning. The lower triangle shows scatter plots with the corresponding regression line, the diagonal shows the histograms, and the upper triangle shows the correlations. The shaded areas around the regression lines represent the uncertainty in the estimation.

5.2.4.1 Regression with Gradient Boosting and Random Forest

In Table 5.10, the performance from the Gradient Boosting and Random Forest models are summarized. As for the CPTU models, they seem to be able to predict the stabilized shear strength based on the data they were trained on. Both models gave negative R^2 values based on the validation set, but the performance from Random Forest was worse than for Gradient Boosting, with an R^2 value of -1.38 compared to -0.69. The performance plots for the two laboratory models are given in Figure 5.12 and Figure 5.13.

Model	Training			Testing		
	R^2	RMSE	MAE	R^2	RMSE	MAE
Gradient Boosting	1.00	15.23	11.06	-0.69	233.09	173.05
Random Forest	1.00	2.39	0.82	-1.38	276.60	234.42

Table 5.10: Summary of the performance from the laboratory machine learning models.

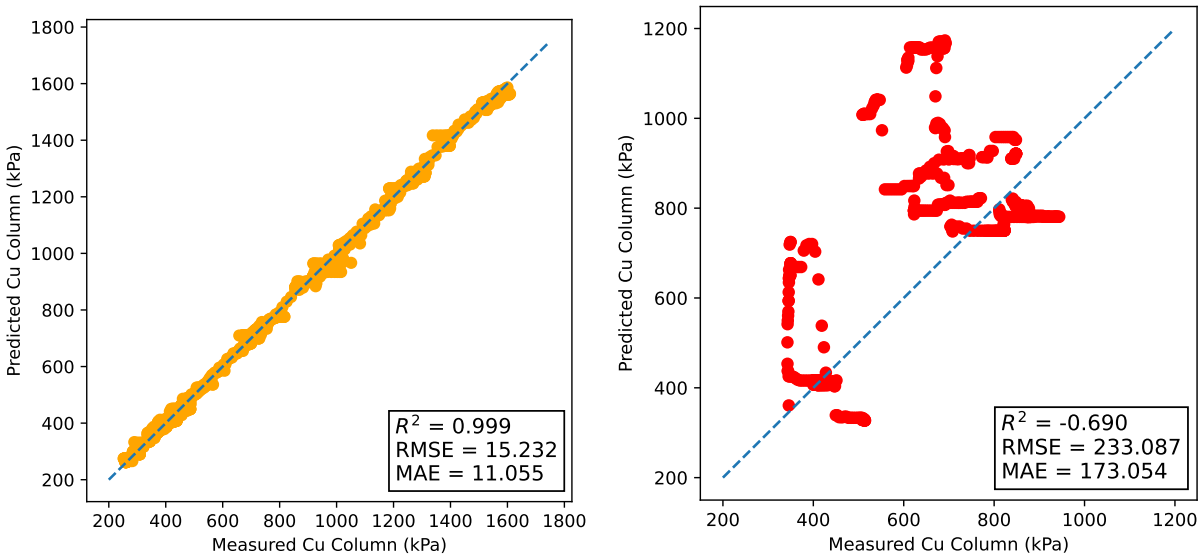

(a) Training data Lab E6. **(b)** Testing data Lab E6.

Figure 5.12: The difference in performance for testing and training data from Gradient Boosting.

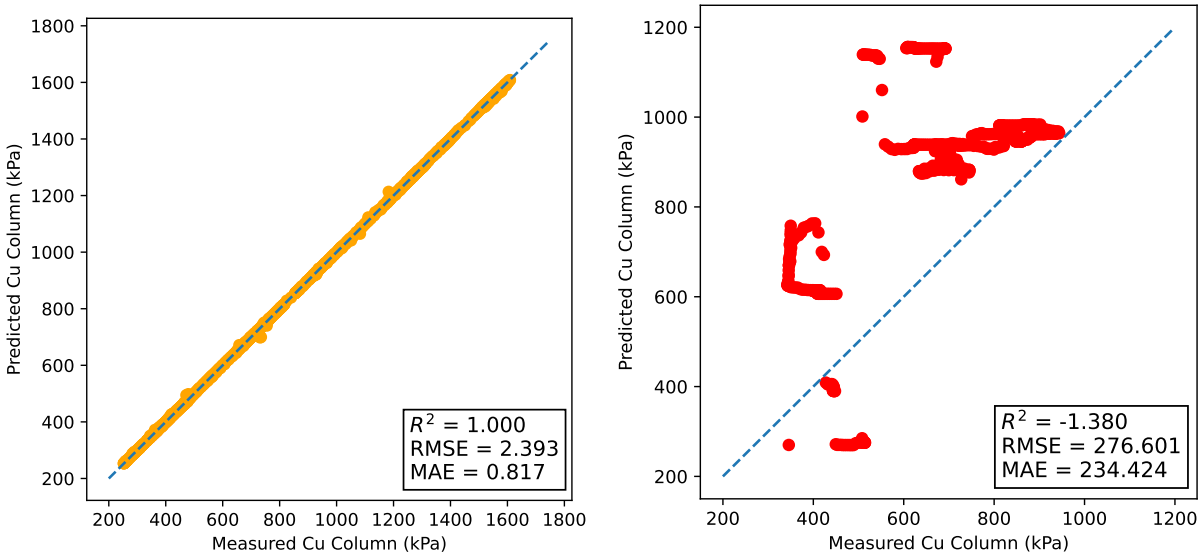

(a) Training data Lab E6. **(b)** Testing data Lab E6.

Figure 5.13: The difference in performance for testing and training data from Random Forest.

Since less laboratory data were available compared to CPTU, only one column was left for validation. In Figure 5.14, the predictions are displayed against this column's elevation and measured strength. Although there was a large difference in the R^2 value of the two models used, the predictions were quite similar. However, it seems like Random Forest overestimated the

strength of the column to a greater extent than Gradient Boosting.

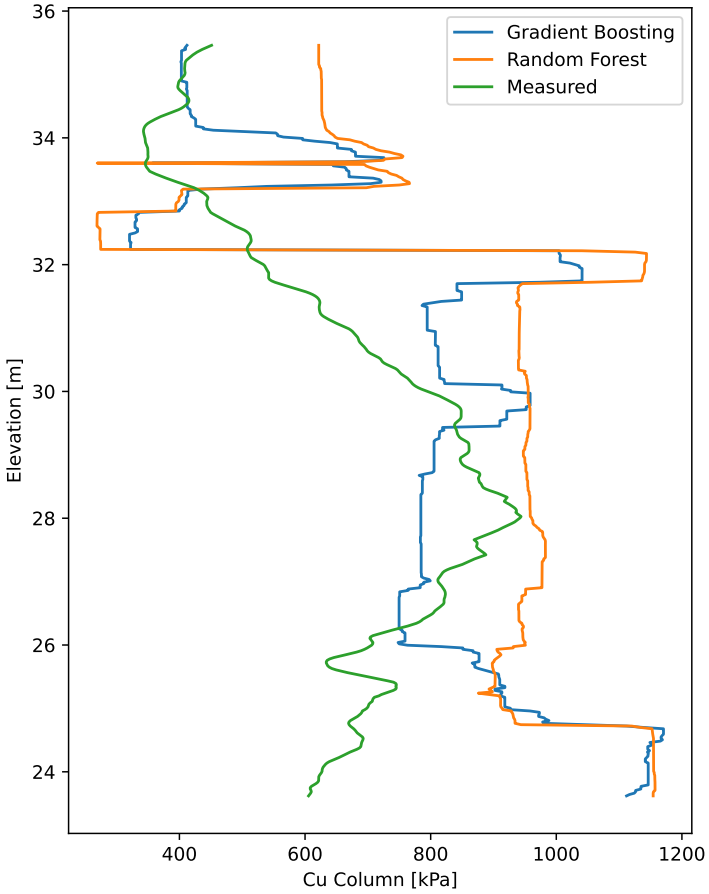

Figure 5.14: The predicted shears strength from Gradient Boosting and Random Forest compared with the actual shear strength.

5.3 The Norwegian Database

5.3.1 Correlation Analysis Norwegian Database

In Table 5.11, the descriptive statistics for the Norwegian database are provided. There were varying degrees of data points for the different variables, where sensitivity and CKD content were the ones with the fewest. Compared with the laboratory database from E6 Kvithammar-Åsen, values were more evenly distributed within a wider range for the different variables. On the other hand, due to the predominant use of the binder quantity of 100 kg/m^3 with a 50/50 mixture of either lime or CKD along with cement, there was very little variation in binder variables. In Figure 5.15, the clear peak in the histograms indicates this observation. This is particularly evident for cement, where this peak is prominent.

	$w_{in\,situ}$ [%]	S_t [–]	γ [kN/m^3]	w_P [%]	w_L [%]	I_P [%]	I_L [–]	Lime cont. [kg/m^3]	Cem. cont. [kg/m^3]	CKD cont. [kg/m^3]	Porosity unstab. [–]	wbr [–]	C_u, 28 days [kPa]
count	256	86	246	195	198	195	195	192	292	108	246	246	292
mean	34.74	42.58	18.65	19.87	33.13	13.18	1.37	46.27	52.33	46.31	0.48	4.90	224.13
std	7.36	57.28	0.86	3.82	9.70	6.95	0.76	10.10	10.78	12.41	0.05	0.90	92.87
min	20.00	3.50	16.90	15.00	18.00	3.00	0.00	23.75	25.00	19.00	0.37	3.45	30.23
25 %	29.00	8.00	17.90	16.50	23.50	7.25	0.78	45.00	50.00	50.00	0.44	4.37	165.81
50 %	33.25	21.67	18.60	19.50	33.00	12.00	1.20	50.00	50.00	50.00	0.49	4.76	207.32
75 %	40.60	62.00	19.30	22.00	40.00	18.80	1.83	52.50	53.50	50.00	0.53	5.28	281.68
max	59.00	280.00	20.60	38.00	67.50	29.80	4.33	75.00	90.00	75.00	0.61	7.89	516.48

Table 5.11: Descriptive statistics of the Norwegian database. For each variable, the number of data points, the mean, the standard deviation, the minimum value, the maximum value, the 25^{th}, 50^{th}, and 75^{th} percentile are provided.

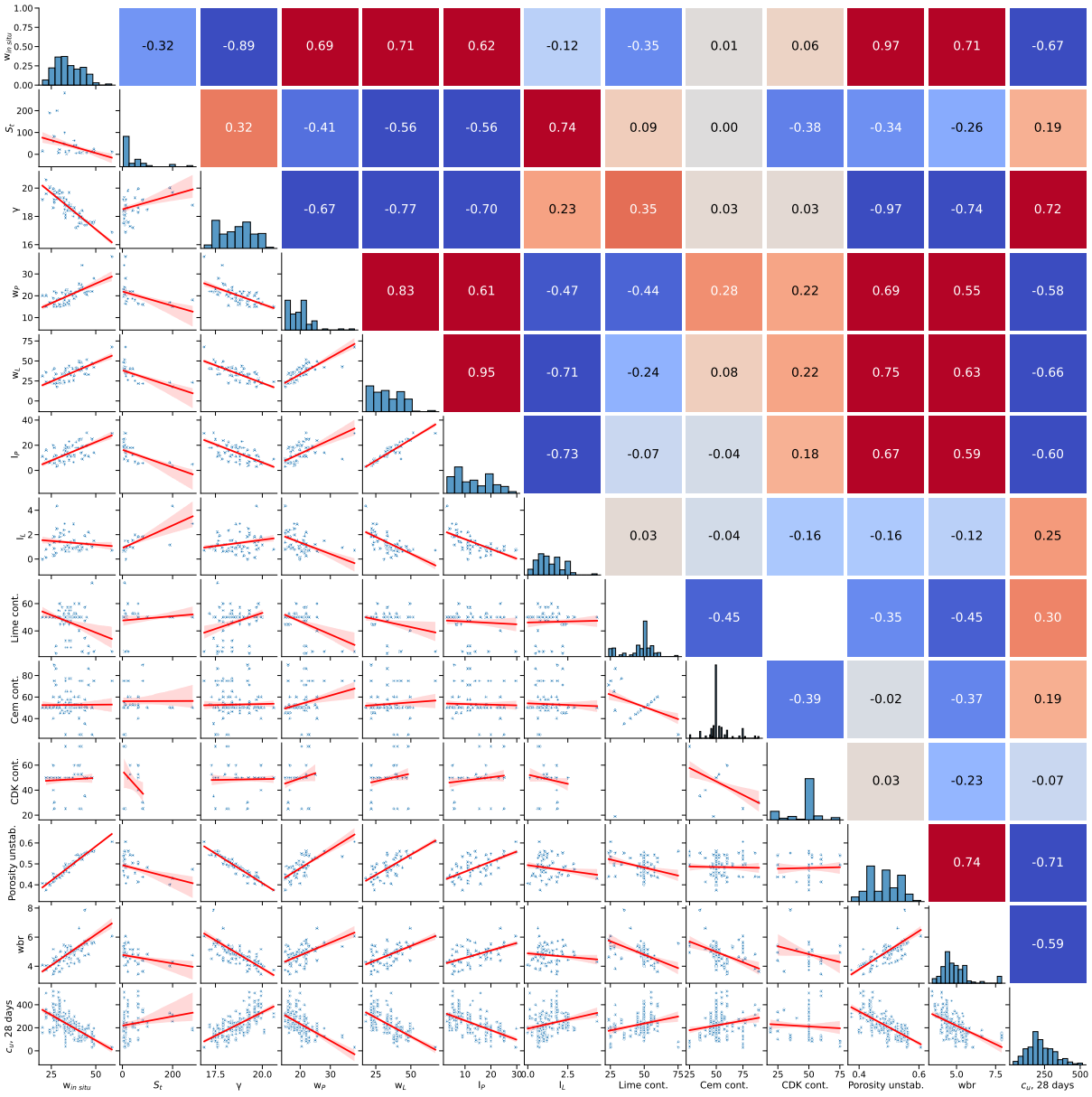

Figure 5.15: The Scatter Plot Matrix of the Norwegian database. The lower triangle shows scatter plots with the corresponding regression line, the diagonal shows the histograms, and the upper triangle shows the correlations. The shaded areas around the regression lines represent the uncertainty in the estimation.

The correlation coefficients in Figure 5.15 are summarized in Table 5.12. The correlations were

calculated between the laboratory data and the stabilized shear strength of the soil samples. There were large variations in the calculated correlations, ranging from -0.71 to 0.72, and R^2 values varied from 0.01 to 0.52.

Variable	Symbol	Count	R	R^2
Water content	$w_{\text{in situ}}$	256	-0.67	0.45
Sensitivity	S_t	86	0.19	0.04
Unit weight	γ	246	0.72	0.52
Plastic limit	w_P	195	-0.58	0.34
Liquid limit	w_L	198	-0.66	0.44
Plasticity index	I_P	195	-0.60	0.36
Liquidity index	I_L	195	0.25	0.06
Lime content	-	192	0.30	0.09
Cement content	-	292	0.19	0.04
CKD content	-	108	-0.07	0.01
Porosity unstabilized	-	246	-0.71	0.50
Water binder ratio	wbr	246	-0.59	0.35

Table 5.12: Linear correlations between the laboratory data and the stabilized strength from the Norwegian database.

5.3.2 Curve Fitting Water Binder Ratio

The relationship between shear strength and the corrected water binder ratio, as described in [4], was compared with the Norwegian database. The newly calculated equation differed significantly, as seen in Figure 5.16. There were generally too low shear strengths for what the given water binder ratio value should have indicated. In this analysis, the corrected water binder ratio was not used since there was no information regarding the active CaO percentage in the various binders used in the Norwegian database.

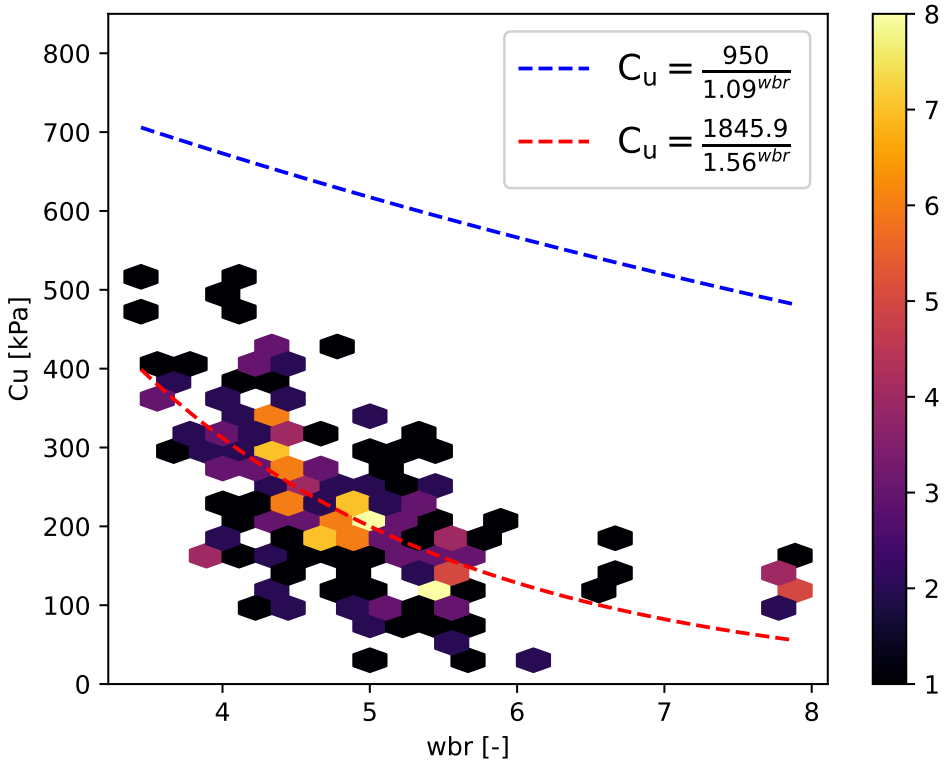

Figure 5.16: Curve fitting wbr from the Norwegian database. The red dotted line shows the equation found by curve fitting, the blue is from [4].

5.3.3 Regression with Gradient Boosting and Random Forest

The Norwegian database showed variations in the number of data points across the different given variables. To be able to train the machine learning algorithms, the missing values had to be handled. Firstly the Lime and CKD content columns were removed since the database only consisted of a few data points where all three binder types were used together. Furthermore, all sensitivity values were removed since this feature had significantly less data than the other variables. The final step was the removal of any row with a missing value. After preparing the database for further analysis with machine learning, 185 data points remained for each variable. The established models were made with these features: Water content, unit weight, plastic limit, liquid limit, plasticity index, liquidity index, cement content, porosity unstabilized, and water binder ratio.

The performance of the best fit from the models is shown in Table 5.13. As seen, the two models generally had little difference in performance. The performance was significantly improved compared to the models based on field data. The highest performance from the models based on the Norwegian database had an R^2 value of 0.82. This performance differs from the highest-performing model in the E6 laboratory database, where the best achieved R^2 value was -0.69.

Model	Training			Testing		
	R^2	RMSE	MAE	R^2	RMSE	MAE
Gradient Boosting	0.89	32.07	21.61	0.82	44.72	32.68
Random Forest	0.88	35.56	24.96	0.79	38.80	29.91

Table 5.13: Summary of the performance of the models from the Norwegian database.

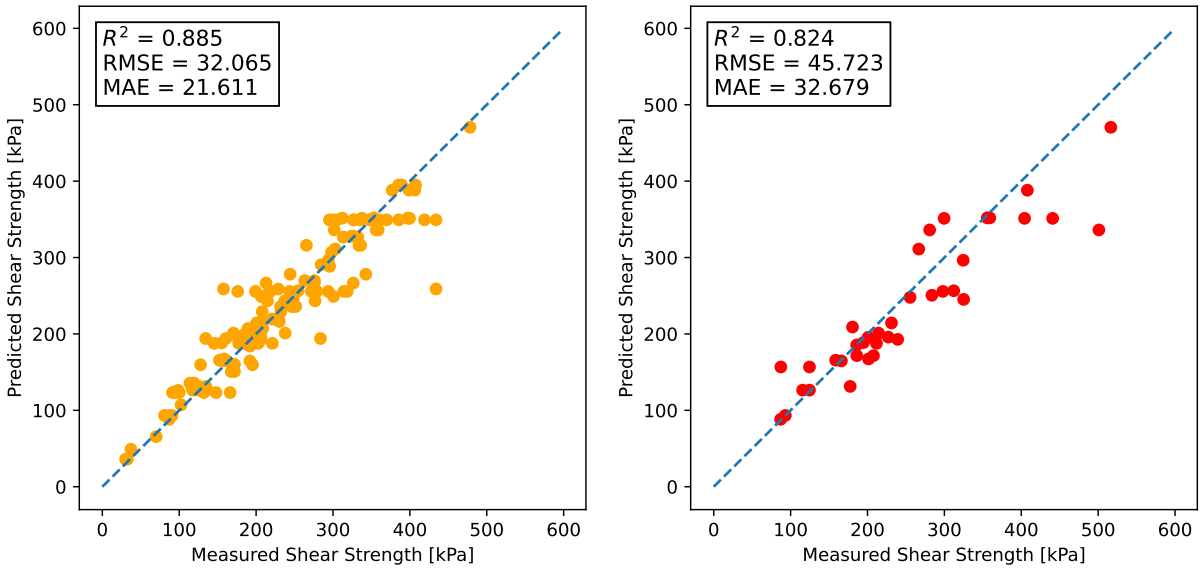

(a) Training data Norwegian database. **(b)** Testing data Norwegian database.

Figure 5.17: The difference in performance for the training and testing set from the Norwegian database from Gradient Boosting.

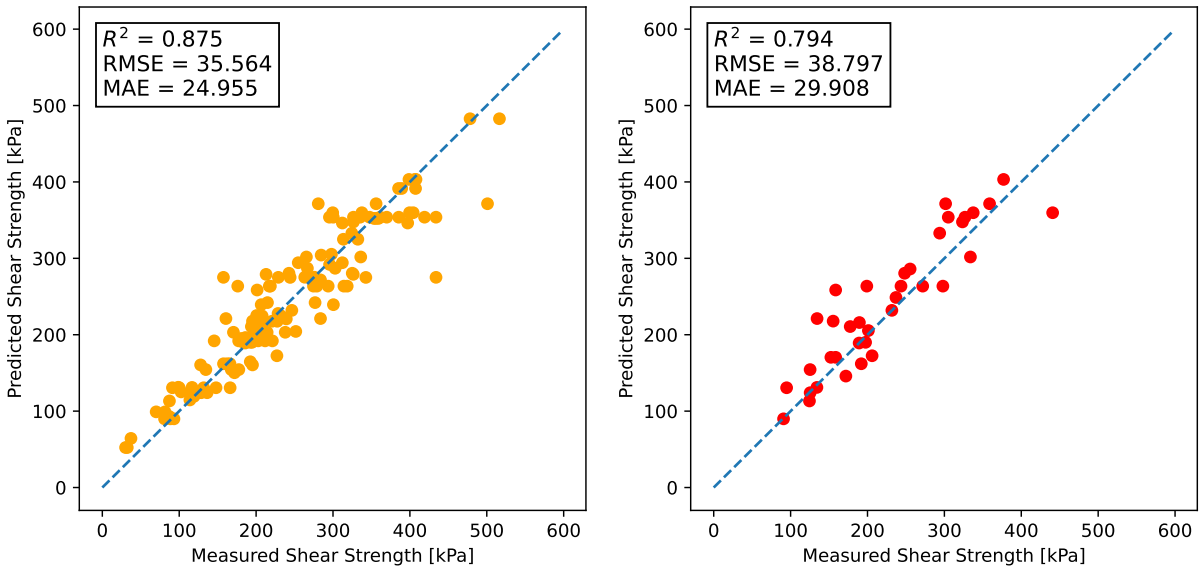

(a) Training data Norwegian database. **(b)** Testing data Norwegian database.

Figure 5.18: The difference in performance for the training and testing set from the Norwegian database from Random Forest.

The permutation importance is a method that can be used to rank how important the different training properties are to the model. The permutation score is found by shuffling the different variables randomly and then evaluating whether it impacts the model's performance. Each feature in the model is given a score between 0 and 1, where the total sum adds up to 1. This was calculated for the Gradient Boosting and Random Forest model features, as shown in Figure 5.19. The calculation was done by using Scikit-Learn. From the permutation feature importance of the models from the Norwegian models, the porosity had the highest importance, with a score > 0.4. The water binder ratio and unit weight also seemed to influence the performance of the models.

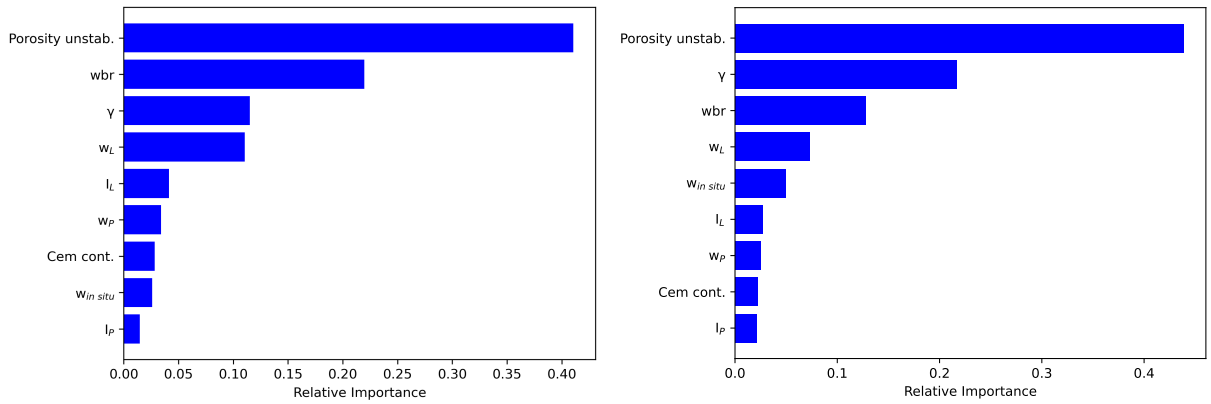

(a) Gradient Boosting **(b)** Random Forest

Figure 5.19: The permutation importance for the two models.

To explore the importance of each parameter further, machine learning models were created where each variable independently predicted the shear strength of the stabilized soil. Sensitivity, Lime content, and CKD content could be analyzed since only individual parameters would be assessed. Large differences in performance were observed within the individual models. To minimize the risk that the R^2 value from the best fit from a given model was an outlier, the average R^2 value from 10-fold cross-validation was used. These R^2 values are summarized in Figure 5.20. All variables, except cement content, had an R^2 value ≥ 0.4. The porosity was the best-performing parameter, with an R^2 value of 0.67.

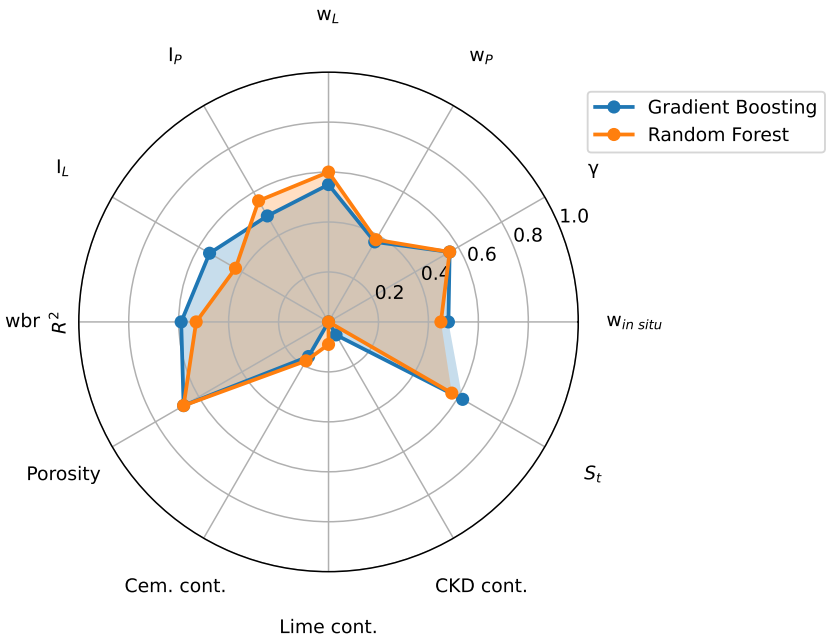

Figure 5.20: Each parameter's ability to predict the stabilized shear strength alone, visualized by the mean cross-validation score, R^2.

5.4 The Swedish Database

5.4.1 Correlation Analysis Swedish Database

From Table 5.14 and Figure 5.21, it can be seen that the Swedish soils are different from the Norwegian. The water content of Norwegian soils typically varies from ∼20-60%. The range of the water content from the Swedish database was much broader, with a variation between ∼30-270%. To be able to stabilize soil with such high water content, large quantities of binder are needed. This compensating binder amount can be seen in Table 5.14, where up to 400 kg/m^3 of cement was used to stabilize the soils.

	ρ $[Mg/m^3]$	$w_{in\,situ}$ [%]	Lime cont. $[kg/m^3]$	Cem. cont. $[kg/m^3]$	CKD cont. $[kg/m^3]$	Porosity unstab. [–]	Dry weight clay $[kg/m^3]$	wbr [–]	C_u, 28 days $[kPa]$
count	874	874	473	874	383	874	874	874	874
mean	1.56	72.58	43.36	68.42	55.32	0.64	993.96	5.99	180.56
std	0.15	36.38	14.54	41.62	22.20	0.08	194.59	1.38	81.44
min	1.09	34.00	17.50	27.00	12.00	0.47	396.56	2.14	23.98
25 %	1.49	52.00	33.00	45.00	45.00	0.58	872.29	5.17	129.80
50 %	1.59	60.00	40.00	60.00	50.00	0.63	1055.29	5.92	169.65
75 %	1.68	80.00	50.00	75.00	60.00	0.69	1136.71	6.94	216.75
max	1.87	272.00	105.00	400.00	200.00	0.89	1496.61	10.13	636.58

Table 5.14: Descriptive statistics of the Swedish database. For each variable, the number of data points, the mean, the standard deviation, the minimum value, the maximum value, the 25^{th}, 50^{th}, and 75^{th} percentile are provided.

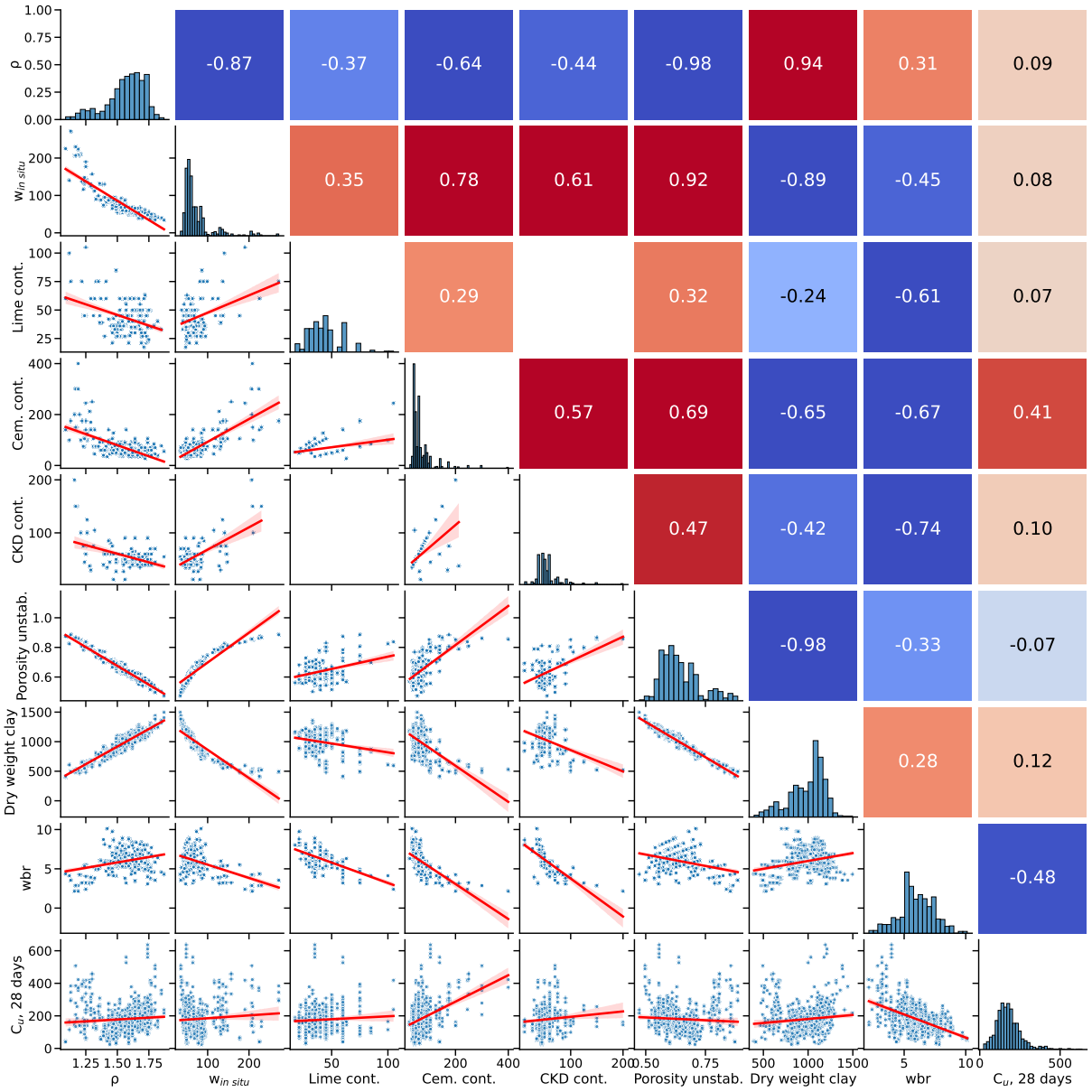

Figure 5.21: The Scatter Plot Matrix of the Swedish database. The lower triangle shows scatter plots with the corresponding regression line, the diagonal shows the histograms, and the upper triangle shows the correlations. The shaded areas around the regression lines represent the uncertainty in the estimation.

The results from the linear correlation analyses between the stabilized strength and the remaining variables are visualized in Table 5.15. Only the cement content and the water binder ratio correlated with the stabilized strength from the given variables. The remaining parameters showed correlation coefficients weaker than $\pm$ 0.12, corresponding to an R^2 value of 0.01.

Variable	Symbol	Count	R	R^2
Bulk density	ρ	874	0.09	0.01
Water content	$w_{in\,situ}$	874	0.08	0.01
Lime content	-	473	0.07	0.01
Cement content	-	874	0.41	0.17
CKD content	-	383	0.10	0.01
Porosity unstabilized	-	874	-0.07	0.01
Dry weight clay	-	874	0.12	0.01
Water binder ratio	wbr	874	-0.48	0.23

Table 5.15: Linear correlations between the laboratory data and the stabilized strength from the Swedish database.

5.4.2 Curve Fitting Water Binder Ratio

In [2], the relationship between the ultimate compressive strength and the water binder ratio is described. The Figure 5.22 has included the lower and upper limits from the curve fittings made in [2]. These were based on Swedish organic clays and gyttja, and inorganic clays. As seen from the red dotted line in Figure 5.22, the newly calculated equation established itself between the upper and lower boundary. The data in this analysis was based on the same dataset as [2].

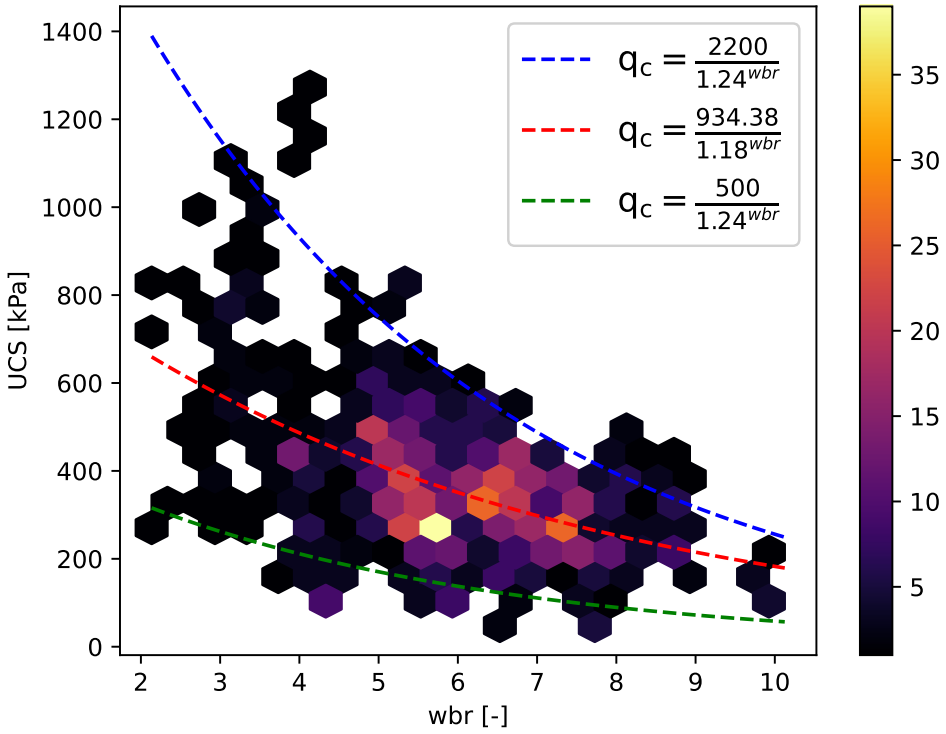

Figure 5.22: Curve fitting wbr from the Swedish database. The green dotted line is given for organic clays and gyttja, while the blue dotted line is established for inorganic clays. The red dotted line is found from the curve fitting analysis.

5.4.3 Regression with Gradient Boosting and Random Forest

The number of data points for the different variables was more similar in the Swedish database. However, Lime and CKD content was removed before the machine learning models could be created on the data. The initial water content, bulk density, porosity, water binder ratio, cement

content, and dry weight clay were used. Each variable had 874 data points. Compared to the Norwegian database, this was about five times more data points used for the machine learning analysis.

In Table 5.16, the performance of the best fit from Gradient Boosting and Random Forest models are compared. As seen from the testing sets, the models had varying capabilities in predicting the shear strength, visualized by an R^2 value between 0.71 to 0.80, where Random Forest performed the best. Of the two, Random Forest performed best based on the training data. The performance plots for the two models are shown in Figure 5.23 and Figure 5.24.

Model	Training			Testing		
	R^2	RMSE	MAE	R^2	RMSE	MAE
Gradient Boosting	0.83	33.04	25.75	0.71	44.84	33.94
Random Forest	0.95	17.91	12.69	0.80	38.62	28.76

Table 5.16: Summary of the performance of the models from the Swedish database.

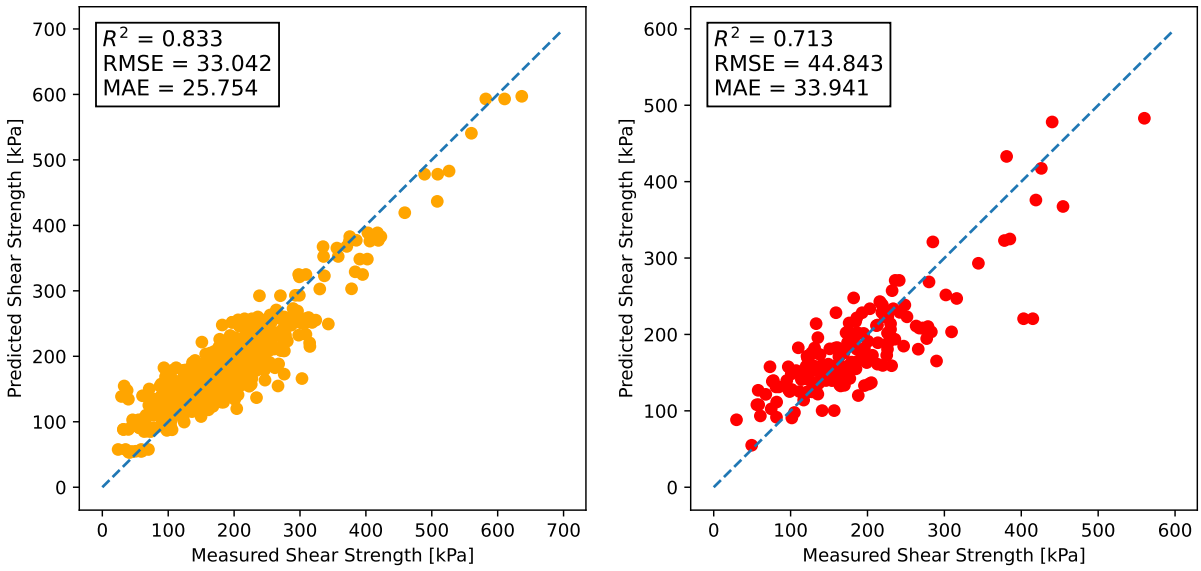

(a) Training data Swedish database.

(b) Testing data Swedish database.

Figure 5.23: The difference in performance for the training and testing set from the Swedish database from Gradient Boosting.

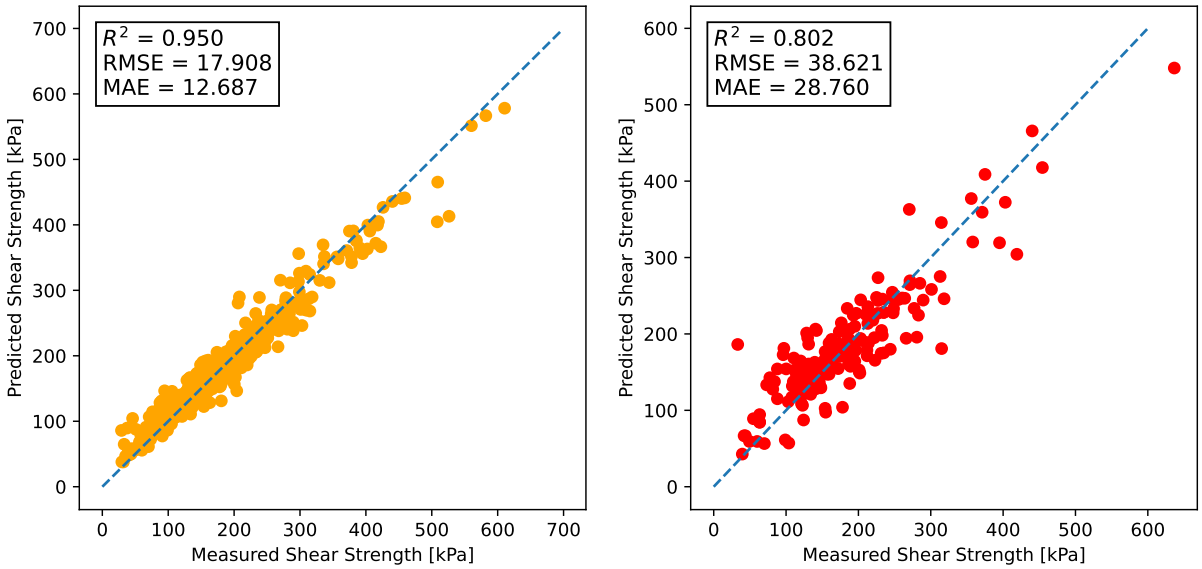

(a) Training data Swedish database. **(b)** Testing data Swedish database.

Figure 5.24: The difference in performance for the training and testing set from the Swedish database from Random Forest.

From the permutation importance analysis of the two models, as seen in Figure 5.25, the water binder ratio seemed to have the biggest influence on the performance of the models.

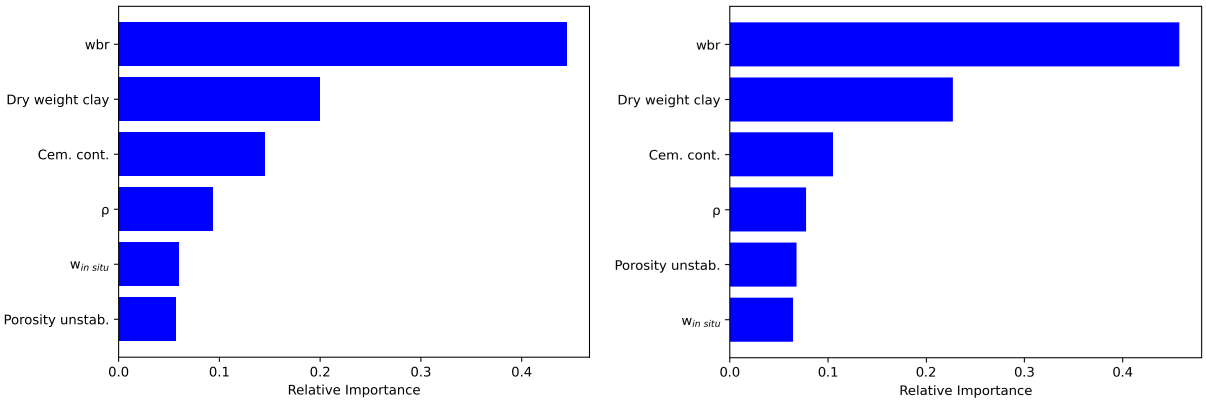

(a) Gradient Boosting **(b)** Random Forest

Figure 5.25: The permutation importance for the two models from the Swedish database.

A similar analysis of parameter importance, as for the Norwegian database, was conducted for the Swedish database. The result is shown in Figure 5.26. As seen, the water binder ratio performed the best, where the Random forest model had an R^2 value of 0.69. This was about the same R^2 value as the Gradient Boosting model with all the features.

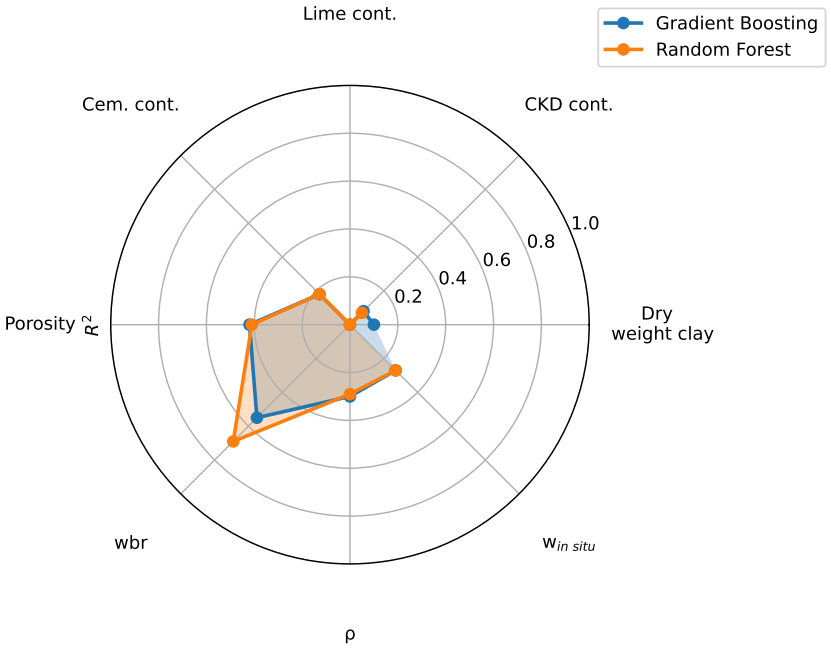

Figure 5.26: Each parameter's ability to predict the stabilized shear strength alone, visualized by the mean cross-validation score, R^2.

6 Discussion

This chapter is divided into four sections. First, the CPTU results are discussed in Section 6.1 followed by the discussion of the laboratory results in Section 6.2. In Section 6.3, the fitted curves from the water binder ratios are discussed and compared with the established relationships from the literature. In the final section, Section 6.4, the performance of the different machine learning models is discussed.

6.1 Correlation analyses CPTU Data

According to [40], it is possible to assume the given type of soil based on the cone resistance q_c and the pore-pressure ratio B_q. Overconsolidated stiff soil is categorized with a high q_c and a corresponding B_q of 0. On the other hand, very soft clays are typically featured with low q_c values and B_q values in the interval 1-1.2. Since softer soils require less energy to sufficiently mix and distribute the binder evenly, more uniform columns with higher shear strength can be expected. This hypothesis has been explored by comparing it with the correlations found in the CPTU database from E6 Kvithammar-Åsen.

In Section 5.1.1, various correlation analyses were performed. There were challenges related to the fact that the CPTUs were not performed at the exact same coordinate as the stabilized columns. Therefore, it was assumed that the CPTU closest to each stabilized column was the most correct. However, due to cases with large distances between performed tests, it was uncertain whether the given CPTU values corresponded to the ground conditions where the stabilized columns were located. Therefore, in the correlation analyses in Section 5.1.2, the distance between the tests performed was considered. The data were grouped by distance and divided into 20 m intervals. The innermost interval, consisting of only data pairs with a maximum distance of 20 m, was considered the most correct. This analysis gave the correlation coefficients for q_c of -0.13 and B_q of 0.22. Although the given variables correlated in the direction that suggested increased strength with softer and more sensitive clays, the correlations were too weak to establish a real pattern. This also applied to the remaining variables: Q_t, f_s, F_r and u_2. None of these parameters showed any clear correlation with the column strength. Of all variables, u_2 had the highest correlation with the column strength, with an R^2 of 0.05. This indicates that providing accurate predictions about the column strength is difficult based on only CPTU data.

From the correlation analysis carried out in Section 5.1.2, it could indicate that some of the variables were dependent on depth. Furthermore, it could be seen in Figure 5.1 that u_2 correlated with the shear strength of the stabilized columns, with a correlation coefficient of 0.61, indicating a relatively strong relationship. Further analysis was performed to ensure that the established correlations were not simply based on the column's shear strength increasing with depth. In the performed correlation analyses, where only the innermost distance interval was analyzed, no correlation was identified between depth and column strength. The established correlation coefficient was given by 0.14, or an R^2 value of 0.02. However, the data was explored further by grouping it based on depth level. The groups were based on two-meter intervals all the way down to 15 m, where correlation calculations were performed for each interval. It was decided not to go deeper than 15 m due to few data points. The results of this analysis are given in Figure 6.1. The depth and shear strength correlation ranged from around -0.12 to 0.15. This implied that there was no detectable correlation between an increase in shear strength and an increase in depth.

Figure 6.1 further shows how the remaining variables correlated with the column strength at the different depth intervals. The number of data points used to calculate the various correlations is given in Figure D11.1.

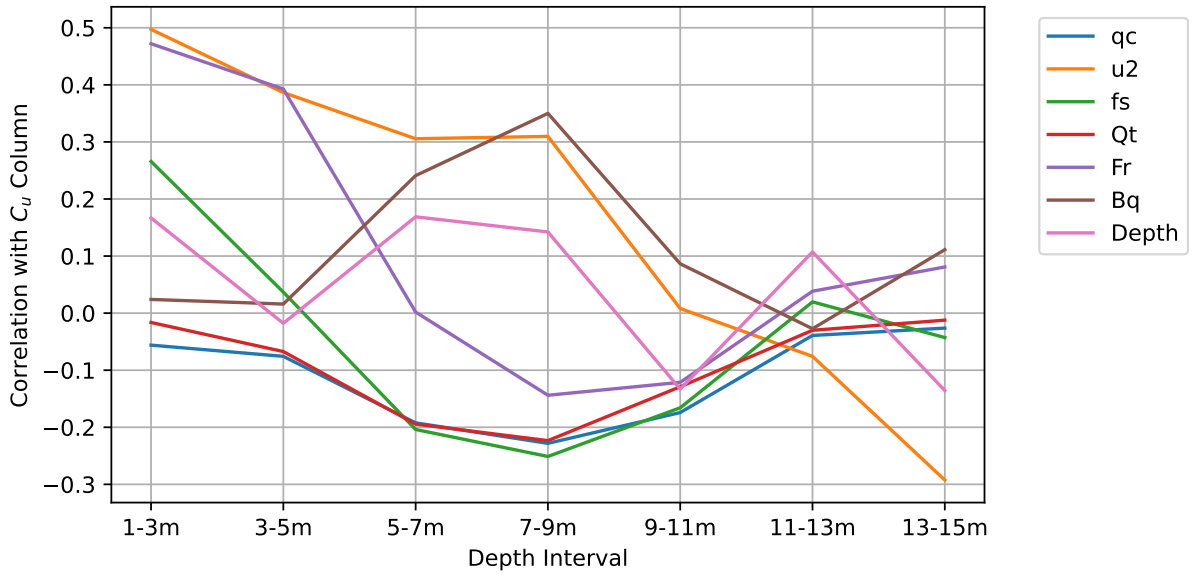

Figure 6.1: The correlation of the CPTU data and Cu Column at different depths. The different correlations are calculated based on 2 m intervals.

6.2 Correlation analyses Laboratory Data

6.2.1 E6 Kvithammar-Åsen

The correlation analyses between the stabilized columns and their closest performed laboratory test point had the same challenge as the CPTU data, with large distances between data pairs. The distances were even greater for the Laboratory data than the CPTU data, meaning even more uncertainty. Weak correlations were observed for the correlation analysis, as seen in Table 5.7, where the correlation coefficients varied from -0.37 to 0.10. Nevertheless, the correlations were improved after removing the data pair with the highest uncertainty caused by large distances. The results of the correlation analysis, considering the spatial variability, showed that the correlations appear to be consistent within 40 m between the data pairs. The results of this analysis, as depicted in Table 5.8, revealed correlation coefficients ranging from -0.60 to 0.32.

In Section 2.2, the strength development in DDM soils with the influencing factors were presented. The strength development is divided into four main categories: Characteristics of stabilizing agent, characteristics and conditions of soil, mixing conditions, and curing conditions. The strength development of the stabilized columns in the E6 Kvithammar-Åsen project can be described primarily by the characteristics and conditions of the soil and the curing conditions. Since all columns in the project utilized the same binder, binder quantity, and BRN, these variables were assumed to have a negligible impact on the difference in shear strength in the columns.

The correlations between the column strength and the soil water content, liquid limit, plastic limit, and plasticity index are summarized in Table 6.1 and Table 6.2. The established correlations from the E6 Kvithammar-Åsen project are comparable to other established relationships where similar studies have been conducted, except for the plastic limit from [14]. Furthermore, the

trends found in the laboratory analysis are consistent with what is expected from the theory. The linear correlations correspond to an R^2 value in the interval 0.21 to 0.36, which suggests that weak correlations have been found.

Reference	Correlation with undrained shear strength		
	w_P	w_L	I_P
E6 Kvithammar-Åsen	-0.60	-0.52	-0.46
Tran, 2022 [14]	0.16	-0.27	-0.34
Tinoco, 2021 [15]	-0.53	-0.59	-
Das, 2011 [16]	-	-0.50	-0.55

Table 6.1: Comparison of correlations between stabilized shear strength and Atterberg limits.

Reference	Correlation with undrained shear strength
	$w_{\text{in situ}}$
E6 Kvithammar-Åsen	-0.49
Tinoco, 2021 [15]	-0.62
Das 2011 [16]	-0.52

Table 6.2: Comparison of correlations between stabilized shear strength and water content.

The correlation matrix in Figure 5.7 shows strong correlations between water content and the unit weight, bulk density, porosity, and water binder ratio. The unit weight and bulk density were negatively correlated with water content, as indicated by a correlation coefficient -0.84. This means that an increase in water content results in a decrease in unit weight and bulk density. Both variables correlated with the column strength with a correlation coefficient of 0.32. A positive correlation was expected, as a higher unit weight and bulk density indicate a lower water content, which is known to increase the strength of the stabilized soil.

Figure 5.7 further shows the correlation between the water content against porosity and water binder ratio, indicated by a correlation coefficient of 0.97. This suggests a near-perfect linear relationship, which was expected because the porosity was calculated based on the water content. The porosity is a measure of the level of voids in a material. In soils with higher porosity, there will be room for more water. This was reflected in the correlation coefficient of -0.47 between porosity and column strength, which means an increase in porosity leads to a reduction in strength. The water binder number showed identical correlations to porosity since the calculation was derived from the porosity divided by the binder quantity. In the E6 Kvithammar-Åsen project, all columns were executed with the same binder quantity. This meant the water binder ratio would only be a scaled version of the porosity. However, the correlation was consistent with what was expected, where a higher water binder ratio resulted in a lower strength.

The shear strengths of the unstabilized clay from both uniaxial compression and fall cone all showed zero correlation with the column strength. This is consistent with the results from [12].

In the CPTU analysis, it could not be proven that the softer the clay, the higher the stabilized strength. This seemed to be consistent with the findings from the laboratory analysis. The remolded shear strength, sensitivity, and liquidity index all showed zero correlation with the column strength.

As seen in Figure 5.7, the shear strength from uniaxial compression and the sensitivity shows a

moderate positive correlation with depth. Even though the correlation between the depth and column strength was given by a correlation coefficient of 0.08 (Table 5.8), which indicated zero correlation, a correlation analysis was performed concerning the depth effect. In Figure 6.2, the correlation between the various laboratory parameters and the shear strength of the stabilized columns was calculated based on 2 meters depth intervals. This eliminated the effect of in-situ stress, which increases with depth. Only the data with a maximum of 40 m between the stabilized columns and the laboratory test points were used in this analysis. Based on the results in Figure 6.2, the shear strength did not appear to depend on depth. The correlations varied from weak positive in the uppermost meters and decreased to weakly negative in the lower meters. The figure also shows how the remaining variables correlated with the shear strength at various depth intervals. The number of data points used to calculate the various correlations is given in Figure D13.1.

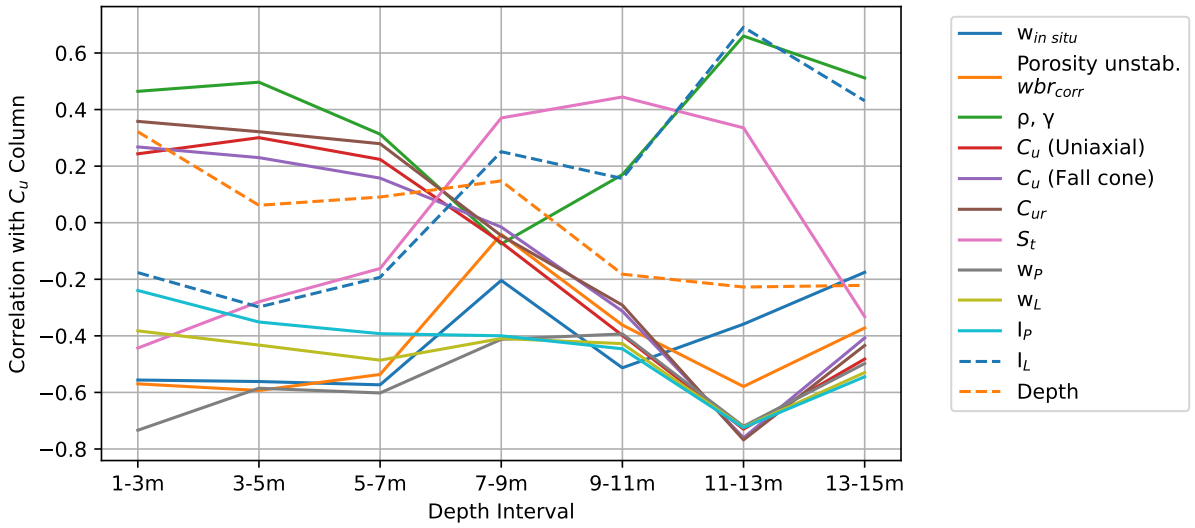

Figure 6.2: The correlation of the Lab data with C_u Column at different depth intervals.

6.2.2 The Norwegian and Swedish Databases

Although greater uncertainties were associated with the field data from E6 Kvithammar-Åsen, the correlations were more or less consistent with the Norwegian database, as seen in Figure 6.3. However, the general trend was that the correlations were stronger in the Norwegian database. The reason for the improved correlations may be due to the laboratory test being performed under controlled conditions. This makes it less likely that external factors have affected the result. Standardized tests are used in the laboratory, where strict standards are followed to minimize uncertainty. The same ideal conditions for testing are difficult to replicate in the field.

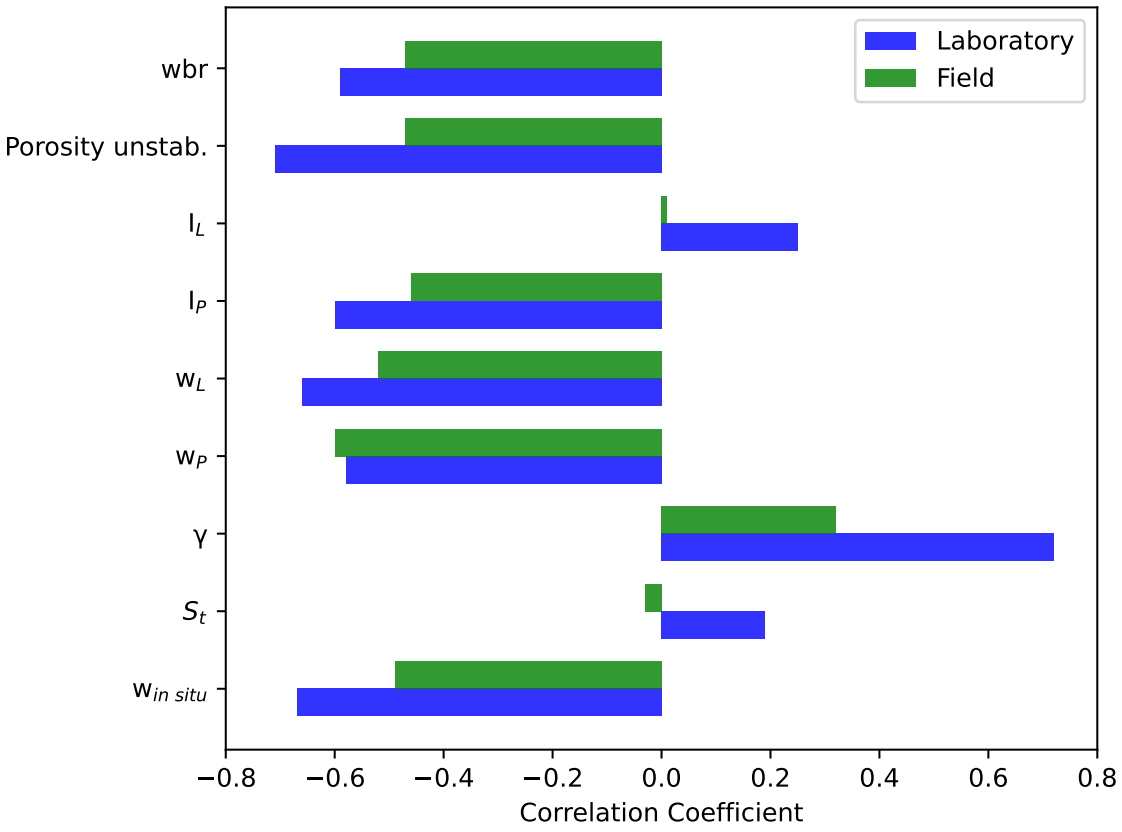

Figure 6.3: Comparison of correlations between the Norwegian database and the correlations from the Laboratory database from E6 Kvithammar-Åsen.

In Figure 6.4, the correlation between the shear strength of the stabilized soil of the common variables from the Swedish and Norwegian databases is summarized. Surprisingly, the water content from the Swedish database did not affect the stabilized strength as it should, according to theory. The correlation was slightly positive, the opposite of what was expected. The reason for the lack of correlation was that the Swedish database consisted of soils with a water content of up to 270%. To stabilize these soils, a lot of cement was needed. This connection can be seen in Figure 5.21, where a positive correlation of 0.78 between water and cement content exists. In the scatter plot between these two variables (Figure 5.21), it is evident that soils with high water content still can achieve a high shear strength if they are stabilized with a sufficient amount of cement. In Table 6.3, the correlation between the water content and the stabilized shear strength from the Swedish database is compared to a similar study by [18], where Irish Moss Peat with a mean water content 400% was used. The quantity of binder was between 100–500 kg/m^3. It can be observed that the correlations in both studies are roughly similar. Since the porosity was calculated based on the water content, it was natural that the correlations were correspondingly low for the Swedish and high for the Norwegian database.

Reference	Correlation with UCS/τ_{max}
	$w_{\text{in situ}}$
Swedish Database	0.08
Yousefpour, 2021 [18]	-0.09

Table 6.3: Comparison of correlations between stabilized shear strength and water content for the Swedish Database.

There were differences in how well the binders performed for the different soil conditions in Norway and Sweden. Lime seemed to have a better-stabilizing effect than cement for Norwegian soil, which was the opposite compared to Swedish soil. CKD appeared to have little influence on the strength increase in both databases. It was difficult to draw any conclusions from these results, as there was little variation in the amount of binder in the Norwegian database, which may have affected the result. Furthermore, it was somewhat surprising that lime showed the highest correlation in the Norwegian database. Cement is usually the binder that gives the earliest strength development, while lime usually has a long-term strength development. Due to the relatively short curing times, assessing how much the pozzolanic reactions had affected the stabilized strengths was difficult. However, the soil was not stabilized with lime alone, it was a mixture with cement. Lime also has another property that generates much heat in contact with water. It is possible that the heat from the lime provided good conditions for the hydration process. Since the pozzolanic reactions are highly temperature dependent, this may indicate that the Norwegian soils reacted better to the pozzolanic reactions than the Swedish ones.

The water binder ratio was the only variable that showed consistent correlations from the Norwegian, Swedish, and E6 Kvithammar-Åsen databases, with correlation coefficients ranging from -0.47 to -0.59.

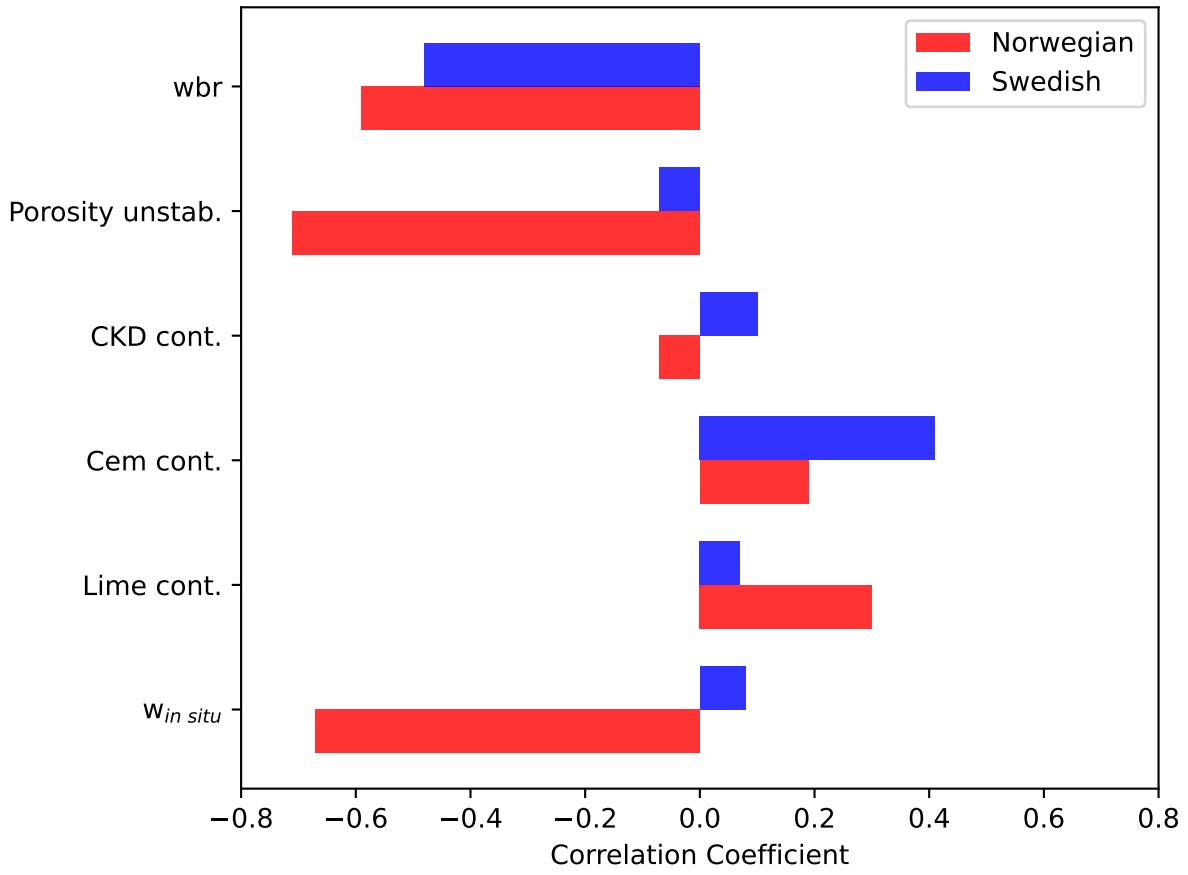

Figure 6.4: Comparison of the common variables' correlation with the stabilized soil's shear strength from the Swedish and Norwegian databases.

6.3 Curve Fitting Water Binder Number

It has been established in previous studies that the relationship between the water binder ratio and shear strength of the stabilized soil is not linear but follows an expression given by [25]. The established relationships in [4] and [2] were compared to the databases.

The curve fitting from the Swedish database was irrelevant, as it used the same database on which the relationship was established. It was, therefore, natural that the equation would fit as well as shown in Figure 5.22. However, a somewhat deviant B constant was found. This may be because the shear strengths in this thesis were converted to 28 days strength using Equation (3.10). This meant the shear strengths would differ from those used in [2].

Regarding the results from the Norwegian and E6 Kvithammar-Åsen databases, the fitted curves showed different results than those established in [4]. Even though the shear strengths from the relationship from [4] also was after 28 days, it was not necessarily that the new relationships were comparable. There may be great uncertainty associated with adjusting the shear strength using Equation (3.10) as the strengths after 28 days were estimated and not physically measured. However, many of the shear strength measurements from the Norwegian database were tested after 28 days, so in these cases, the formula did not provide any uncertainties related to shear strength. Although the relationship established in [4] was specific to clays in Trondheim, it was assumed that the relationship should be transferable to other clays from Norway. The general observations from the curve fitting of the Norwegian database were that the shear strengths were far too low compared to what they should have been for the given water binder ratio values. This may indicate that the established correlation between the water binder number and shear strength of the stabilized soil is not transferable to other clays outside Trondheim.

The data from E6 Kvithammar-Åsen revealed a notable trend in the fitted curves. The curve fitting indicated significantly higher obtained shear strengths than the values reported in [4]. The strength of the soil tested in the field was much higher than that reproduced in the laboratory, especially for lower water binder ratios. One possible reason for the difference in strength is that it is difficult to reproduce the high temperatures in the soil that occurs during the mixing of the binder. The methods used to measure shear strength are also different in the field and laboratory. In [4], the relationship was based on shear strength measurements from uniaxial compression. However, in the E6 Kvithammar-Åsen, all shear strength measurements were from KPS or FOPS. It thus appears that it is challenging to determine the stabilized shear strength based on relationships established in the laboratory.

6.4 Machine learning models

6.4.1 E6 Kvithammar-Åsen

As seen in Table 6.4, all the machine learning models based on the data from the E6 Kvithammar-Åsen project had a negative R^2 for the testing sets, indicating a poor fit. This meant the models failed to explain any shear strength variation based on the input parameters. From the other evaluation metrics, RMSE and MAE, the CPTU models had an average margin of error between 377.5 kPa and 449.2 kPa, while the laboratory models were between 173.1 kPa and 276.6 kPa. The error was larger in the CPTU models since the range of the shear strength in the CPTU test set was more extensive than in the Laboratory test set. Based on the field data used, it may appear that it is difficult to create reliable machine learning models. Why the models were

performing so poorly is challenging to determine. There were spatial uncertainties since the data pairs were not from exactly the same coordinates. Furthermore, there were fewer data points from the laboratory tests compared to CPTU and KPS/FOPS. More points were created by interpolating between the laboratory tests performed in the same borehole. It was, therefore, not certain that the correct physical properties were used. At the same time, there were large differences in recorded shear strength, which ranged from 4-2778 kPa. It was difficult to know how accurate the results from KPS/FOPS were because the testing was not executed under the same controlled conditions as in a laboratory.

Multiple studies have been conducted where reliable models predicted the strength of laboratory-stabilized soil. The given studies are summarized in Table 2.7. These models were all based on measurements from uniaxial compression. Therefore, it may seem that the shear strength tests from Uniaxial compression are more reliable than those from KPS/FOPS.

Model	Gradient Boosting	Random Forest
CPTU	-0.70	-0.84
Laboratory	-0.69	-1.38

Table 6.4: Comparison of R^2 from the test set from the CPTU and Laboratory ML models from E6 Kvithammar-Åsen.

6.4.2 The Norwegian and Swedish Databases

The machine learning models in the Norwegian and Swedish databases performed better than the models in the E6 database when it came to predicting the stabilized shear strength. These were based on shear strength measurements from uniaxial compression, which strengthens the theory that a large uncertainty is associated with the shear strength measurements from KPS/FOPS. The data used in laboratory studies originate from more controlled environments, which provides less uncertainty. The comparison of the R^2 values from the testing sets from the different machine learning models are shown in Table 6.5. The average margin of error from the outputs was in the range of 29-45 kPa, from both MAE and RMSE. Based on all the evaluation metrics, it can be said that the models' performance is reasonably good, with the highest achieved R^2 value of 0.82.

Model	Gradient Boosting	Random Forest
Norwegian	0.82	0.79
Swedish	0.71	0.80

Table 6.5: Comparison of R^2 from the Norwegian and Swedish ML models test set.

To further explore the performance of the models, 10-fold cross-validation was used. Differences in performance were observed each time the different models were trained. The performance was particularly affected by how the data was split for training and testing. The results from the 10-fold cross-validation of the models are shown in Figure 6.5 and Figure 6.6. These plots consist of a box showing the range from the first to the third quartile. The orange horizontal line inside the box represents the median. Two vertical lines extend from the box to the minimum and maximum values. As seen in the plots from the Swedish database, there are some small circles. These values were interpreted as outliers and have thus not been considered by the box plot in the statistical calculations.

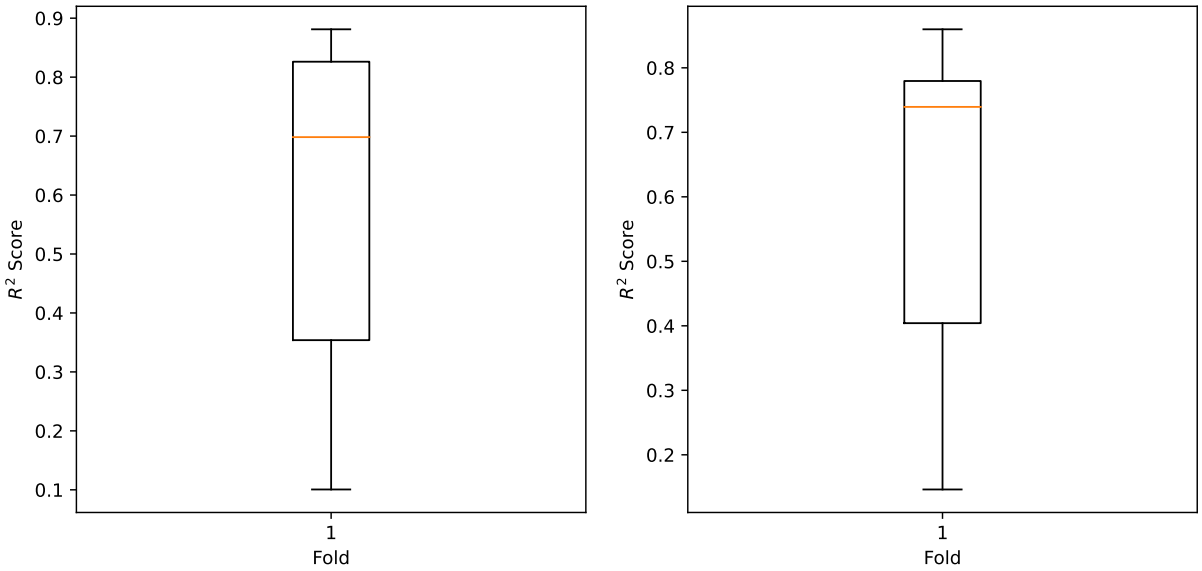

(a) Gradient Boosting. **(b)** Random Forest.

Figure 6.5: 10-fold cross-validation of the Norwegian models.

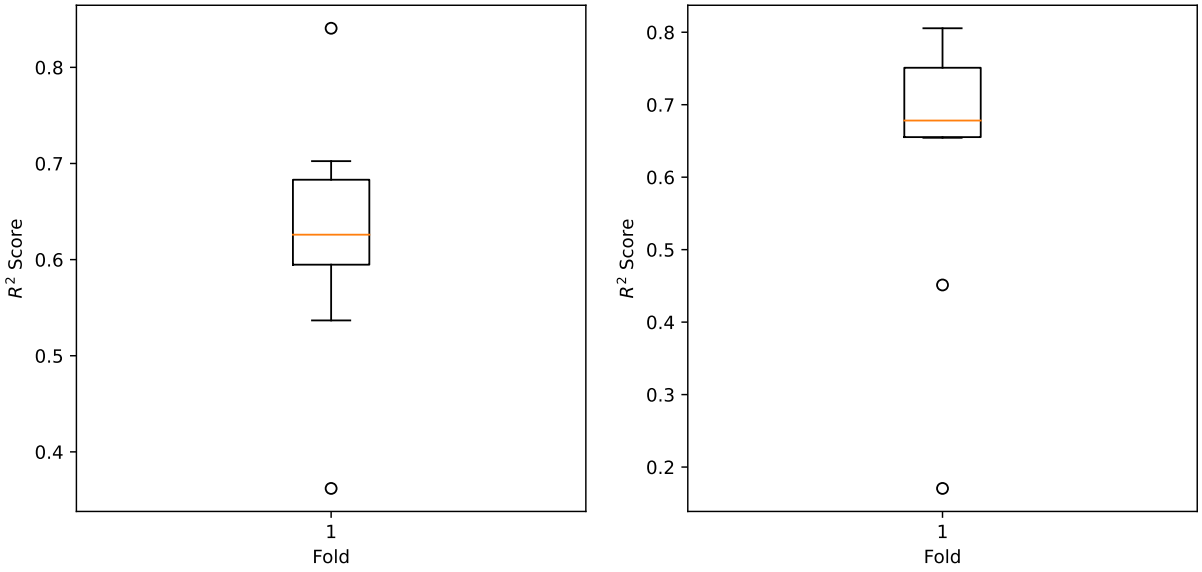

(a) Gradient Boosting. **(b)** Random Forest.

Figure 6.6: 10-fold cross-validation of the Swedish models.

As seen in Figure 6.5 and Figure 6.6, there was great variation in the performance achieved when using cross-validation, where the mean cross-validation scores are shown in Table 6.6. The scores from the cross-validation were significantly lower than the performance obtained from evaluating the entire dataset. This means there is a possibility that the models are overfitting the training data, which indicates that the models may not give accurate predictions for unseen data. Nevertheless, based on an R^2 value of around 0.63, this is similar to what has been found in [30] and [28], where the R^2 values were between 0.63 and 0.69. In these articles, the training features were many of the same ones used in the models for the Norwegian database. However, the analyzed soil in [30] and [28] did not include soil from Norway, so it is difficult to know how comparable the studies are.

Model	Gradient Boosting	Random Forest
Norwegian	0.59	0.63
Swedish	0.63	0.64

Table 6.6: Mean Cross-Validation Score R^2 for the ML models.

The performance of the machine learning models based on each parameter's ability to predict the stabilized strength individually was compared with the R^2 from the linear correlation analyses, as seen in Figure 6.7 and Figure 6.8. The used R^2 values were from 10-fold cross-validation, as this produced the most accurate representation. For the Norwegian database, where there were strong linear correlations, there was generally a slight performance improvement from the non-linear models for most parameters. However, there was a massive improvement for the sensitivity and liquidity index. This may indicate that it is possible to find a relationship between these parameters and the stabilized strength, even though no linear correlation was found. In the Swedish database, machine learning showed a clear increase in performance for the water binder ratio and porosity.

Figure 6.7: Comparison of R^2 from non-linear and linear analysis of the Norwegian database.

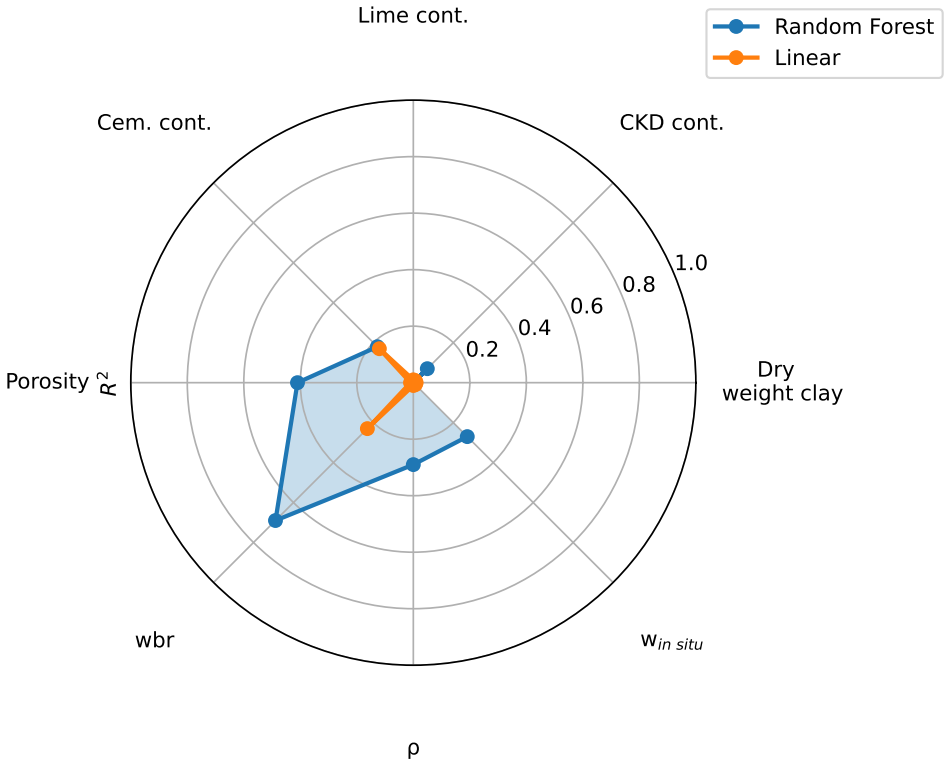

Figure 6.8: Comparison of R^2 from non-linear and linear analysis of the Swedish database.

In Figure 6.9, the performance of the shared variables from the Norwegian and Swedish databases is compared. The R^2 of the different binder contents and the water binder ratio seemed consistent for both databases. However, there were variations in the performance of the water content, porosity, and unit weight/ bulk density. The water binder ratio was the only variable to provide reliable results even in varying soil conditions. The Random Forest model from the Swedish database showed a mean cross-validation score (R^2) of 0.69. Compared to the mean score of the models containing all variables, as seen in Table 6.6, the water binder ratio model performed slightly better.

Based on permutation importance analysis, the most influential parameters on both databases were consistent with the variables that achieved the best performance in predicting the shear strength on their own. For the Norwegian database, porosity had the highest R^2 of 0.67 and by far the highest permutation importance score. However, for the Swedish, the water binder ratio with an R^2 of 0.69 showed the highest permutation importance score. There seemed to be no correlation between high R^2 and a high permutation score for the remaining variables.

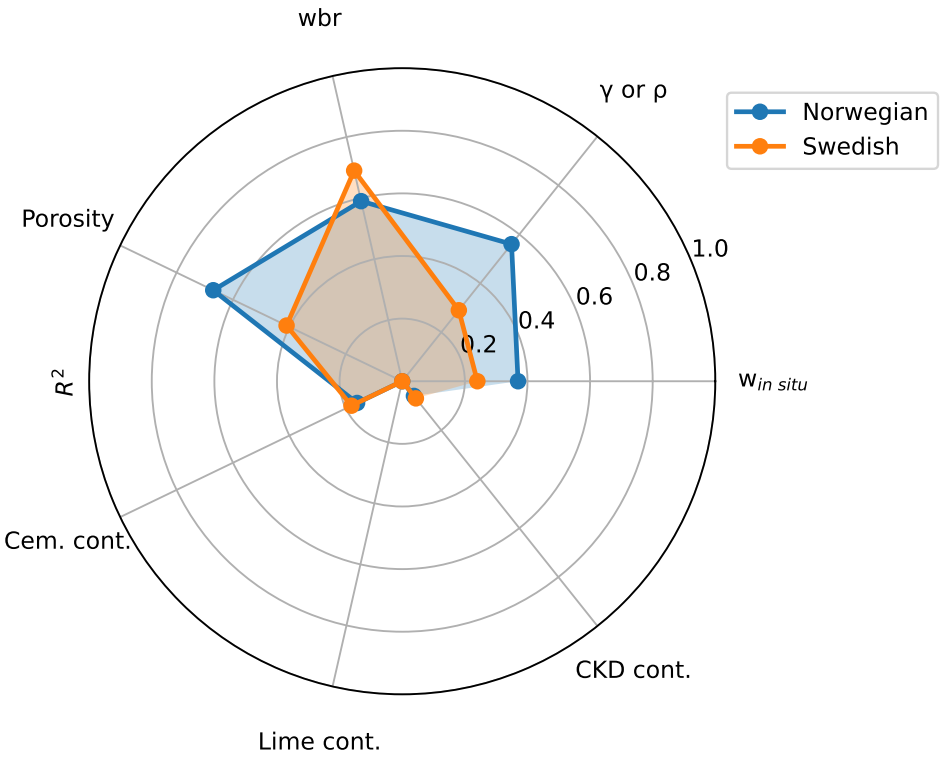

Figure 6.9: Spider plot Swedish database vs. Norwegian database. The R^2 are based o the random forest models from both databases.

7 Conclusion and Further Work

7.1 Main Findings

In this master thesis, the objective was to investigate whether it was possible to find reliable correlations between various parameters, specifically in-situ soil and binder parameters, and the shear strength of stabilized soil. The analysis was based on data from three different sources. Two databases were established on laboratory-stabilized soil from Norway and Sweden, while the final one consisted of field data from various field tests conducted in the E6 Kvithammar-Åsen project. The tests performed at the E6 project were CPTUs, Laboratory tests of the unstabilized soil, and KPS/FOPS tests of the shear strength of the stabilized columns. Based on this data, two databases were established: A CPTU database and a laboratory database.

Based on CPTU parameters cone resistance (q_c) and pore-pressure ratio (B_q), it is, according to [40] possible to classify the specific type of soil. A high q_c value with a correspondingly low B_q value characterizes overconsolidated, stiff soils. In contrast, a low q_c value with a B_q value typically between 1-1.2 is common for soft clays. Less energy is required to mix soft clays than stiff ones. This means that it will be easier to achieve good binder distribution throughout the entire column, which is believed to result in a higher achieved stabilized strength.

The correlation analysis from the CPTU data indicated no relationship between the CPTU data and the strength of the stabilized soil. The problem was that the database contained large uncertainties associated with significant distances between the compared CPTU values and shear strength values obtained from the KPS and FOPS tests in the field. Therefore, a new correlation analysis was performed, with an upper limit for the distance between the test for a more correct result. The smallest interval analyzed was 0-20 m between the data pairs. However, no significant improvement in the correlations was observed. The q_c and B_q gave correlation coefficients of -0.13 and 0.22. Thus, no clear indication was found that softer clays result in higher stabilized shear strength. The highest R^2 was given by the pore-pressure in the probe (u_2) of 0.05. Based on the research, no correlation has been found between the CPTU data and the stabilized strength of the soil.

In the correlation analyses between the in-situ soil parameters obtained from laboratory tests and the stabilized strength of the columns from E6 Kvithammar-Åsen, a significant improvement was observed by only considering the data pairs with the least distance. The correlations were consistent up to 40 m between the laboratory and shear strength data. The water content, porosity, plastic limit, liquid limit, plasticity index, and corrected water binder ratio all showed a weak correlation with the column strengths, with R^2 values ranging from 0.22 to 0.36. The unit weight and bulk density showed the same correlation with the column strength, with an R^2 value of 0.11.

The more sensitive the soil is, the less mixing energy is required to adequately mix the soil so that the binder is evenly distributed throughout the column. This means an increased stabilized strength was expected for soils with high sensitivity. On the other hand, more energy is required to mix soil with high intact shear strength. Thus, higher stabilized strength could have been expected in soils with lower intact shear strength. Conversely, the intact and remolded shear strength, sensitivity, and liquidity index showed no correlation, with a best R^2 value of 0.01. This was consistent with the findings from the CPTU analysis, which also found no correlation between

increased stabilized shear strength for softer clays. The findings were further in agreement with a previous study, which found that there was no correlation between the stabilized and unstabilized strength of the soil [12].

The correlations from the Norwegian database showed similar results as the E6 Kvithammar-Åsen database, but the correlations were generally stronger. However, the correlations from the Swedish database were much weaker. This can likely be related to the different soil types considered in the Swedish database. The water binder ratio was the only variable with consistent correlations in all laboratory databases.

Random Forest and Gradient Boosting, two machine learning models, were created for all databases. The models were trained on 80% of the data and tested on the remaining 20%. The Gradient Boosting models outperformed the Random Forest models for the CPTU and laboratory data from the E6 project. However, the models could not recreate the stabilized strength in the columns, with R^2 values $<$ -0.69 indicating a poor fit. The assumptions made to establish the databases had too much uncertainty. At the same time, it is also possible that there was great uncertainty related to the results of FOPS and KPS. These uncertainties combined make it very difficult for the models to predict the strength of the columns.

On the other hand, the models based on laboratory data from the Norwegian and Swedish databases could predict the shear strength with a best fit given by an R^2 of 0.82. Gradient Boosting gave the best prediction for the Norwegian database, while Random Forest performed the best for the Swedish database. However, it was uncertain whether the actual performance of the models was as high as the best fit. From the 10-fold cross-verification, the mean R^2 was found to be between 0.59 to 0.64 for all models. This is a lower performance than the model based on only the water binder ratio from the Swedish database, which was R^2 of 0.69. Creating machine learning models based solely on this variable with relatively good results was possible.

7.2 Concluding Remarks

The main findings are summarized in the following concluding remarks:

- There was no observed correlation between the CPTU data and the stabilized strength of the DDM columns.
- However, there were weak correlations between the water content, porosity, plastic limit, liquid limit, plasticity index, and corrected water binder ratio with the stabilized strength of the soil. The plastic limit showed the strongest correlation with an R^2 value of 0.36.
- The data from the E6 Kvithammar-Åsen project proved unsuitable for creating reliable machine learning models. The R^2 value of -0.69 gave the best fit. This may be because there are uncertainties associated with field data.
- However, there are fewer uncertainties associated with laboratory-stabilized soil. All models mode on the two provided laboratory databases performed better than an R^2 value of 0.71. The Gradient Boosting model from the Norwegian database gave the best performance, with an R^2 value of 0.82.
- The water binder ration managed to predict the strength of the stabilized soil relatively well on its own, with an average cross-validation score R^2 of 0.69. Random Forest achieved this from the Swedish database.

7.3 Advice for Future DDM Projects

Based on the analyses made in this master thesis, some recommendations for future DDM projects can be made. laboratory tests are clearly more useful than CPTU, as they showed more reliable correlations. The water content, porosity, plastic limit, liquid limit, plasticity index, and corrected water binder ratio all showed some correlation with the stabilized column strength. These are recommended variables that should be prioritized when performing laboratory tests. In this study, the observed correlations were consistent up to 40 m between the laboratory tests and the stabilized columns. This should be considered when determining the location of the laboratory tests so that the distances are not too great. This is especially true if further research projects are to be carried out. The distance between the data to be compared should be as little as possible.

7.4 Further Work

Machine learning has been shown to have the potential to predict the mechanical properties of soil. The problem is that the stabilized strength of soil is difficult to estimate due to the varying behavior. Recommendations for further work are given below.

- Create a larger database containing data from multiple projects to get more variety in the used training features.
- This thesis has only looked at correlations between the stabilized strength and different CPTU and laboratory parameters. In both the Swedish and Norwegian databases, data regarding the stiffness of the stabilized soil is available. It is possible that there may be some interesting correlations here to explore.
- The models established are Random Forest and Gradient Boosting with default hyperparameters. It is possible that a better performance can be achieved by using more advanced and tuned machine learning models.

Bibliography

[1] Paniagua P, Bache BK, Karlsrud K, Lund AK. Strength and stiffness of laboratory-mixed specimens of stabilised Norwegian clays. Proceedings of the institution of civil engineers-ground improvement. 2022;175(2):150–163.

[2] Hov S, Larsson S. Strength and Stiffness Properties of Laboratory-Improved Soft Swedish Clays. International Journal of Geosynthetics and Ground Engineering. 2023;9(1):11.

[3] Eggen A. Veiledning for grunnforsterkning med kalksementpeler. Norsk geoteknisk forening; 2012.

[4] Hov S, Paniagua P, Sætre C, Rueslåtten H, Størdal I, Mengede M, et al. Lime-cement stabilisation of Trondheim clays and its impact on carbon dioxide emissions. Soils and Foundations. 2022;62(3):101162.

[5] Fayyad U, Piatetsky-Shapiro G, Smyth P. From data mining to knowledge discovery in databases. AI magazine. 1996;17(3):37–37.

[6] González S, García S, Del Ser J, Rokach L, Herrera F. A practical tutorial on bagging and boosting based ensembles for machine learning: Algorithms, software tools, performance study, practical perspectives and opportunities. Information Fusion. 2020;64:205–237.

[7] Vegvesen S. Håndbok V221: Grunnforsterkning, fyllinger og skråninger. Statens Vegvesen, Oslo. 2014;.

[8] Terashi M. Theme lecture: Deep mixing method-Brief state of the art. In: Proc. 14th ICSMFE. vol. 4; 1997. p. 2475–2478.

[9] Åhnberg H, Johansson SE, Retelius A, Ljungkrantz C, Holmqvist L, Holm G. Cement och kalk för djupstabilisering av jord. En kemisk-fysikalisk studie av stabiliseringseffekter. Statens geotekniska institut; 1995.

[10] Norcem. Multicem;. (Accessed on 14/02/2023). Tilgjengelig fra: https://www.norcem.no/no/Multicem.

[11] Åhnberg H. Strength of stabilised soil-a laboratory study on clays and organic soils stabilised with different types of binder. Lund University; 2006.

[12] Larsson S, Kock-Larsen J, Garin H, Ekström J. Correlation between undrained shear strength in dry deep mixing columns and unimproved soft soil. In: DFI Deep Mixing 2015 Conference. Deep Foundation Institute; 2015. p. 573–580.

[13] Broms BB. Stabilization of soft clay with lime columns. In: Proceedings of a Seminar on Soil Improvement and Construction Techniques in Soft Ground, Nanyang Technological Institute, Singapore; 1984. p. 120–133.

[14] Tran VQ. Hybrid gradient boosting with meta-heuristic algorithms prediction of unconfined compressive strength of stabilized soil based on initial soil properties, mix design and effective compaction. Journal of Cleaner Production. 2022;355:131683.

[15] Tinoco J, Correia AAS, Venda Oliveira PJ. Soil-cement mixtures reinforced with fibers: a data-driven approach for mechanical properties prediction. Applied Sciences. 2021;11(17):8099.

[16] Das SK, Samui P, Sabat AK. Application of artificial intelligence to maximum dry density and unconfined compressive strength of cement stabilized soil. Geotechnical and Geological Engineering. 2011;29(3):329–342.

[17] Porbaha A, Shibuya S, Kishida T. State of the art in deep mixing technology. Part III: geomaterial characterization. Proceedings of the Institution of Civil Engineers-Ground Improvement. 2000;4(3):91–110.

[18] Yousefpour N, Medina-Cetina Z, Hernandez-Martinez FG, Al-Tabbaa A. Stiffness and strength of stabilized organic soils—part ii/ii: Parametric analysis and modeling with machine learning. Geosciences. 2021;11(5):218.

[19] Firoozi AA, Guney Olgun C, Firoozi AA, Baghini MS. Fundamentals of soil stabilization. International Journal of Geo-Engineering. 2017;8:1–16.

[20] Larsson S. State of Practice Report–Execution, monitoring and quality control. Deep Mixing. 2005;5:732–785.

[21] Janz M, Johansson SE. The function of different binding agents in deep stabilization. Swedish deep stabilization research centre, report. 2002;9:1–35.

[22] Guimond-Barrett A. Influence of mixing and curing conditions on the characteristics and durability of soils stabilised by deep mixing [Theses]. Université du Havre; 2013. Tilgjengelig fra: https://hal.science/tel-02497429.

[23] Huawen X. Yielding and failure of cement treated soil. 2009;.

[24] Kitazume M, Terashi M. The deep mixing method. CRC press; 2013.

[25] Abrams D. Bulleten 1: Structural Materials Research Laboratory. Chicago: Lewis Instityte) Design of concrete mixtures; 1918.

[26] Keller. Dry soil mixing; 2022. (Accessed on 09/06/2023). Tilgjengelig fra: https://www.keller-geoteknikk.no/en/expertise/techniques/dry-soil-mixing.

[27] Eyo EU, Abbey SJ, Booth CA. Strength predictive modelling of soils treated with calcium-based additives blended with eco-friendly pozzolans—A machine learning approach. Materials. 2022;15(13):4575.

[28] Taffese WZ, Abegaz KA. Prediction of compaction and strength properties of amended soil using machine learning. Buildings. 2022;12(5):613.

[29] Ngo HTT, Pham TA, Vu HLT, Giap LV. Application of artificial intelligence to determined unconfined compressive strength of cement-stabilized soil in vietnam. Applied Sciences. 2021;11(4):1949.

[30] Taffese WZ, Abegaz KA. Artificial intelligence for prediction of physical and mechanical properties of stabilized soil for affordable housing. Applied Sciences. 2021;11(16):7503.

[31] Wang O, Al-Tabbaa A. Preliminary model development for predicting strength and stiffness of cement-stabilized soils using artificial neural networks. In: Computing in Civil Engineering (2013); 2013. p. 299–306.

[32] Tinoco J, Correia AG, Cortez P. Application of data mining techniques in the estimation of the uniaxial compressive strength of jet grouting columns over time. Construction and Building Materials. 2011;25(3):1257–1262.

[33] Oberhollenzer S, Erharter G. TU Graz – NGI Workshop; 2023. 21.04.2023. Presentation.

[34] Sandven R, Senneset K, Emdal A, Nordal S, Janbu N, Grande L. Geotechnics Field and Laboratory Investigations. Compendium in courese TBA4110 Geoteknikk, felt- og laboratorieundersøkelser. 2017;.

[35] Hov S, Madsen J. Prosjektforutsetninger for kalksementstabilisering. E6 Kvithammar – Åsen Byggeplan Stjørdal; 2022. N0-GEOT-07. Prosj. nr 80100408-147, Dok. Nr N0-GEOT-07.

[36] Breiman L. Bagging predictors. Machine learning. 1996;24(2):123–140.

[37] Chicco D, Warrens MJ, Jurman G. The coefficient of determination R-squared is more informative than SMAPE, MAE, MAPE, MSE and RMSE in regression analysis evaluation. PeerJ Computer Science. 2021;7:e623.

[38] Verma U. R-square(r2) and adjusted R-square. Analytics Vidhya; 2020. Tilgjengelig fra: https://medium.com/analytics-vidhya/r-square-r%C2%B2-and-adjusted-r-square-63b77d4a6bd7.

[39] Berrar D. Cross-Validation.; 2019.

[40] Senneset K, Janbu N. Shear strength parameters obtained from static cone penetration tests. Strength testing of marine sediments: laboratory and in-situ measurements Philadelphia, PA, American Society for Testing and Materials. 1985;p. 41–54.

Appendix A: Presentation Data E6 Kvithammar-Åsen

A1 P1 Kvithammar

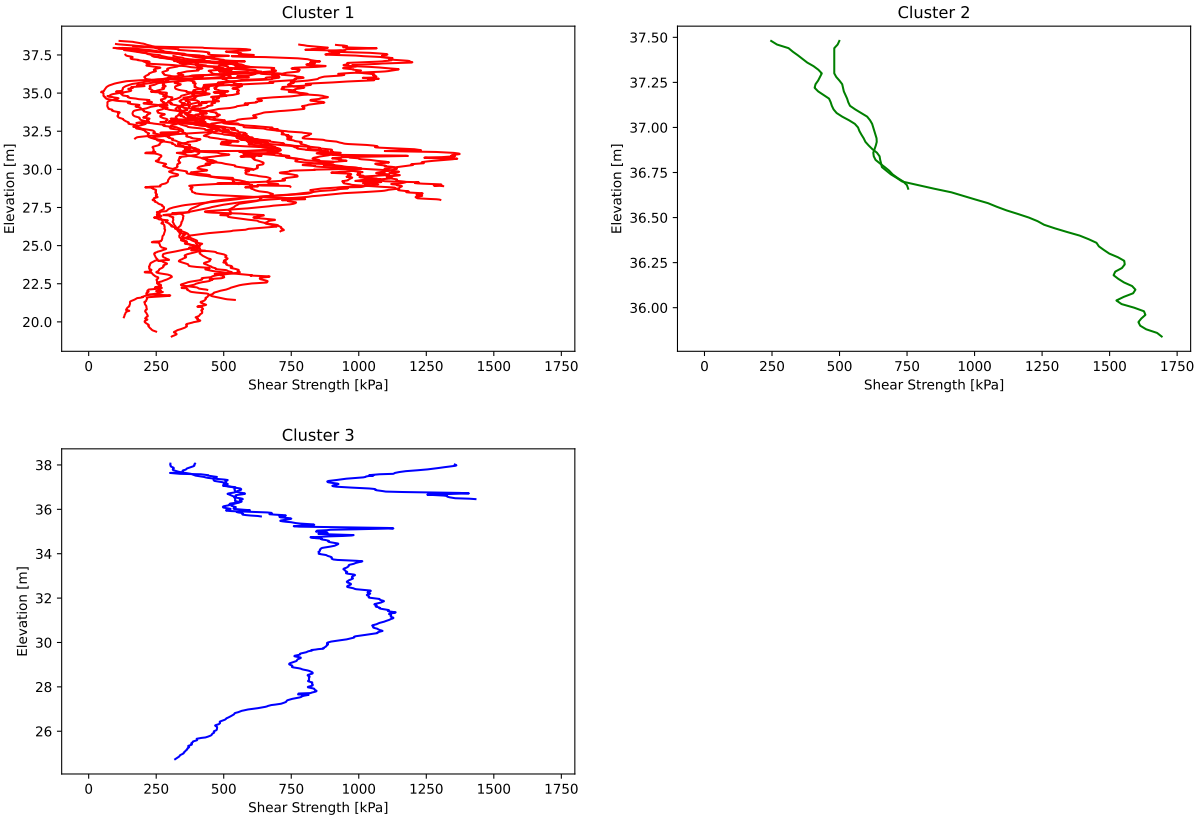

Figure A1.1: KPS clusters from P1.

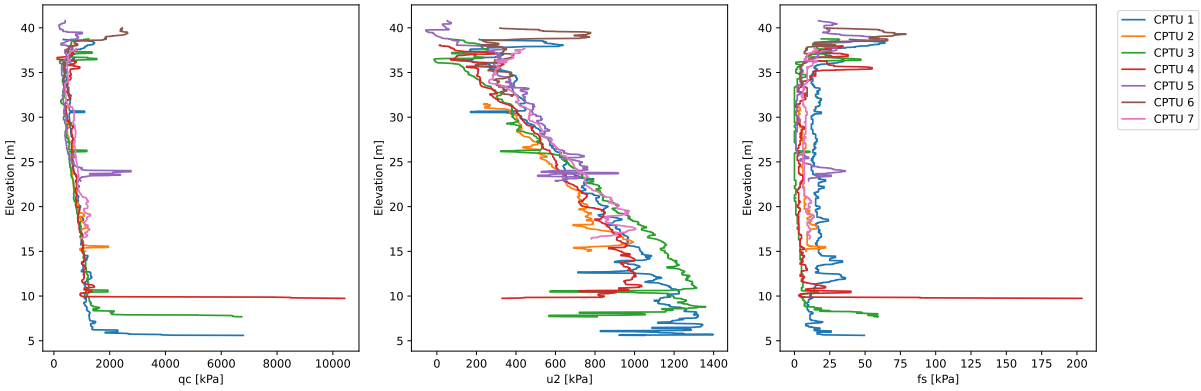

Figure A1.2: qc, u2 and fs from P1.

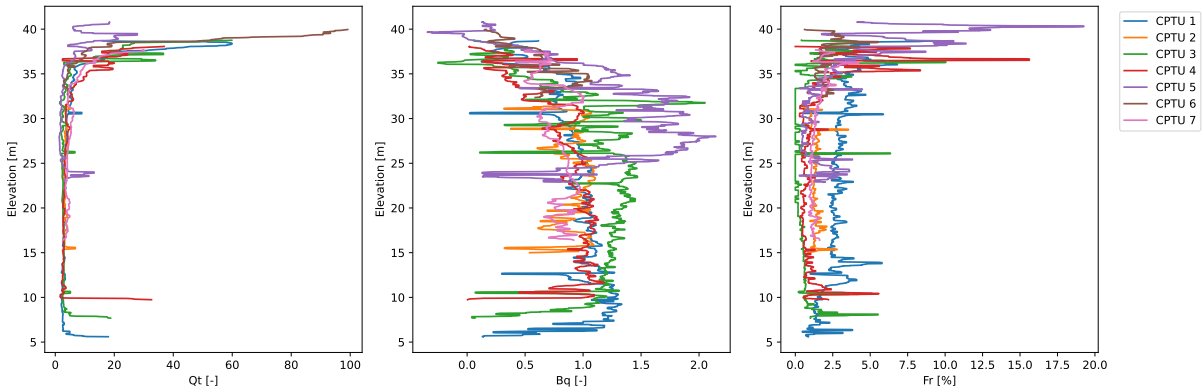

Figure A1.3: Qt, Bq, Fr from P1.

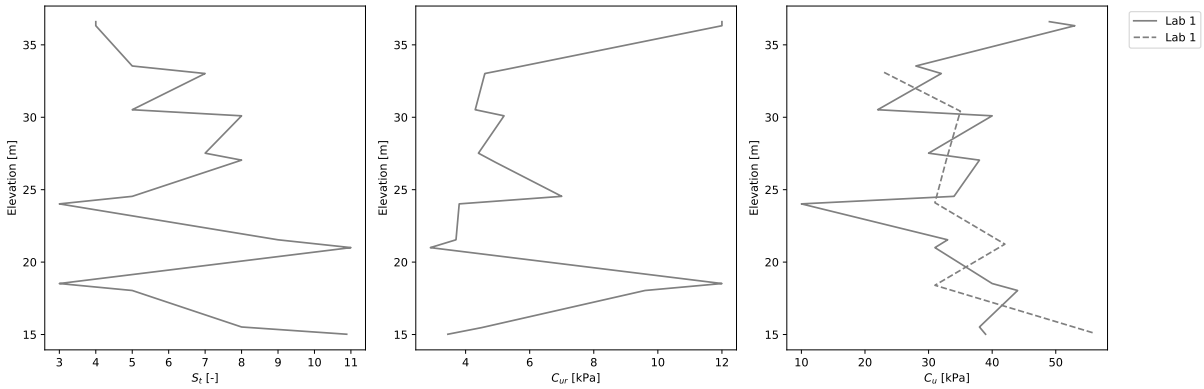

Figure A1.4: Fall Cone data and Uniaxial compression data (Dotted line in right plot) from P1.

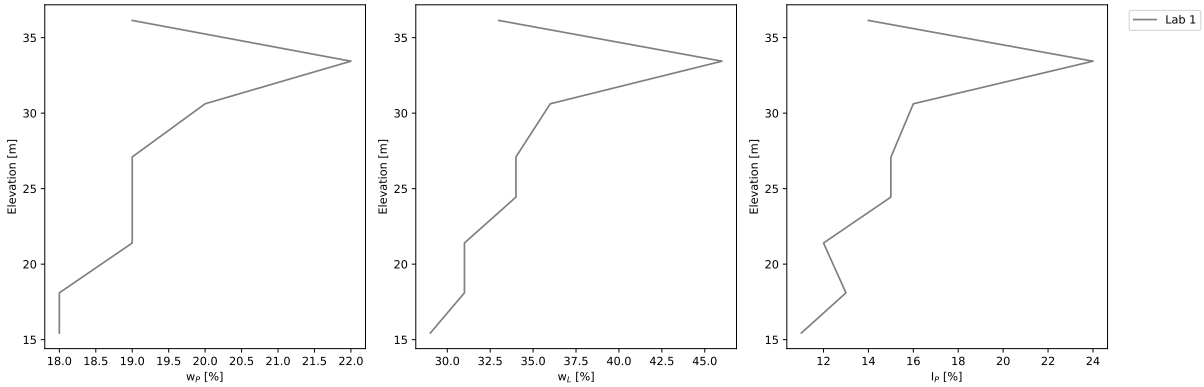

Figure A1.5: Atterberg Limits from P1.

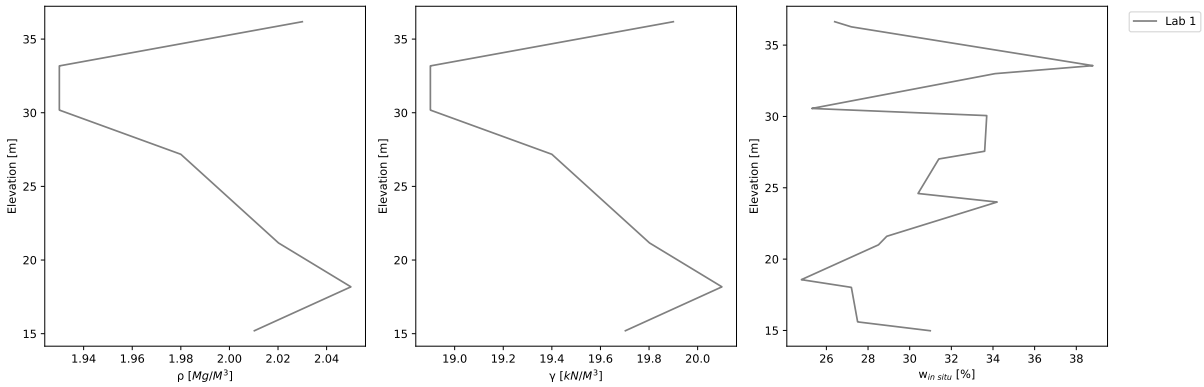

Figure A1.6: Bulk density, unit weight and water content from P1.

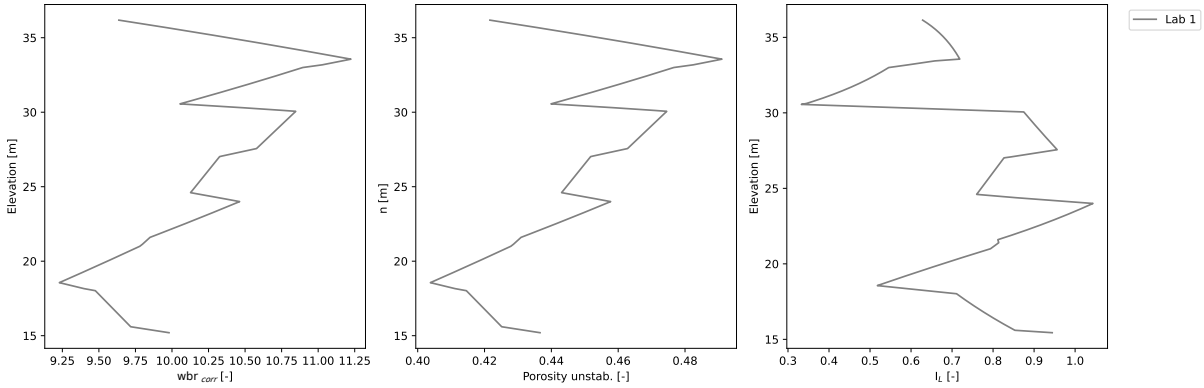

Figure A1.7: Calculated wbr, porosity and I_L from P1.

A2 P3 Langsteindalen

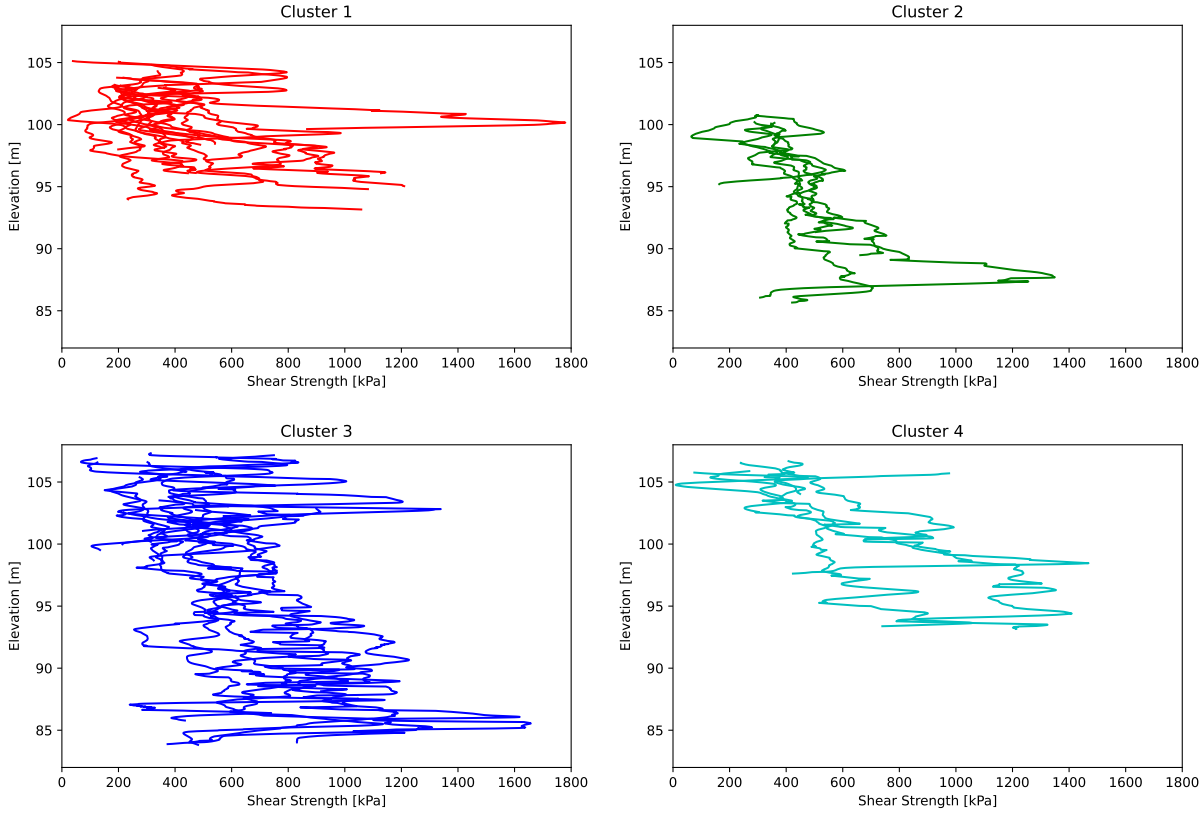

Figure A2.1: KPS/FOPS clusters from P3.

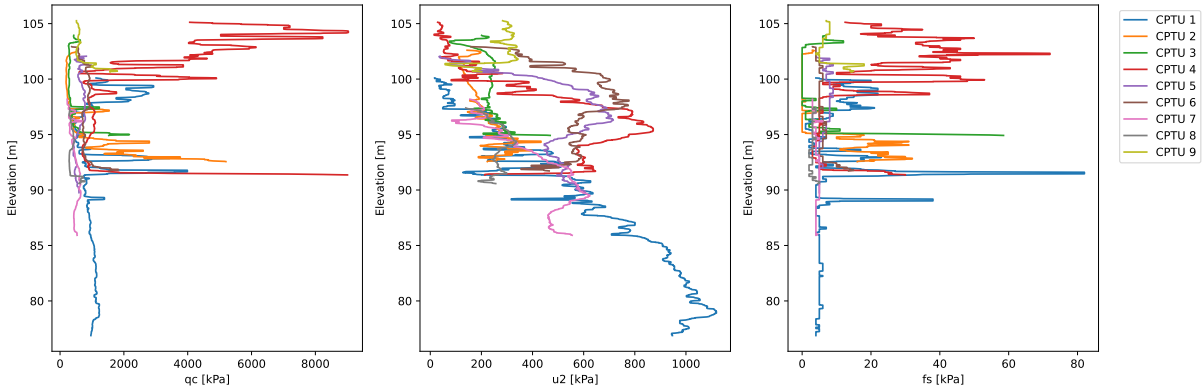

Figure A2.2: qc, u2 and fs from P3.

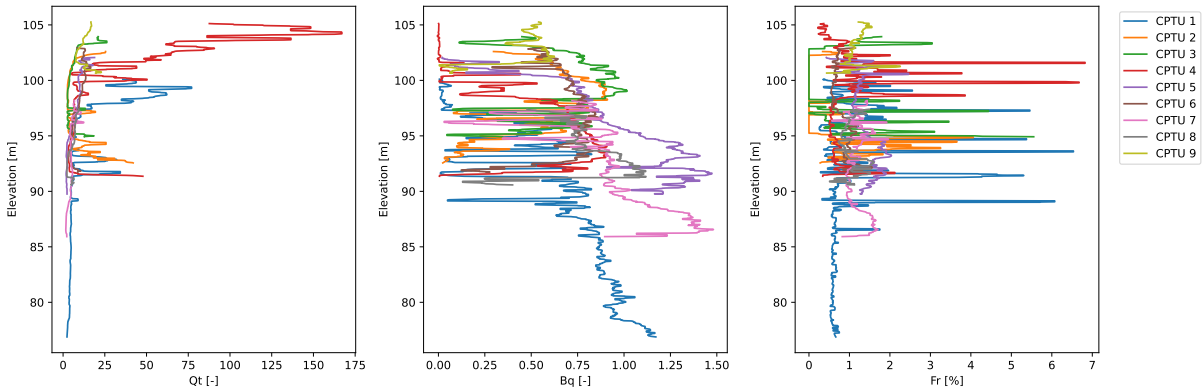

Figure A2.3: Qt, Bq, Fr from P3.

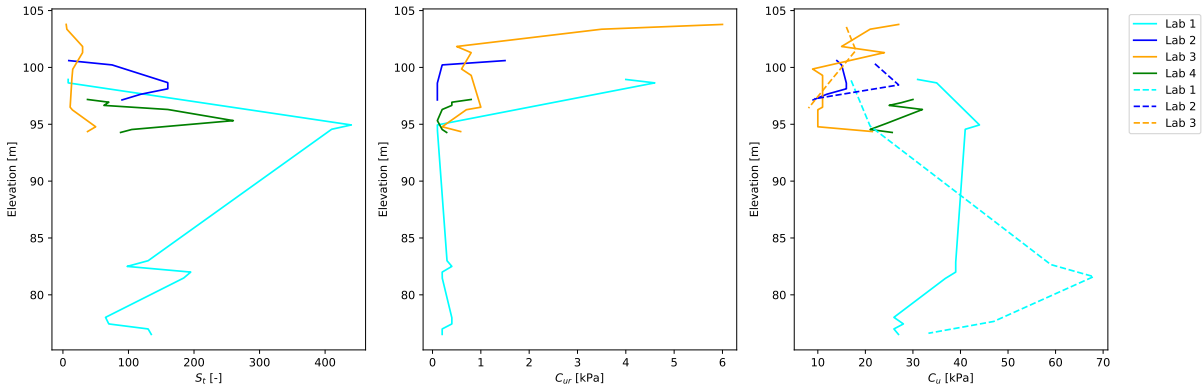

Figure A2.4: Fall Cone data and Uniaxial compression data (Dotted line in right plot) from P3.

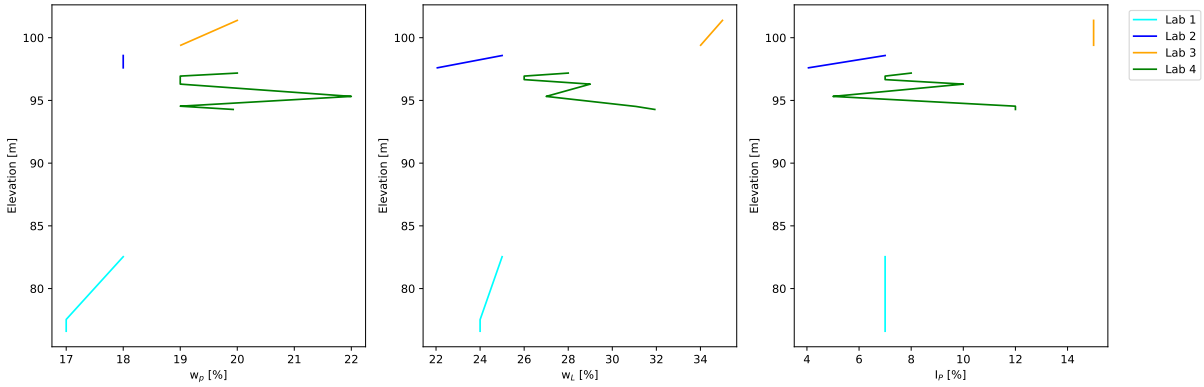

Figure A2.5: Atterberg Limits from P3.

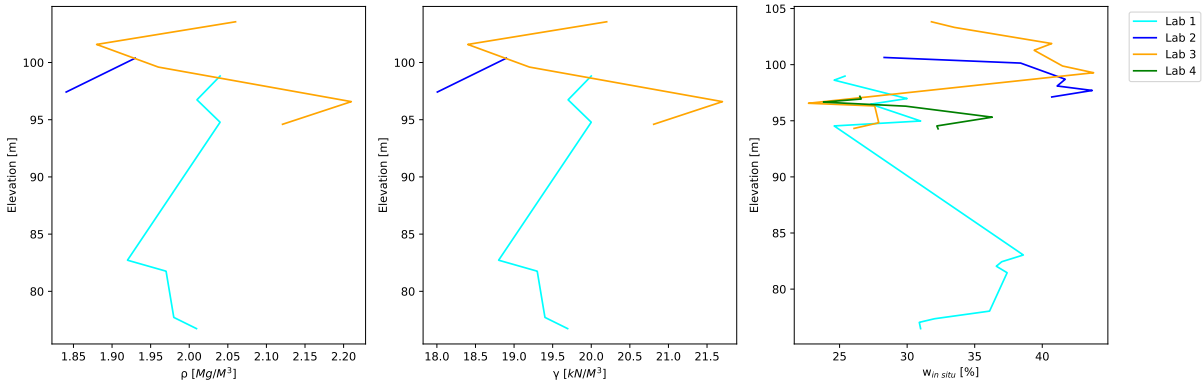

Figure A2.6: Bulk density, unit weight and water content from P3.

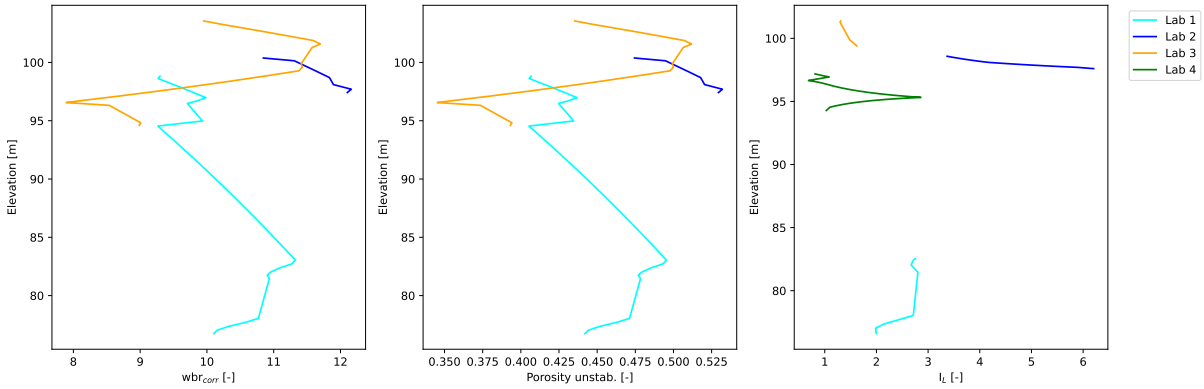

Figure A2.7: Calculated wbr, porosity and I_L from P3.

A3 P7 Kleiva

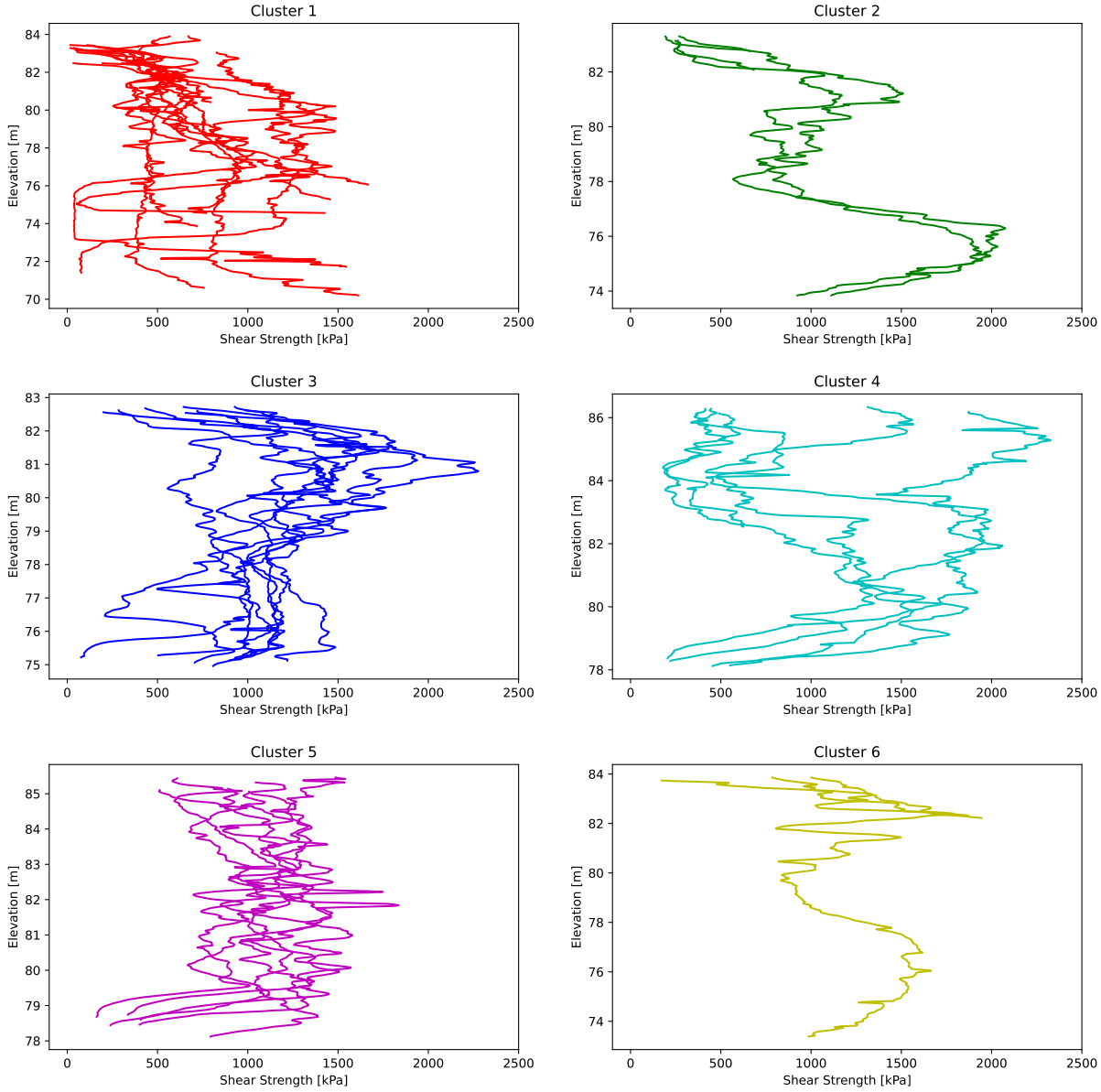

Figure A3.1: KPS clusters from P7.

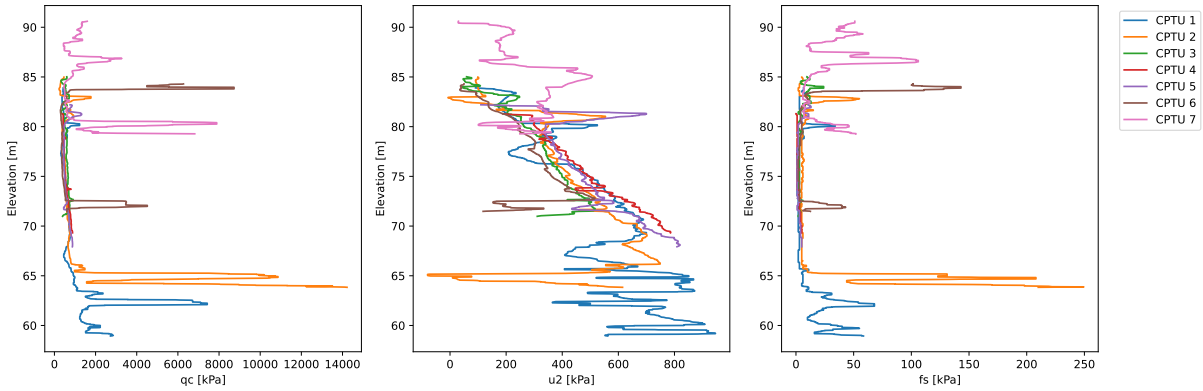

Figure A3.2: qc, u2 and fs from P7.

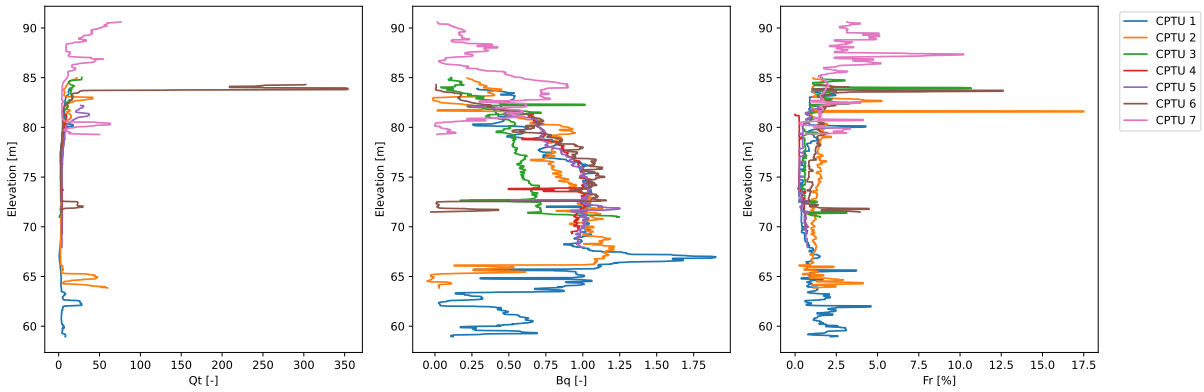

Figure A3.3: Qt, Bq, Fr from P7.

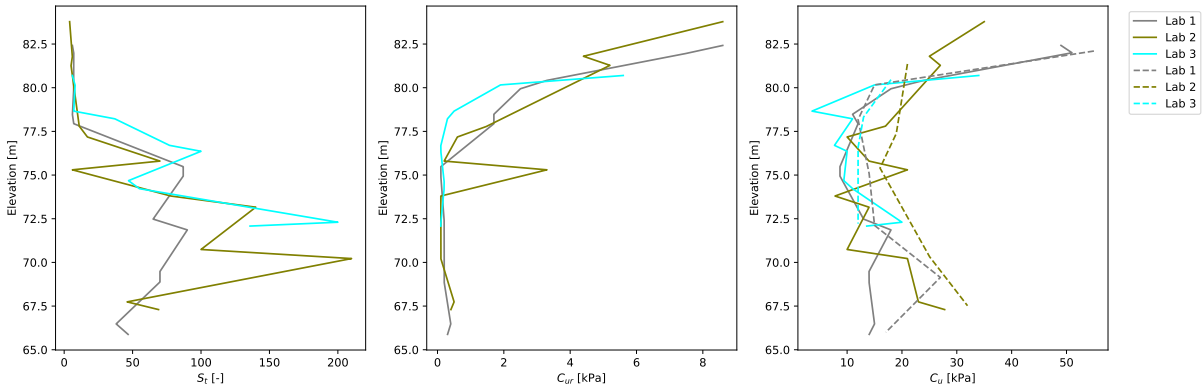

Figure A3.4: Fall Cone data and Uniaxial compression data (Dotted line in right plot) from P7.

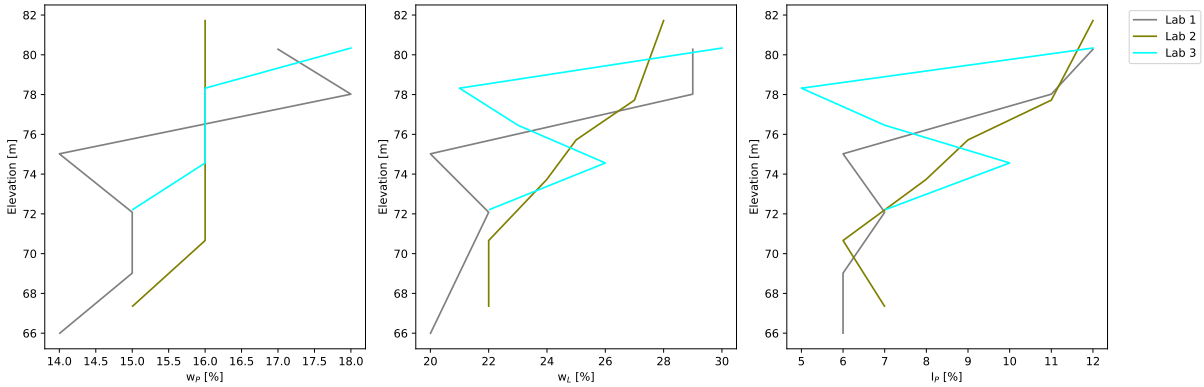

Figure A3.5: Atterberg Limits from P7.

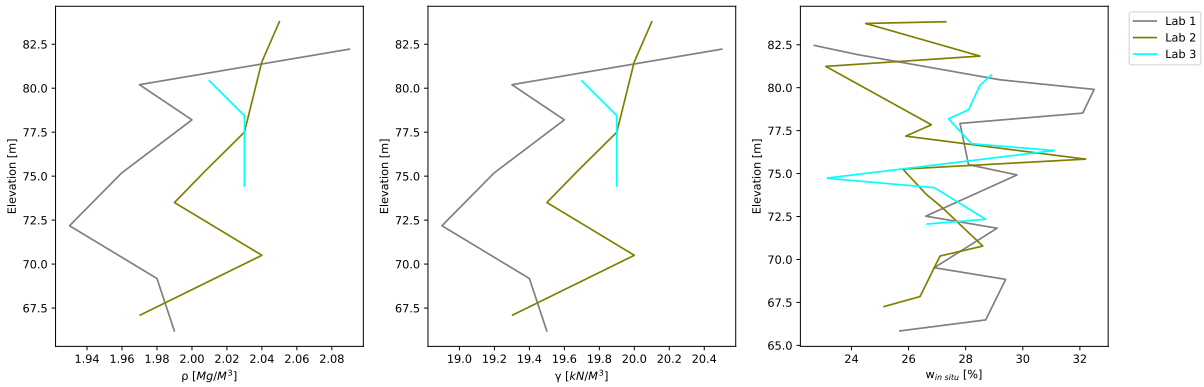

Figure A3.6: Bulk density, unit weight and water content from P7.

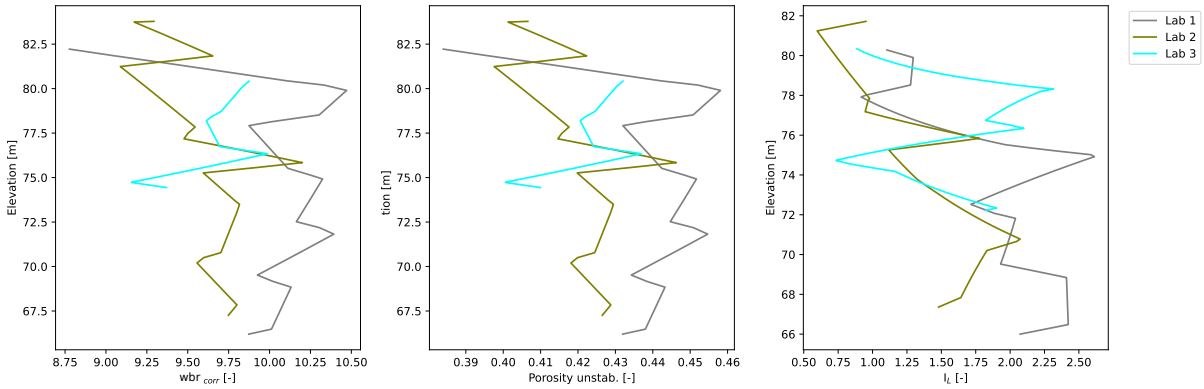

Figure A3.7: Calculated wbr, porosity and I_L from P7.

A4 P9 Stokkan

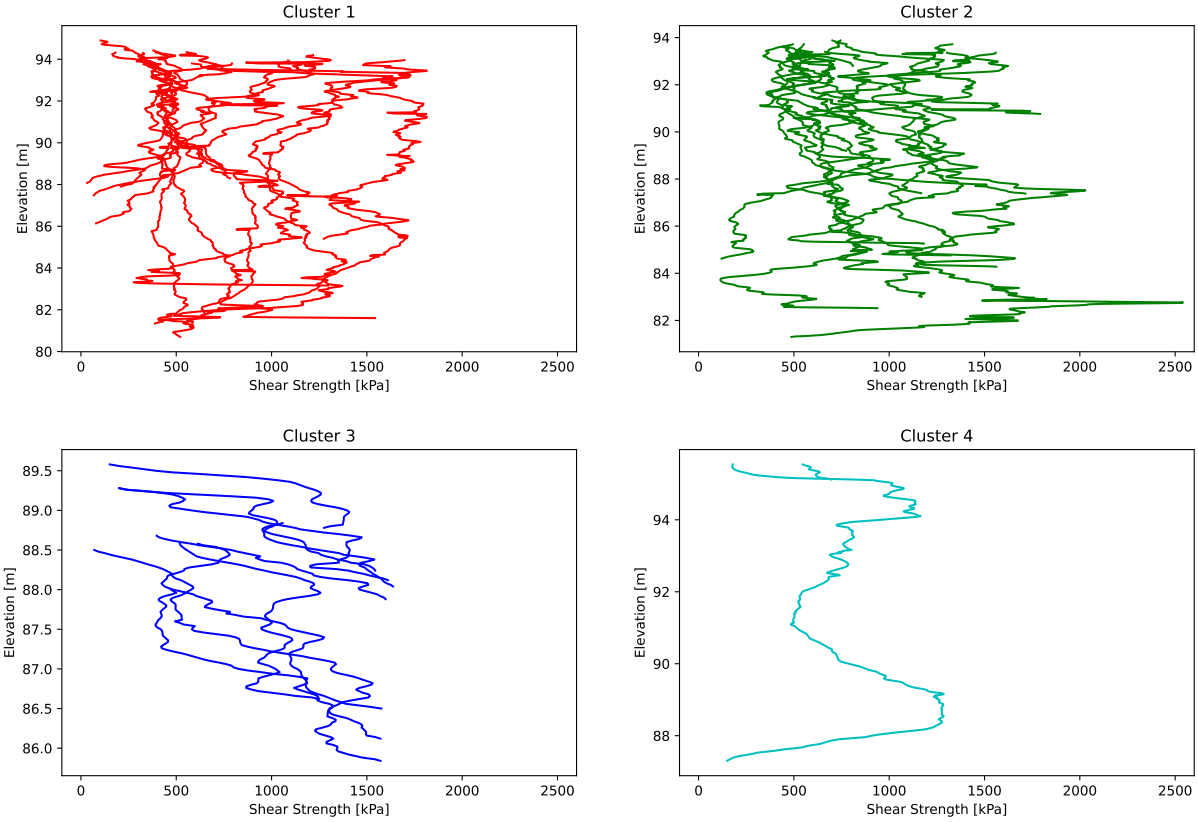

Figure A4.1: KPS clusters from P9.

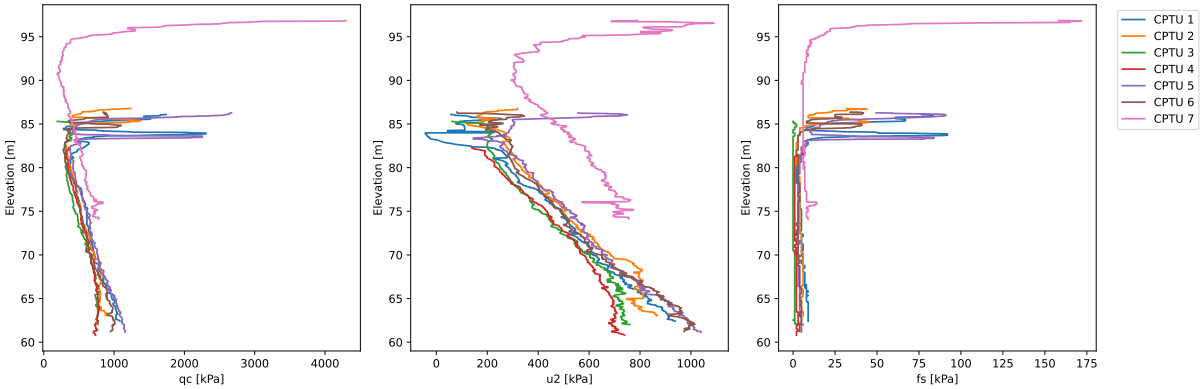

Figure A4.2: qc, u2 and fs from P9.

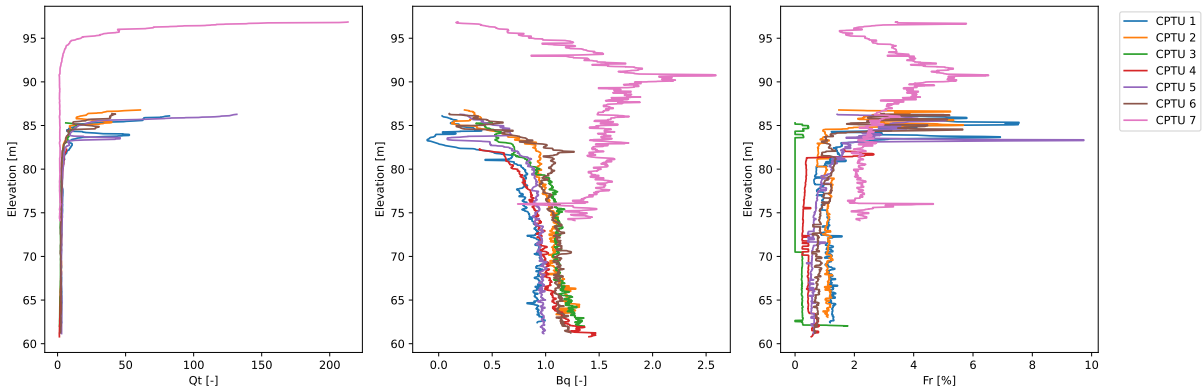

Figure A4.3: Qt, Bq, Fr from P9.

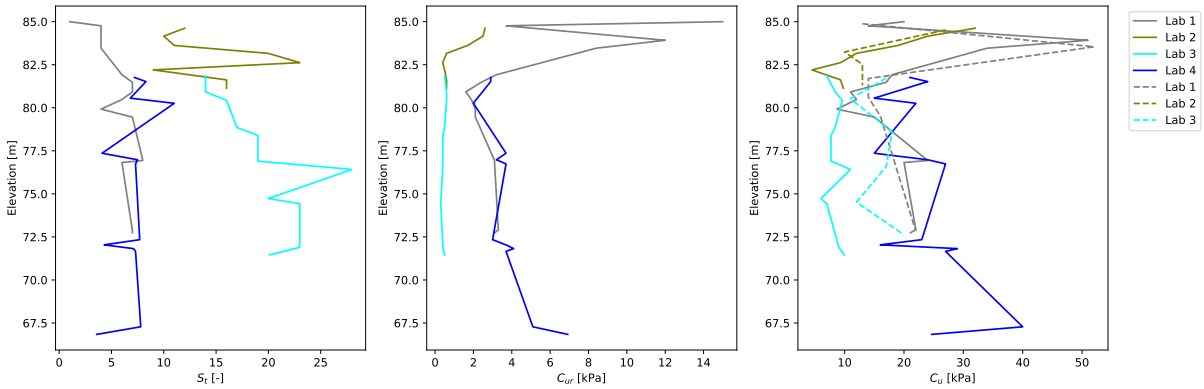

Figure A4.4: Fall Cone data and Uniaxial compression data (Dotted line in right plot) from P9.

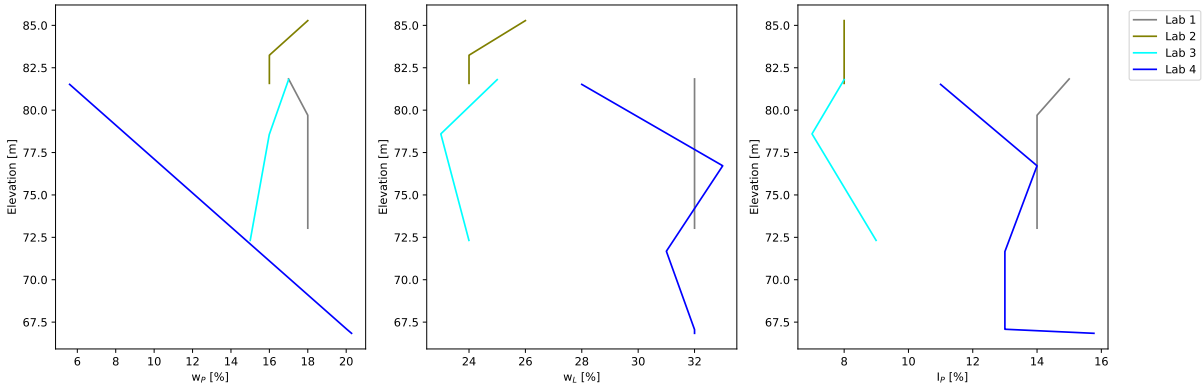

Figure A4.5: Atterberg Limits from P9.

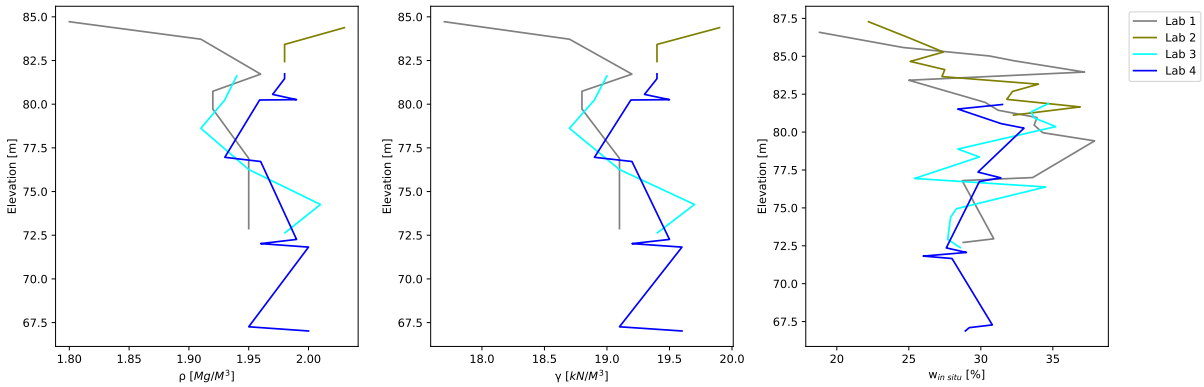

Figure A4.6: Bulk density, unit weight and water content from P9.

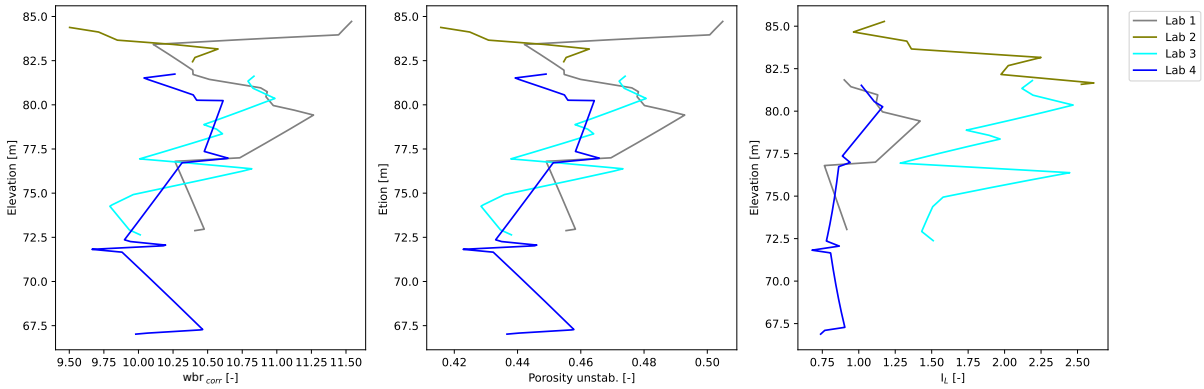

Figure A4.7: Calculated wbr, porosity and I_L from P9.

A5 P11 Vassmarka

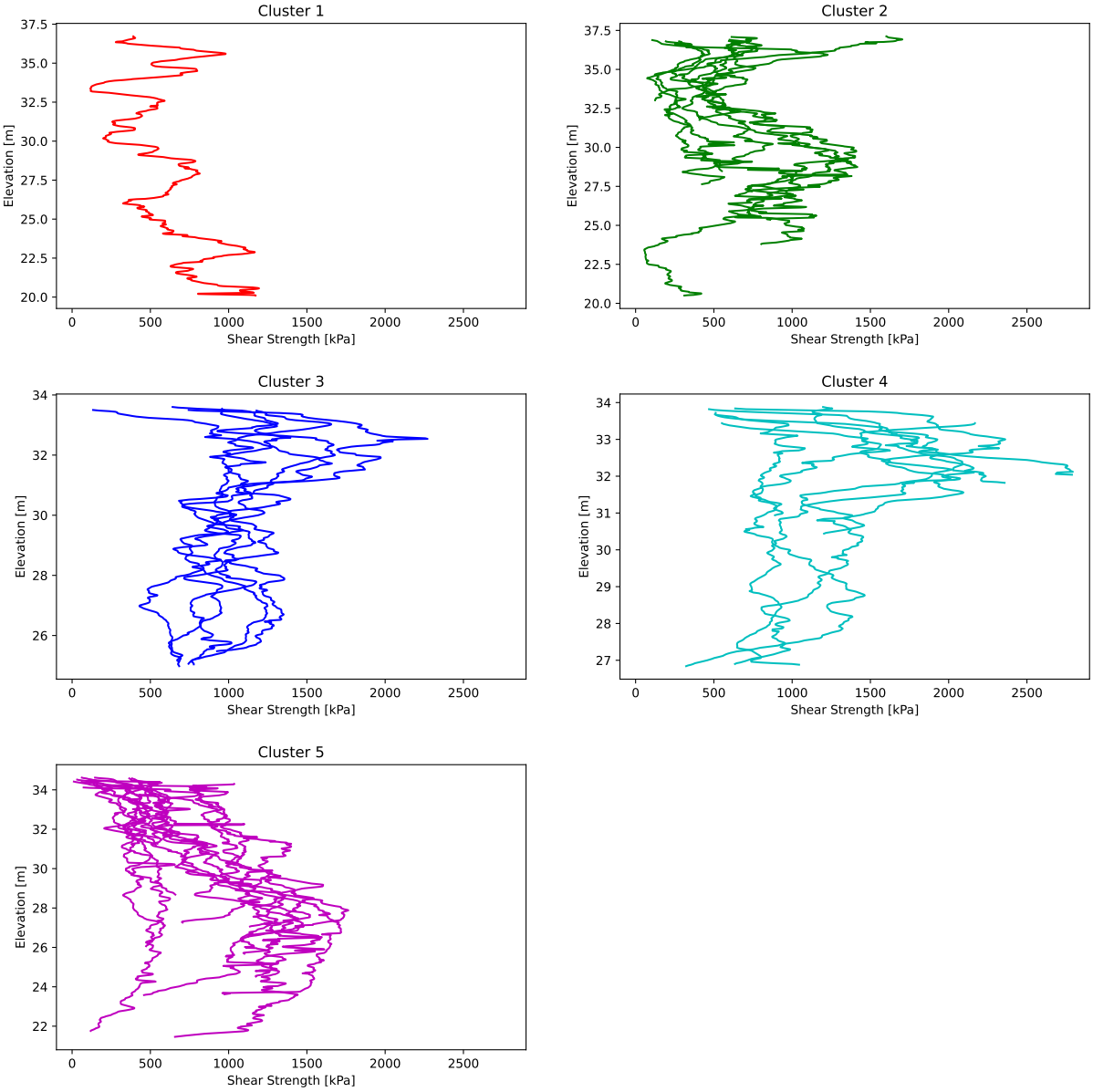

Figure A5.1: KPS clusters from P11.

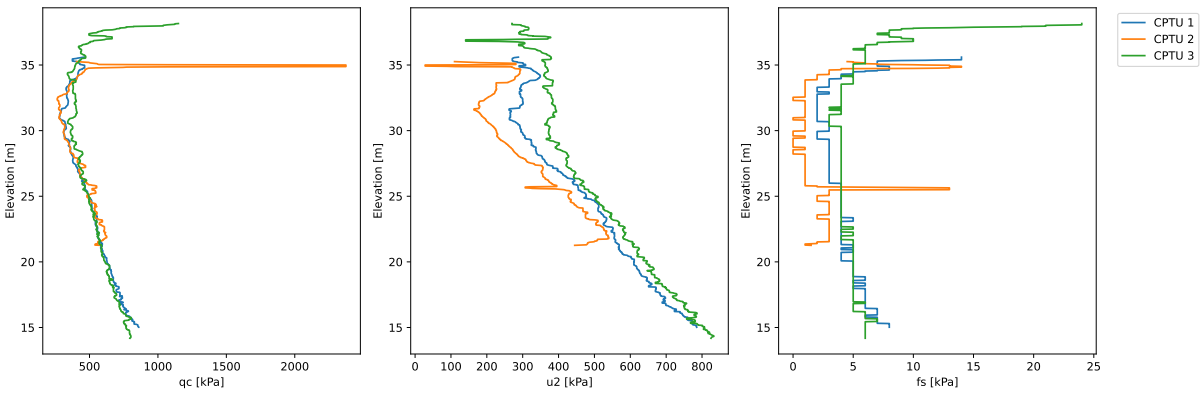

Figure A5.2: qc, u2 and fs from P11.

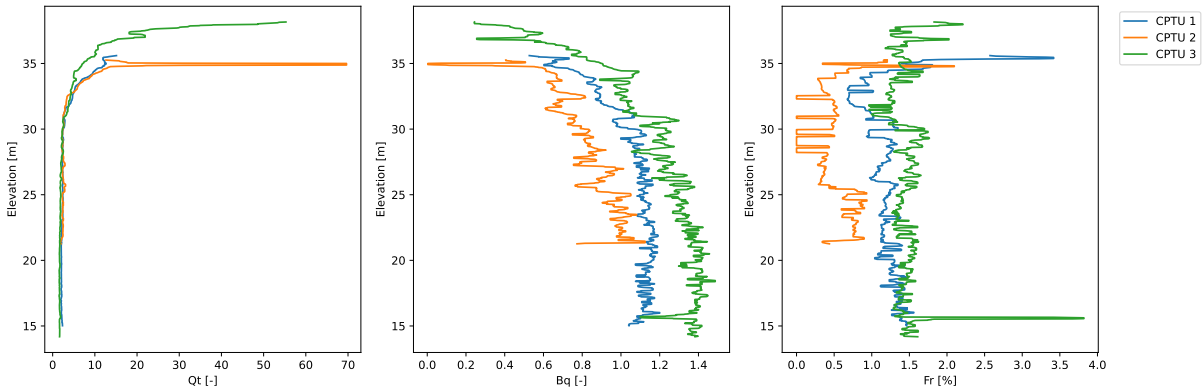

Figure A5.3: Qt, Bq, Fr from P11.

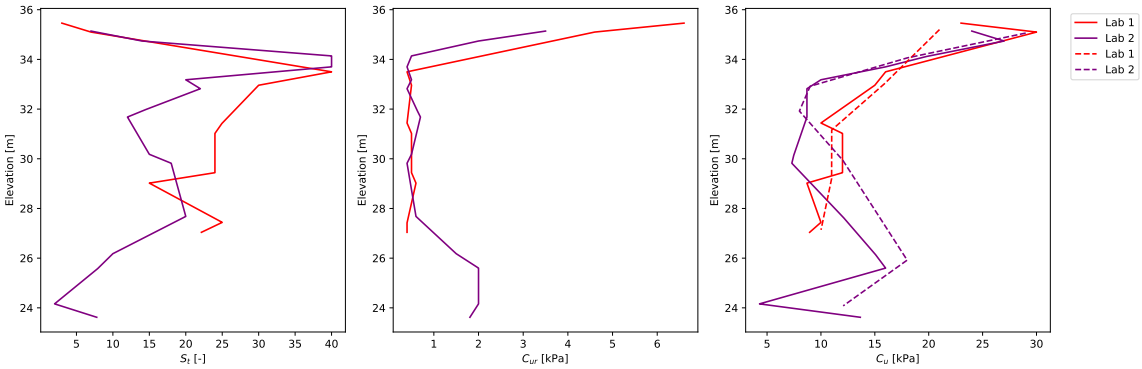

Figure A5.4: Fall Cone data and Uniaxial compression data (Dotted line in right plot) from P11.

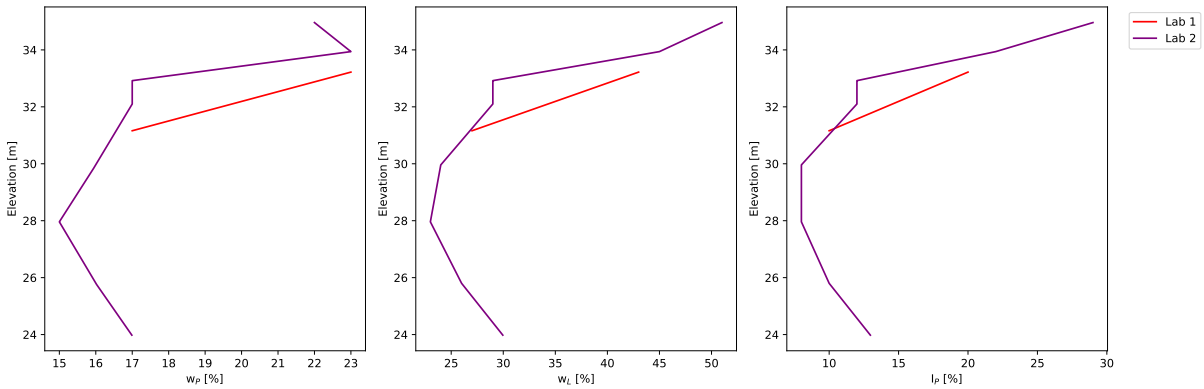

Figure A5.5: Atterberg Limits from P11.

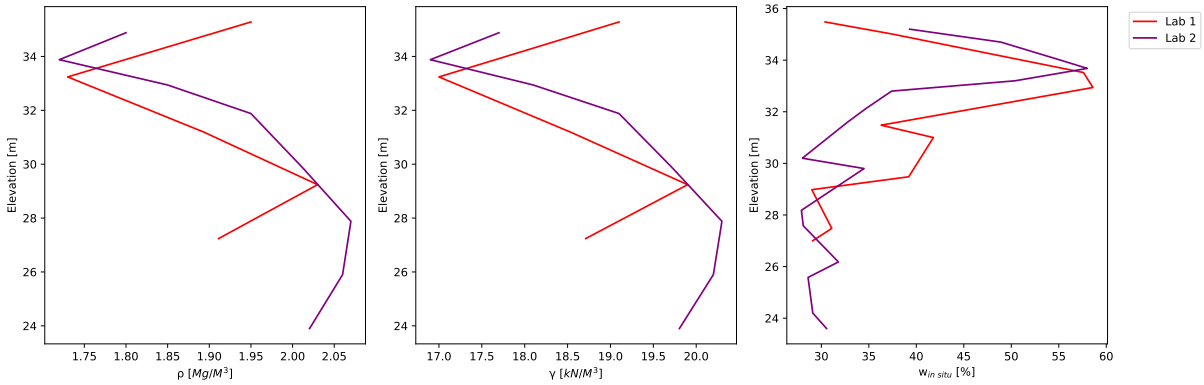

Figure A5.6: Bulk density, unit weight and water content from P11.

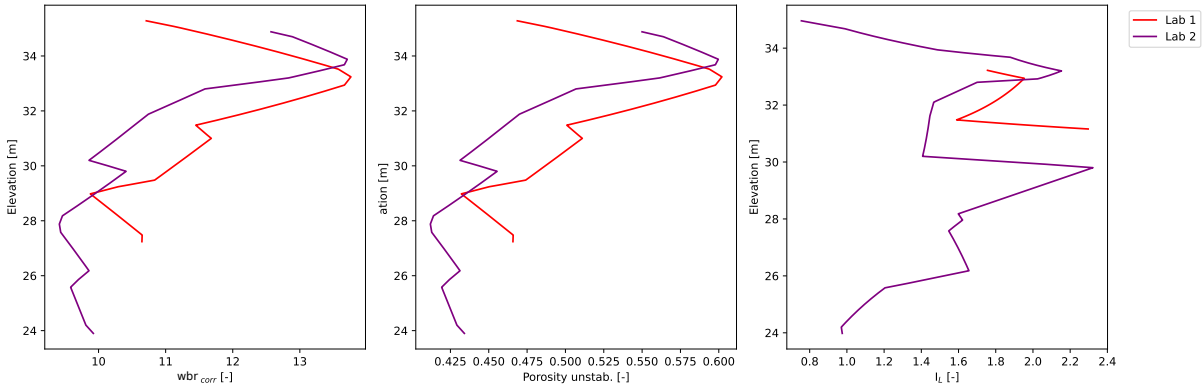

Figure A5.7: Calculated wbr, porosity and I_L from P11.

Appendix B: Shear Strength Clusters ML Database

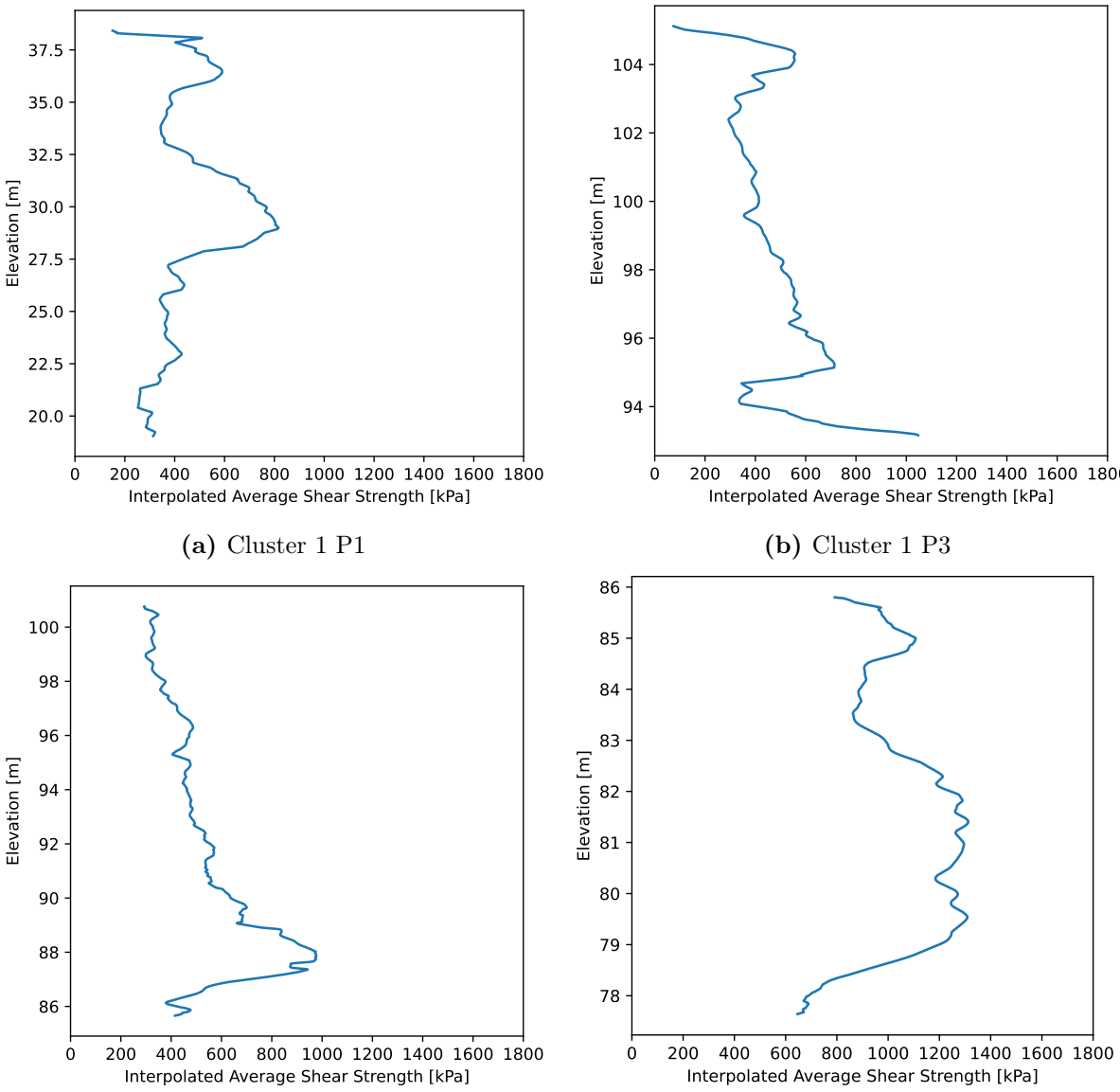

(a) Cluster 1 P1

(b) Cluster 1 P3

(c) Cluster 2 P3

(d) Cluster 4 and 5 P7

Figure B5.8: Interpolated average shear strength for the clusters nearest to the Laboratory tests.

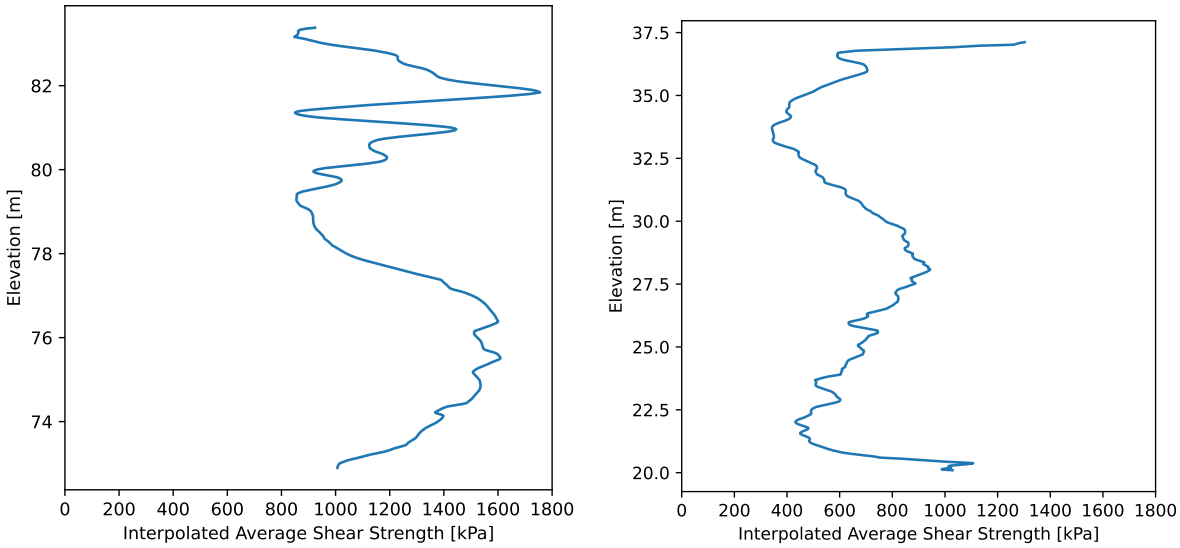

(a) Cluster 6 P7

(b) Cluster 1 and 2 P11

Figure B5.9: Interpolated average shear strength for the clusters nearest to the Laboratory tests.

Appendix C: Scatter plots E6 Kvithammar-Åsen

C6 All CPTU Data

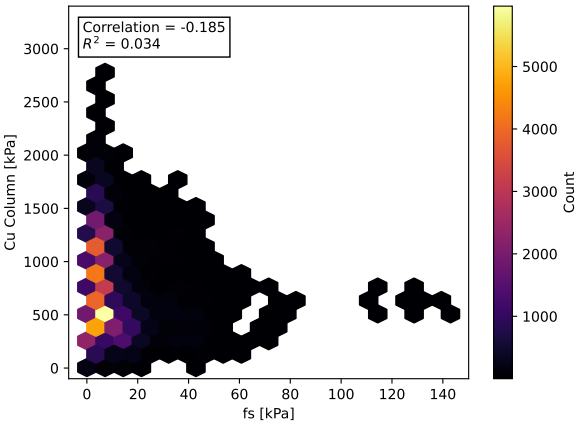

(a) Correlation between fs and Cu Column.

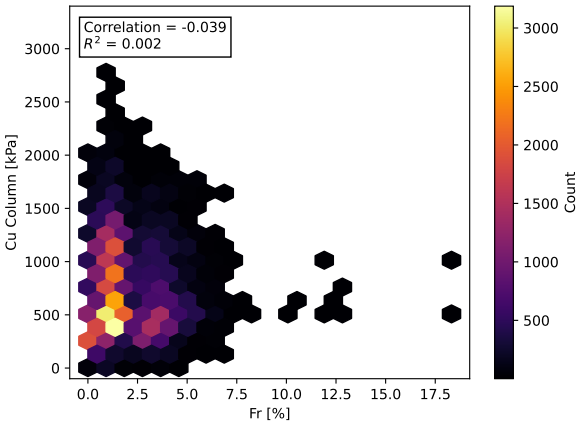

(b) Correlation between Fr and Cu Column.

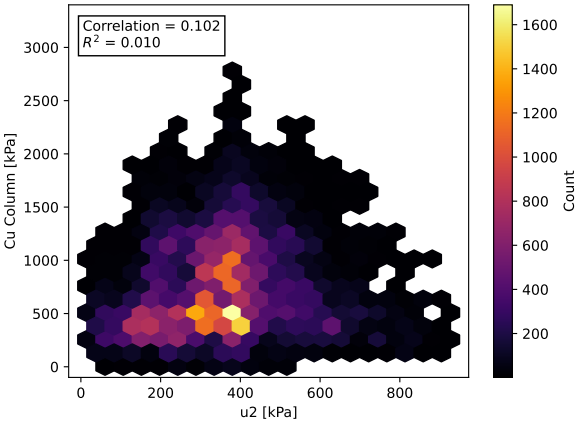

(c) Correlation between u2 and Cu Column.

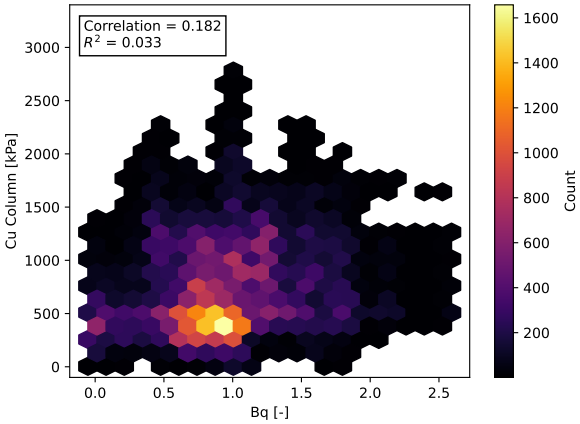

(d) Correlation between Bq and Cu Column.

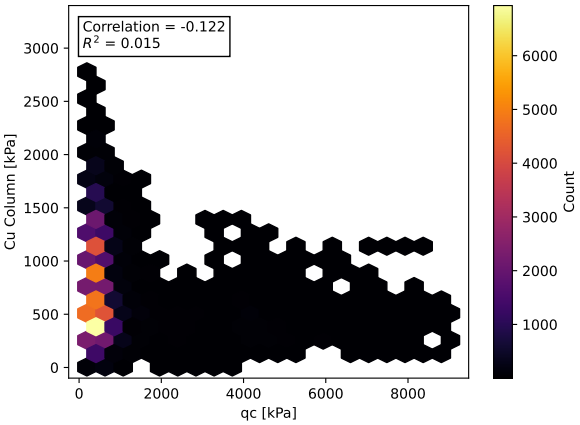

(e) Correlation between qc and Cu Column.

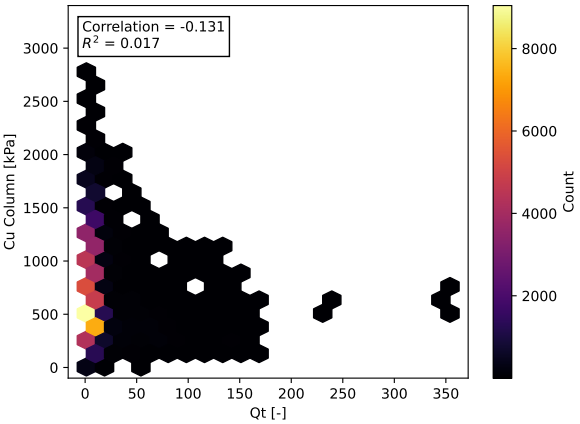

(f) Correlation between Qt and Cu Column.

Figure C6.1: The scatter plots show the correlation between the shear strength of the stabilized columns and the CPTU data from the CPTU closest to each stabilized column.

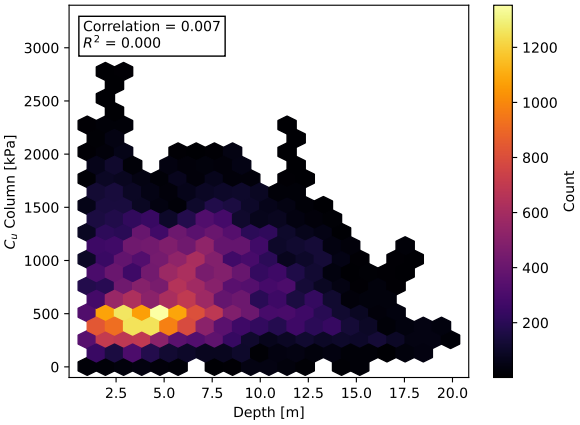

(a) Correlation between Depth and Cu Column.

Figure C6.2: The scatter plots show the correlation between the shear strength of the stabilized columns and the depth data from the CPTU closest to each stabilized column.

C7 Distance Reduced CPTU Data

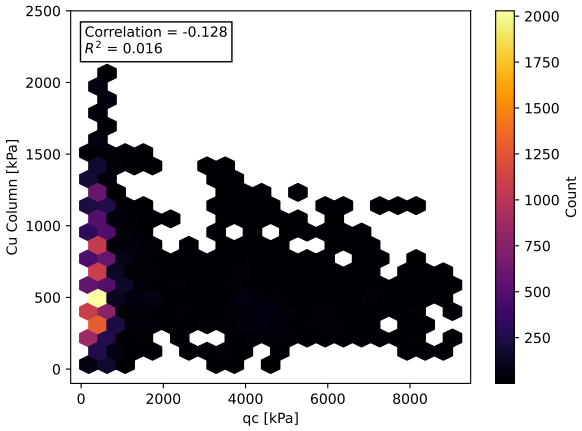

(a) Correlation between qc and Cu Column.

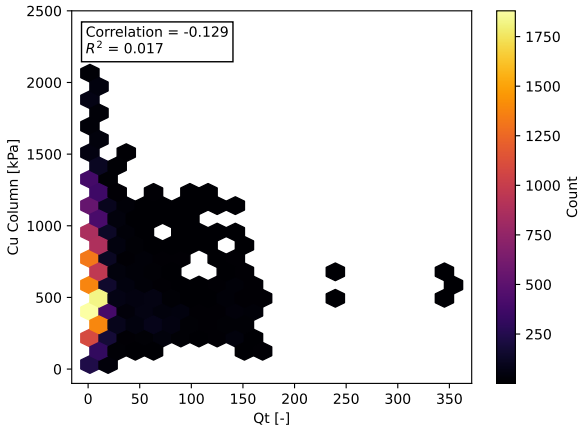

(b) Correlation between Qt and Cu Column.

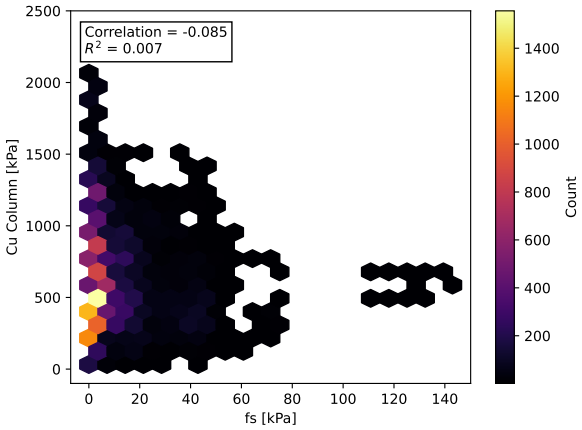

(c) Correlation between fs and Cu Column.

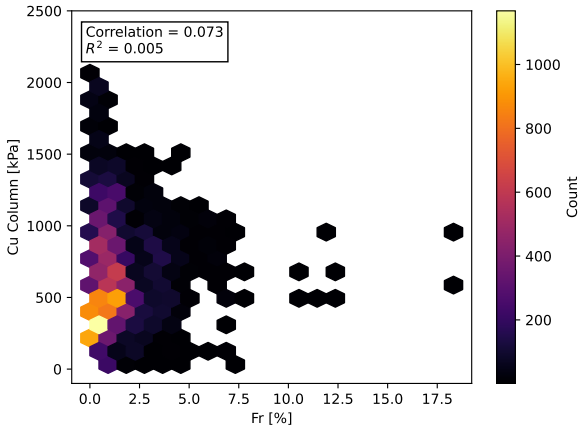

(d) Correlation between Fr and Cu Column.

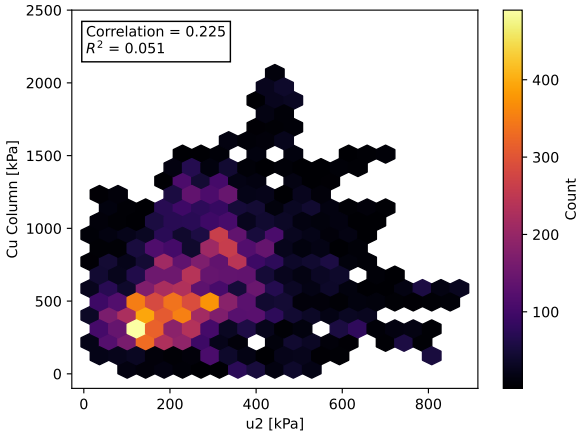

(e) Correlation between u2 and Cu Column.

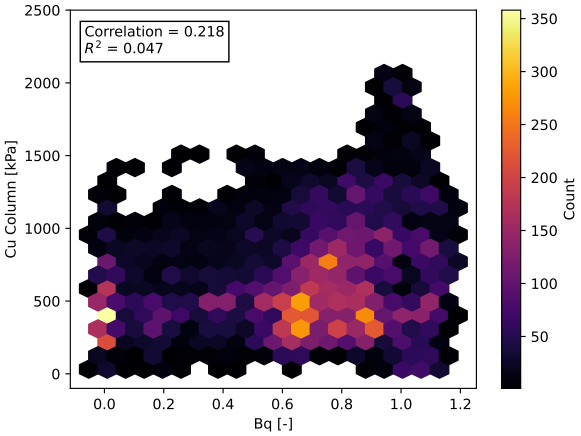

(f) Correlation between Bq and Cu Column.

Figure C7.1: The scatter plots show the correlation between the shear strength of the stabilized columns and the data from the CPTU closest to each stabilized column, where all the data where the distance between the CPTU and the nearest stabilized column is more than 20 meters are removed.

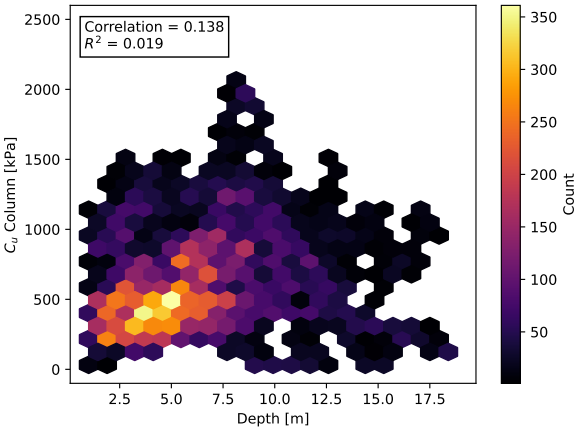

(a) Correlation between Depth and Cu Column.

Figure C7.2: The scatter plots show the correlation between the shear strength of the stabilized columns and the depth data from the CPTU closest to each stabilized column, where all the data where the distance between the CPTU and the nearest stabilized column is more than 20 meters are removed.

C8 All Laboratory Data

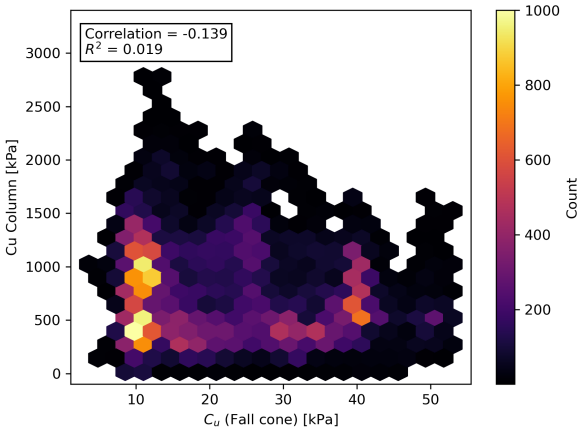

(a) Correlation between C_u and C_u Column.

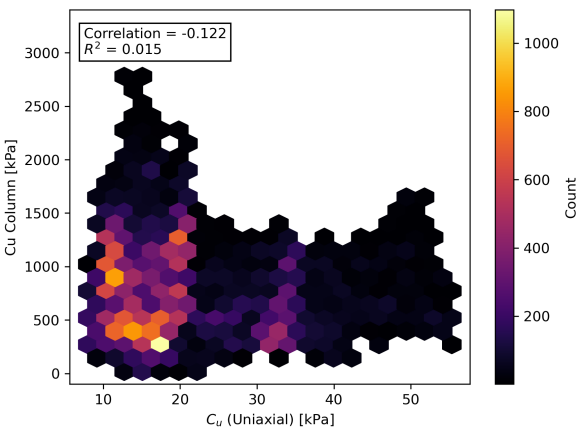

(b) Correlation between C_u and C_u Column.

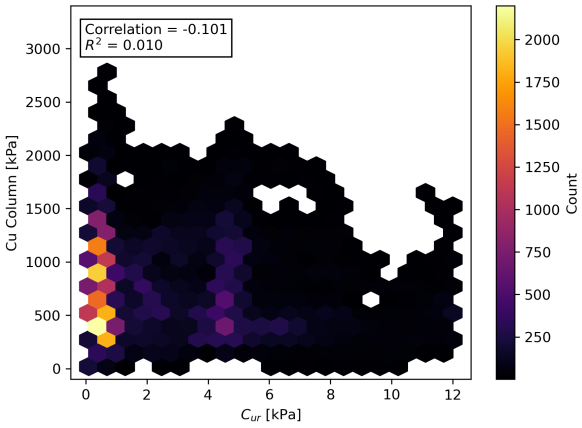

(c) Correlation between C_{ur} and C_u Column.

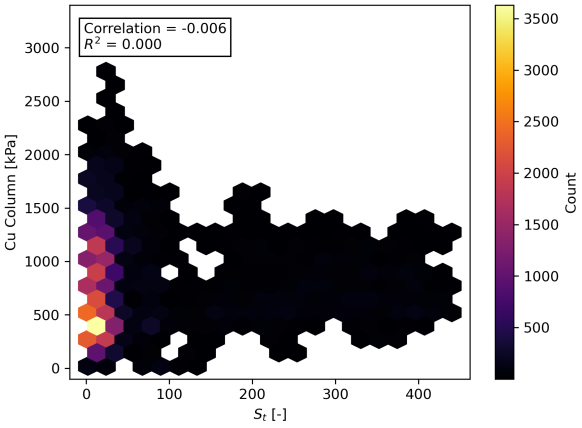

(d) Correlation between S_t and C_u Column.

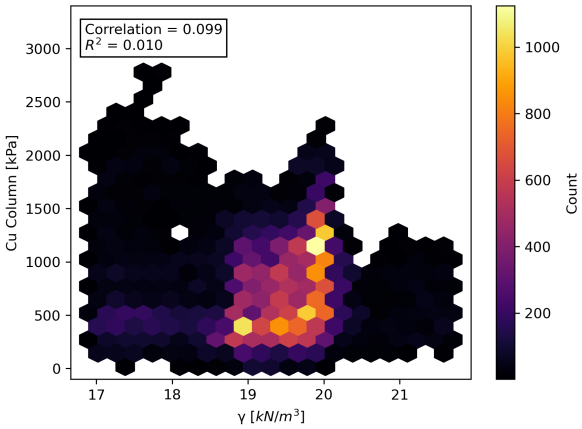

(e) Correlation between γ and C_u Column.

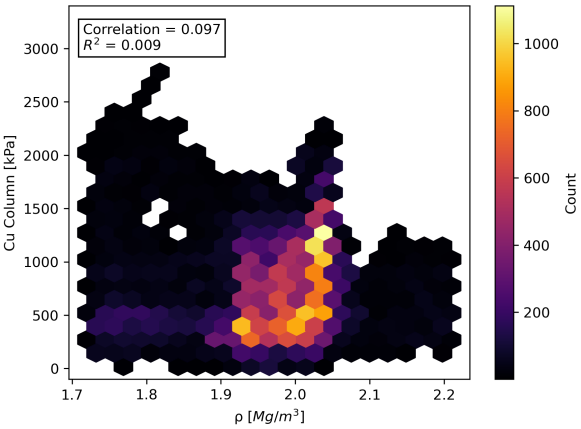

(f) Correlation between ρ and C_u Column.

Figure C8.1: The scatter plots show the correlation between the shear strength of the stabilized columns with the data from the fall cone, uniaxial, unit weight, and bulk density tests closest to each stabilized column.

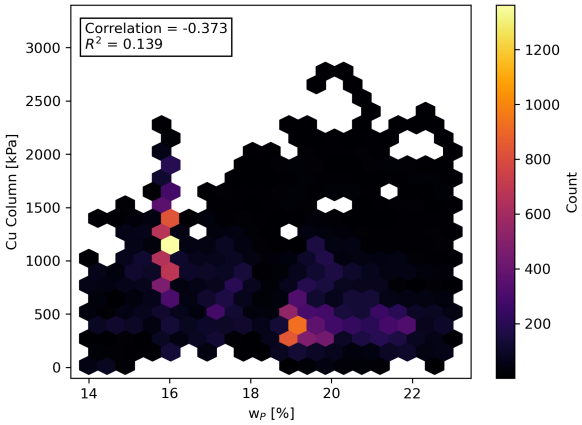

(a) Correlation between w_P and C_u Column.

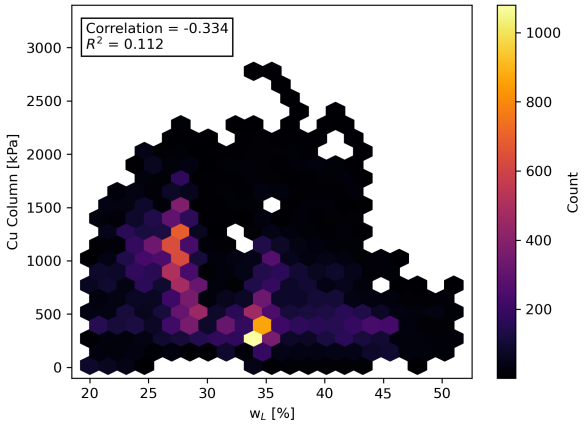

(b) Correlation between w_L and C_u Column.

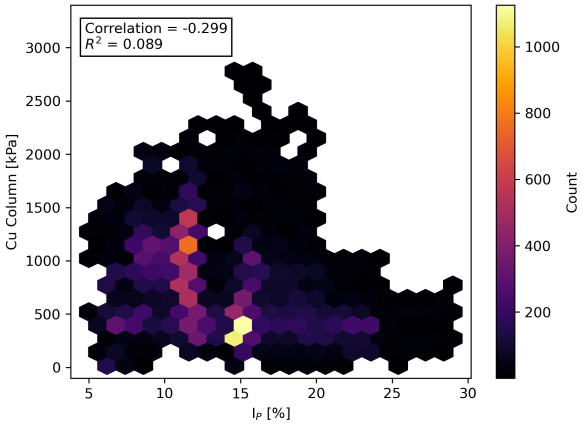

(c) Correlation between I_P and C_u Column.

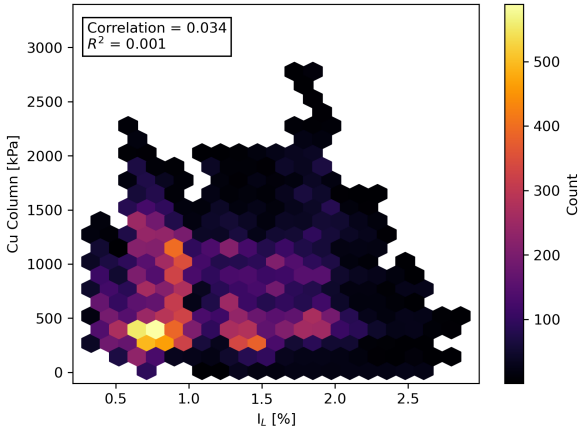

(d) Correlation between I_L and C_u Column.

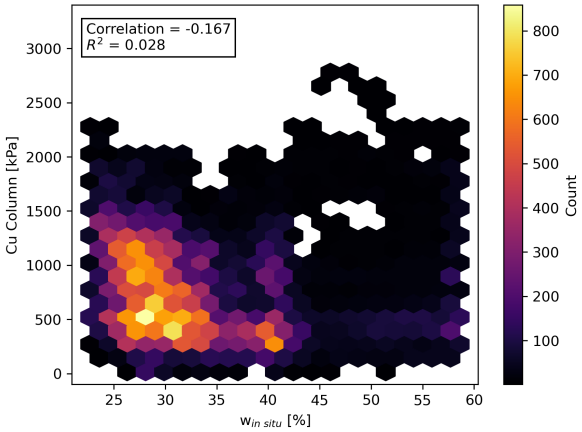

(e) Correlation between $w_{\text{in situ}}$ and C_u Column.

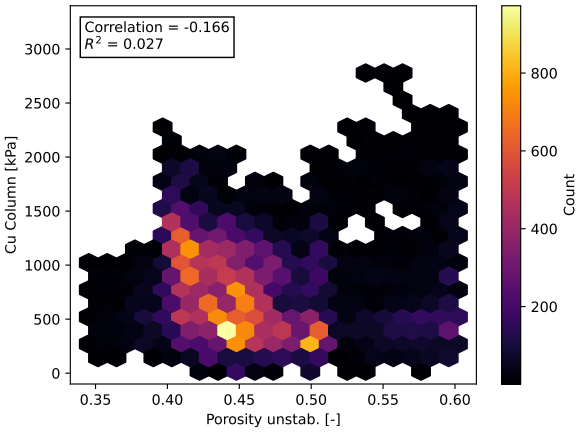

(f) Correlation between porosity and C_u Column.

Figure C8.2: The scatter plots show the correlation between the shear strength of the stabilized columns with the data from the Atterberg limits, water content, and the calculated porosity of the unstabilized soil closest to each stabilized column.

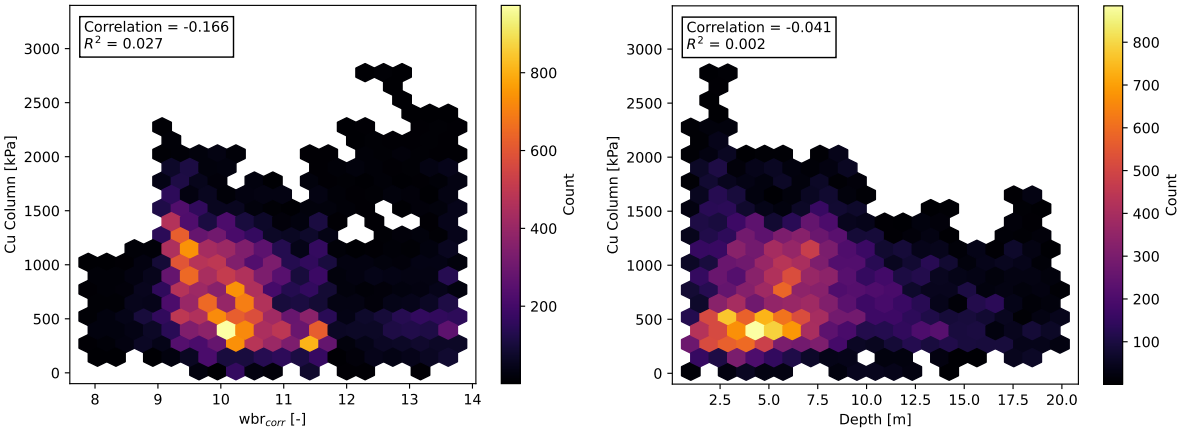

(a) Correlation between wbr and C_u Column. **(b)** Correlation between Depth and C_u Column.

Figure C8.3: The scatter plots show the correlation between the shear strength of the stabilized columns with the data from the calculated water binder ratio and the depth values closest to each stabilized column.

C9 Distance reduced Laboratory Data

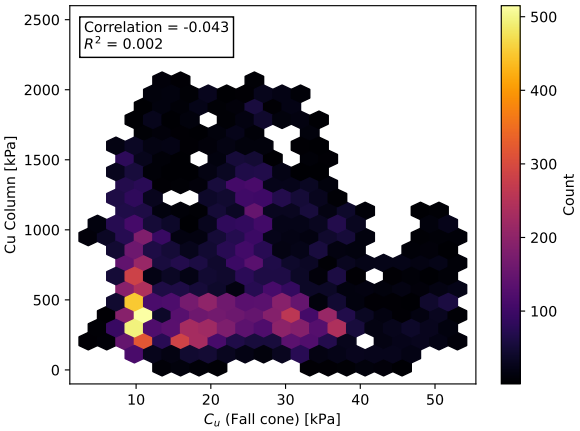

(a) Correlation between C_u and C_u Column.

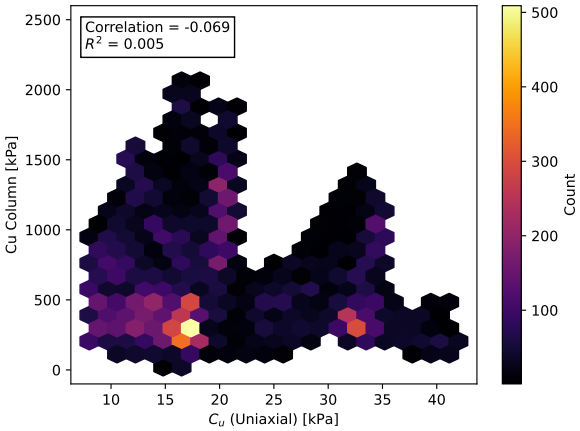

(b) Correlation between C_u and C_u Column.

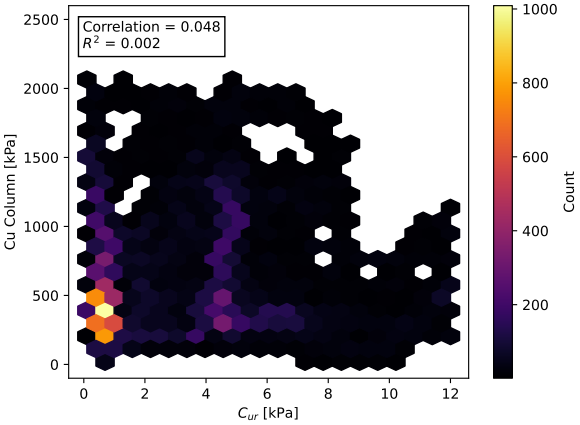

(c) Correlation between C_{ur} and C_u Column.

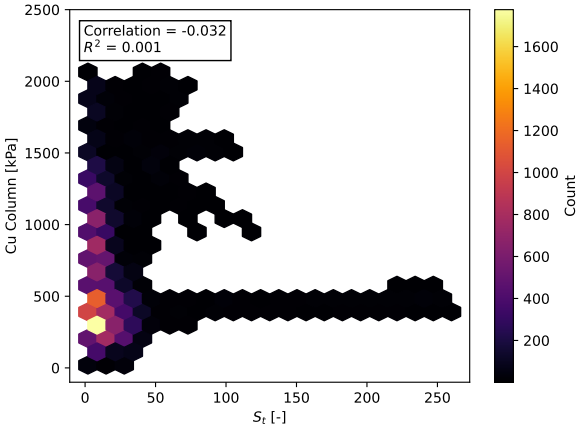

(d) Correlation between S_t and C_u Column.

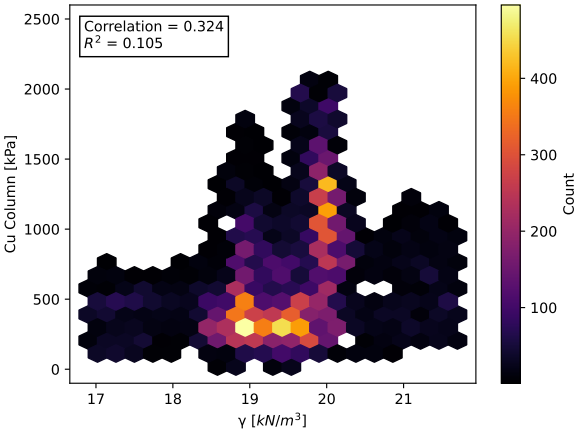

(e) Correlation between γ and C_u Column.

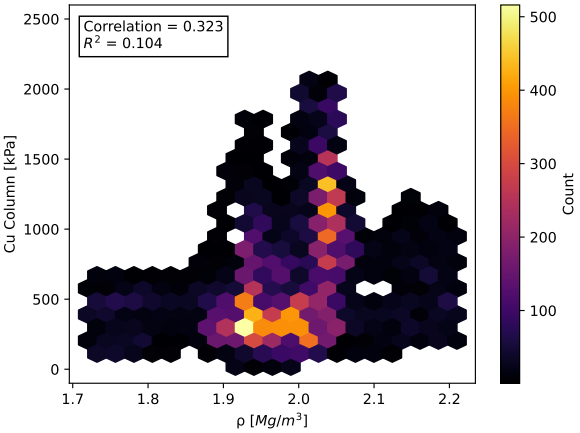

(f) Correlation between ρ and C_u Column.

Figure C9.1: The scatter plots show the correlation between the shear strength of the stabilized columns with the data from the fall cone, uniaxial, unit weight, and density tests closest to each stabilized column, where all the data where the distance between the laboratory tests and the nearest KPS is more than 40 meters are removed.

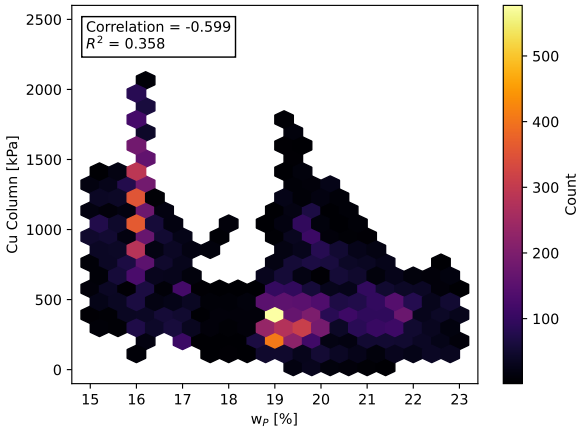

(a) Correlation between w_P and C_u Column.

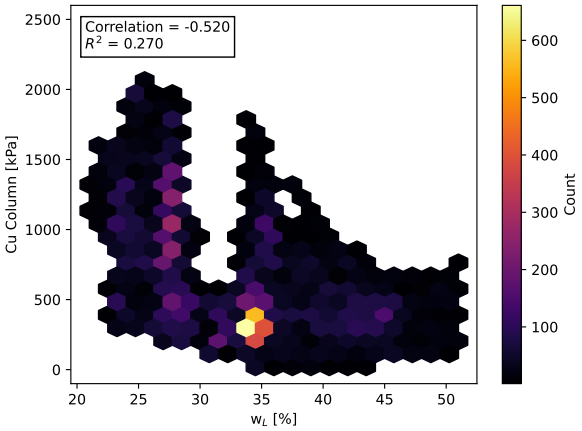

(b) Correlation between w_L and C_u Column.

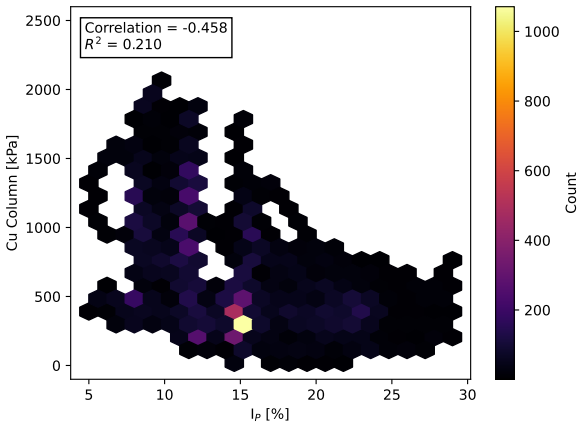

(c) Correlation between I_P and C_u Column.

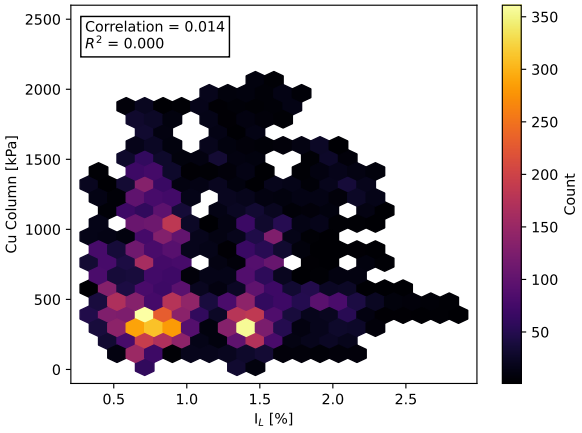

(d) Correlation between I_L and C_u Column.

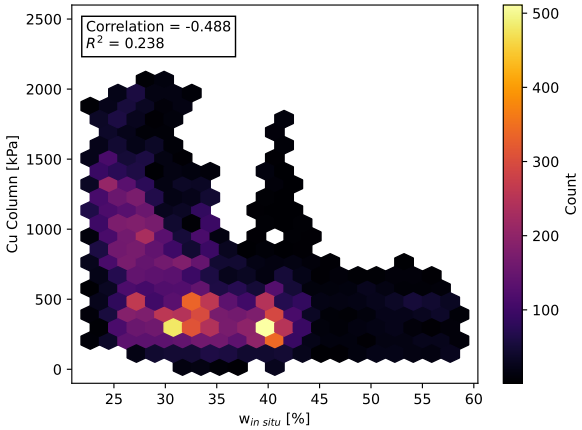

(e) Correlation between $w_{\text{in situ}}$ and C_u Column.

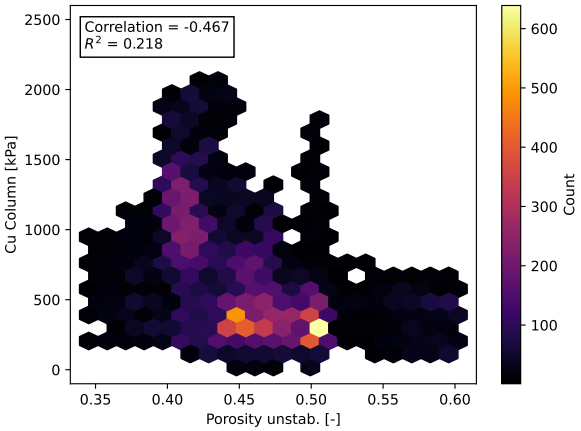

(f) Correlation between porosity and C_u Column.

Figure C9.2: The scatter plots show the correlation between the shear strength of the stabilized columns with the data from the Atterberg limits, water content, and the calculated porosity of the unstabilized soil closest to each stabilized column, where all the data where the distance between the laboratory tests and the nearest KPS is more than 40 meters are removed.

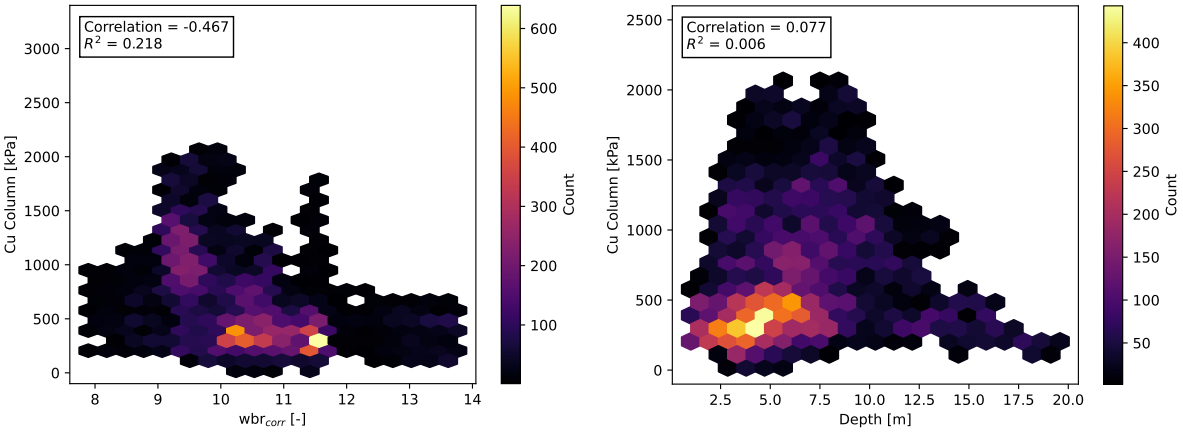

(a) Correlation between wbr and C_u Column. **(b)** Correlation between Depth and C_u Column.

Figure C9.3: The scatter plots show the correlation between the shear strength of the stabilized columns with the data from the calculated water binder ratio and the depth values closest to each stabilized column, where all the data where the distance between the laboratory tests and the nearest KPS is more than 40 meters are removed.

Appendix D: Data Points Correlation Analysis

D10 CPTU Regarding Distance

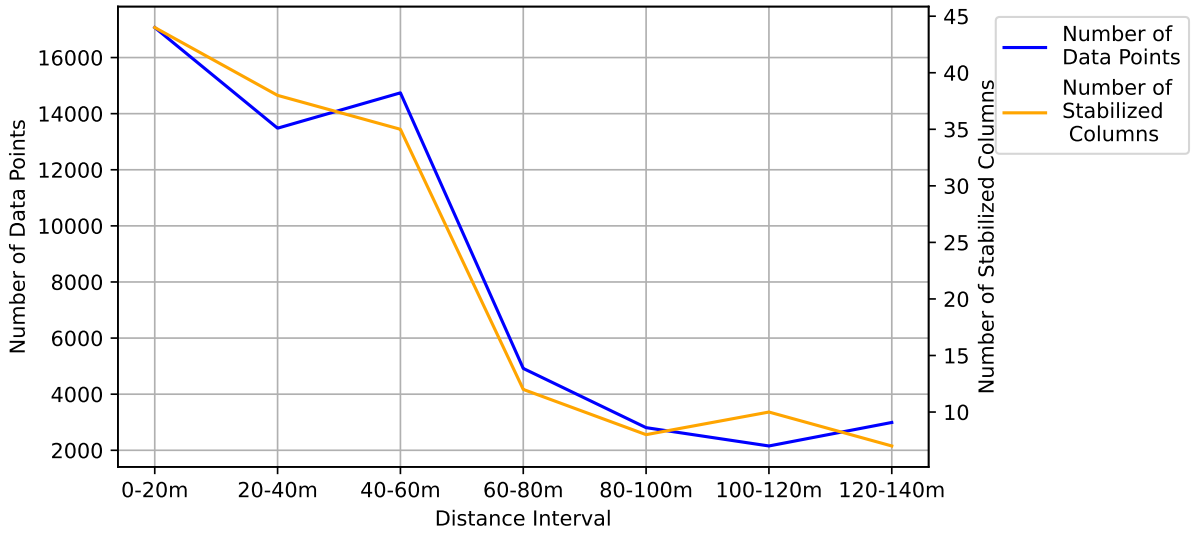

Figure D10.1: The correlation of the CPTU data and Cu Column at different distances. The different correlations are calculated based on 20 meters intervals.

D11 CPTU Regarding Depth

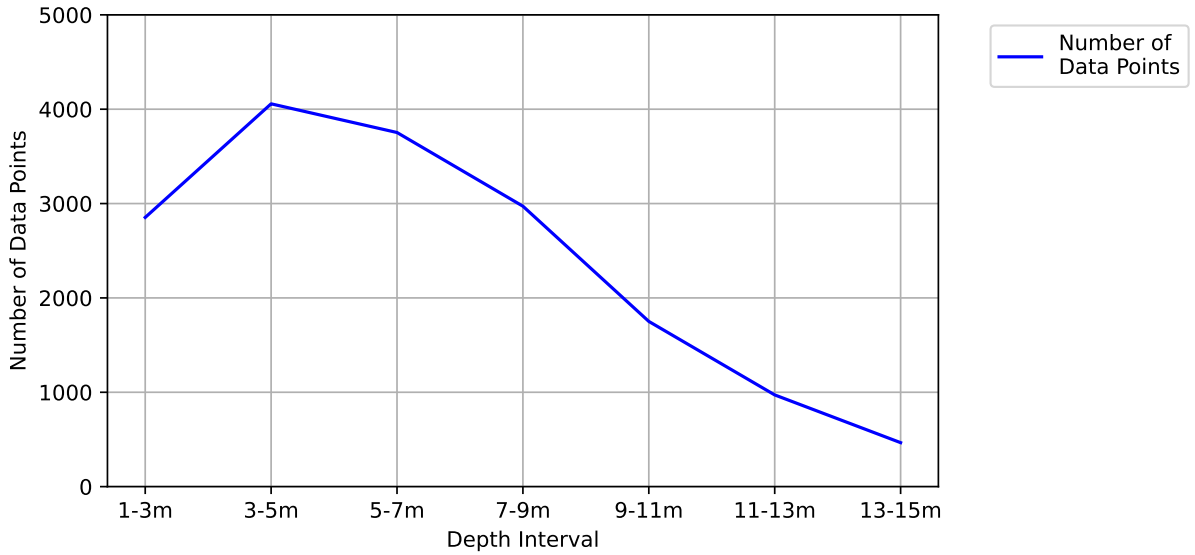

Figure D11.1: The correlation of the CPTU data and Cu Column at different depths. The different correlations are calculated based on 2 meters intervals.

D12 Laboratory Regarding Distance

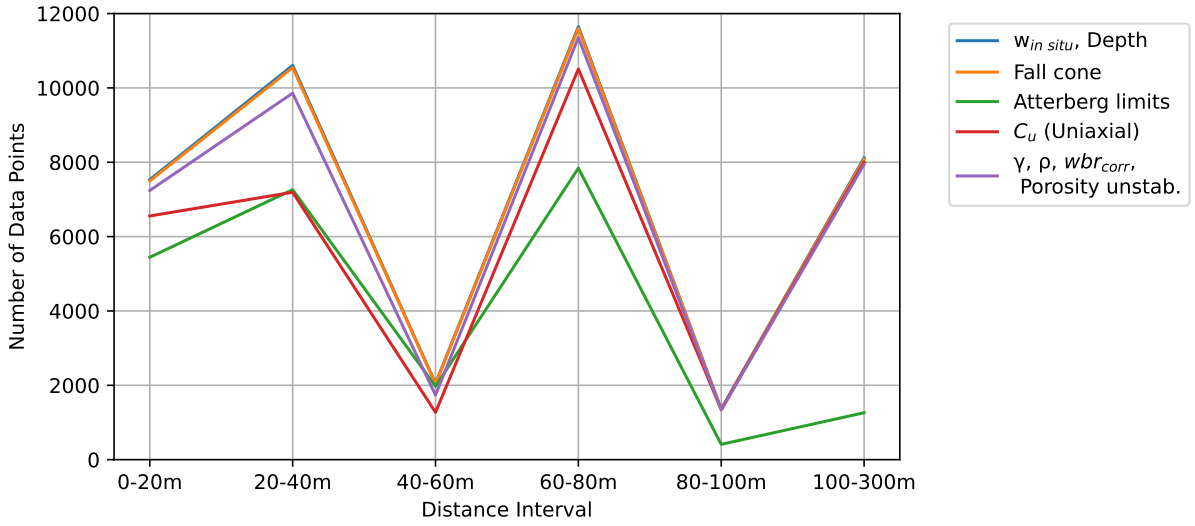

Figure D12.1: Visualization of the number of data points used for the correlation calculations in each interval for the different parameters.

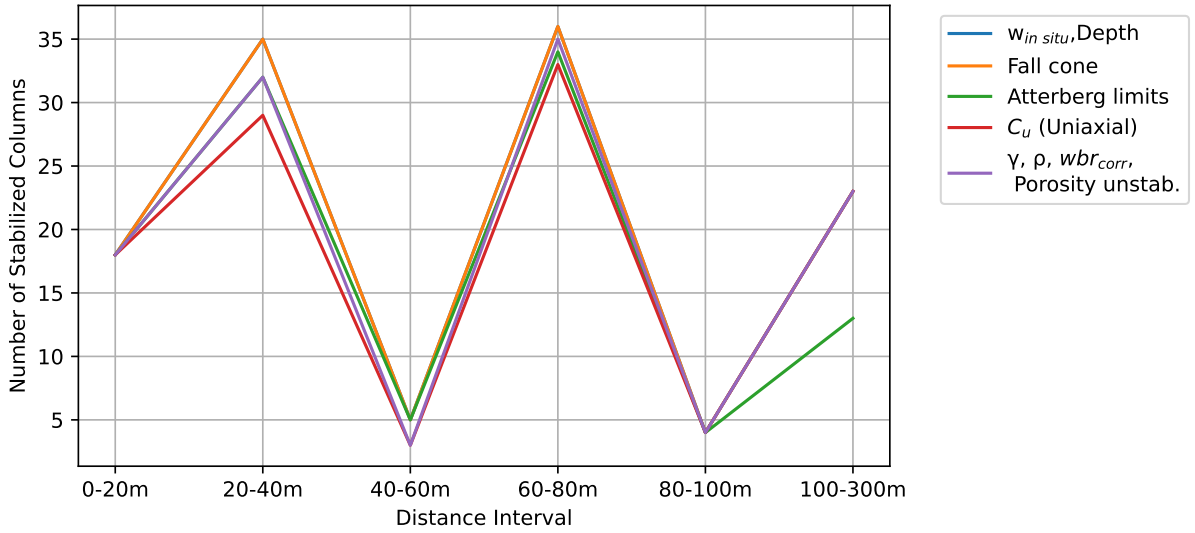

Figure D12.2: Visualization of the number of columns used for the correlation calculations in each interval for the different parameters.

D13 Laboratory Regarding Depth

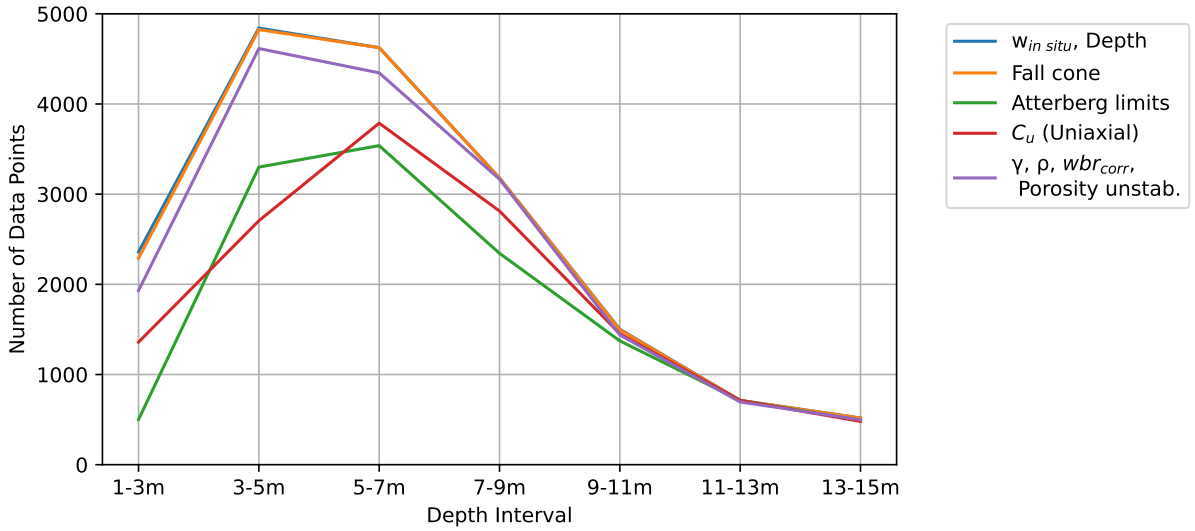

Figure D13.1: Visualization of the number of data points used for the correlation calculations in each depth interval for the different parameters.

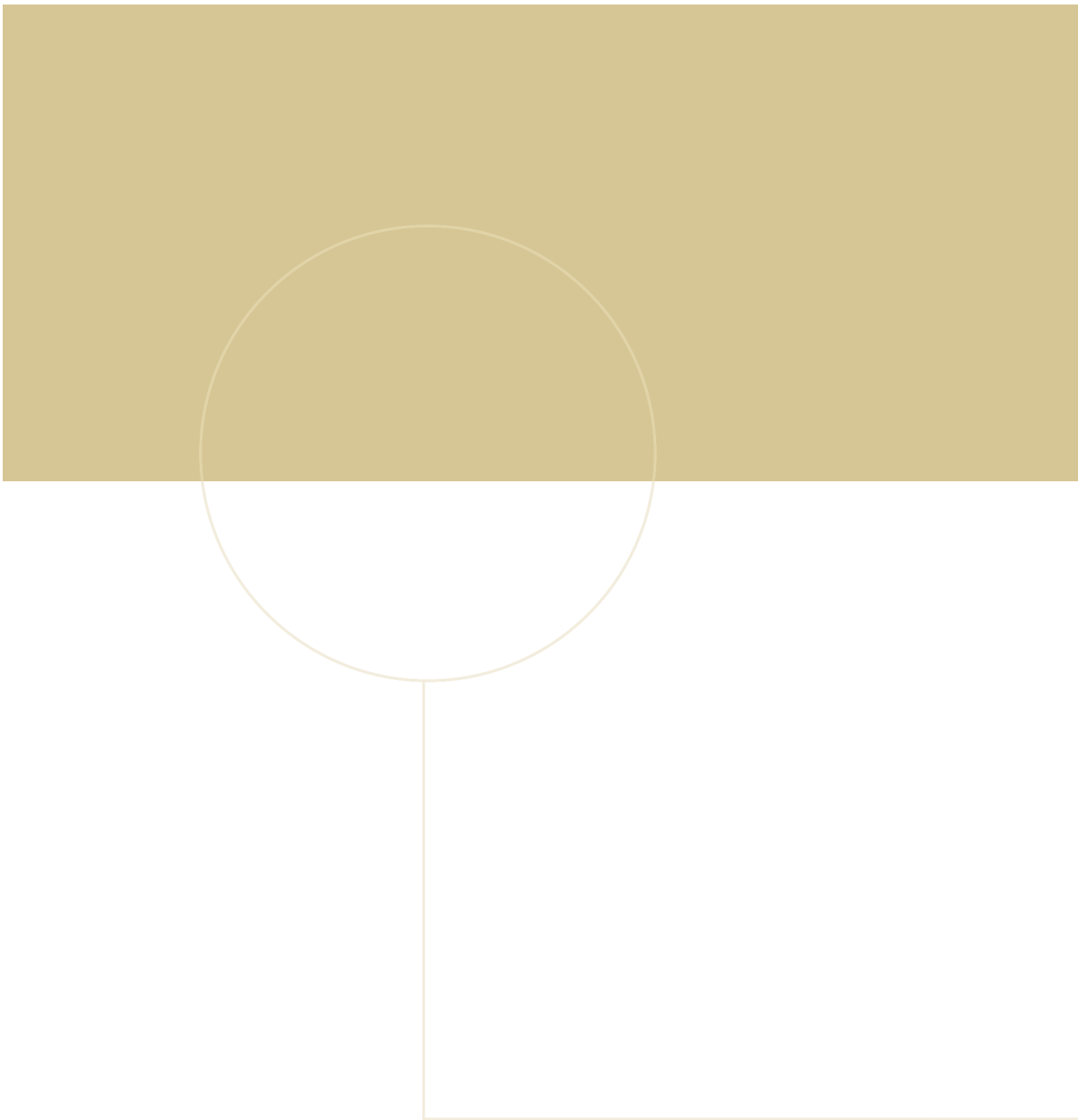

NTNU

Norwegian University of
Science and Technology